

Thesis 5
3238

**University of Nevada
Reno**

**Geophysical Applications to
the Development of a Groundwater Model
of Washoe Valley, Nevada**

**A Thesis submitted in partial fulfillment of the
Master of Science in Hydrology/Hydrogeology**

**By
Ronald Clayton Petersen**

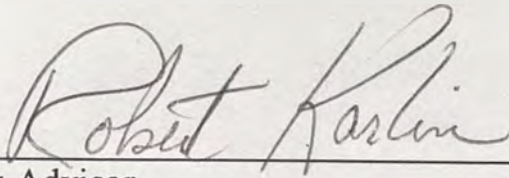
Robert Karlin, Ph.D. Thesis Advisor

December 1993

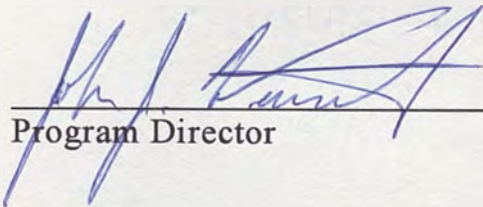
2374304

[0115/94]

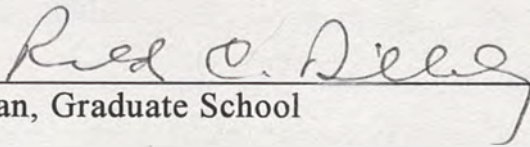
The thesis of Ronald Clayton Petersen is approved:



Thesis Advisor



Program Director



Dean, Graduate School

University of Nevada

Reno

December 1993

ACKNOWLEDGMENTS

Many people helped along the way to the completion of this thesis, and I hereby express my thanks and appreciation to all of them. First there are the members of my thesis committee, Drs. Fred Gifford, Berry Lyons, and Steve Wheatcraft who all offered encouragement and insight. My sincerest appreciation goes to my advisor, Dr. Robert Karlin. He is the one person of whom it can truly be said that this thesis would never have been completed without him.

This thesis was field intensive, and couldn't have been done without the help of several of my fellow students, particularly Georgia Doyle, Andy Morsel, and Janice Murphy. Special thanks go to Jim Granata, who spent almost as much time collecting data in Washoe Valley as I did. Steve Gillette served beyond the call of duty when on two occasions he pulled me out of the mud of Washoe Lake when I got stuck. Alan Ramelli collected and processed the GPS data. Magnetometers were borrowed from Great Basin Geophysical and Western Mining Company. Additionally, the color magnetic contour plot was generated by Great Basin.

Last, but not least, I owe special thanks to my wife Nancy for her patience and perseverance over the last two and a half years, and to my children, Julia and Clayton, who have also been patient and perseverant, even though they are still too young to know what it means.

ABSTRACT

Gravity, ground magnetic, and terrain conductivity surveys were run in Washoe Valley to define subsurface lithology for input to a groundwater model. The gravity results map basin configuration, with a shallower basement on the east indicated. High magnetic and terrain conductivity values reflect a volcanic unit overlying this shallow eastern basement, which is in turn overlain by electrically conductive fine-grained sediments. Together, these units suggest much lower transmissivities on the east side of the valley, relative to a thicker section of coarse-grained sediments to the west. These low transmissivities are required by the groundwater model to fit the 1965 potentiometric surface to which the model is calibrated. This study demonstrates the utility of combining the results of multiple geophysical surveys with conventional hydrological parameters. This integration is particularly useful for mapping spatial distributions of interbasin hydraulic properties, and it provides excellent constraints the groundwater model.

CONTENTS

	Page
ACKNOWLEDGMENTS	ii
ABSTRACT.....	iii
LIST OF FIGURES.....	1
LIST OF TABLES	3
INTRODUCTION.....	4
SCOPE AND OBJECTIVES.....	8
GEOLOGIC SETTING	10
HYDROLOGIC SETTING.....	11
PREVIOUS WORK.....	12
GEOPHYSICS	14
Applications to Groundwater Investigations.....	14
Methods.....	20
Geophysical Results.....	24
Gravity and Magnetic Results.....	24
Joint Gravity and Magnetic Modeling.....	31
Electrical Conductivity Survey.....	38
Discussion	42
THE GROUNDWATER MODEL SIMULATION.....	44
The Conceptual Model.....	44
The Mathematical Model.....	45
Model Layers.....	46
The Unconfined Aquifer	47
The Confining Layer.....	47
The Confined Aquifer	48
Grid Cell Size	49
The Potentiometric Surface	49
Hydraulic Conductivities and Transmissivities	52
Recharge	56
Discharge	57
Boundary Conditions and Initial Heads.....	58
The Steady-State Simulation	58

	Page
Calibration.....	58
Sensitivity Analysis	65
Changes in the Unconfined Aquifer	65
Changes in the Confined Aquifer.....	65
Changes in Both Aquifers	70
Position of the Interface Between Units.....	71
Recharge.....	76
The Confining Layer.....	79
Summary	83
Limitations of the Model	84
CONCLUSIONS AND RECOMMENDATIONS.....	86
REFERENCES.....	89
APPENDIX A: DRIFT CORRECTONS.....	92
APPENDIX B. GRAVITY DATA.....	96
APPENDIX C:. MAGNETIC DATA.....	100
APPENDIX D: TERRAIN CONDUCTIVITY DATA.....	116
APPENDIX E: GLOBAL POSITIONING DATA (GPS).....	118
APPENDIX F: WELL DATA	119

FIGURES

	Page
1. Regional Location Map of Washoe Valley.....	5
2. Local Features of Washoe Valley.....	6
3. Gravity Station Locations.....	21
4. Magnetic Station Locations.....	23
5. EM-34 Profile Locations.....	25
6. Gravity Contours with Interpreted Major Structures.....	26
7. Magnetic Contours (Color).....	27
8. Structural Interpretation Map.....	29
9. Magnetic Contours with Model Profile Locations.....	30
10. Southern Gravity-Magnetic Profile.....	33
11. Central Gravity-Magnetic Profile.....	34
12. Northern Gravity-Magnetic Profile.....	35
13. Locations of Paleoclimate Drill Holes.....	40
14. Coincident EM-34 - Magnetic Data.....	41
15. Generalized Stratigraphic Section of Southern New Washoe City.....	48
16. The Model Grid.....	50
17. The 1965 Potentiometric Surface with Calibration Profiles.....	51
18. Contoured Transmissivities from Specific Capacity Data.....	53
19. Domains I thru V of Similar Hydraulic Properties.....	54
20. Calibrated Model Potentiometric Surface of the Unconfined Aquifer.....	60

21. Northern Profile Calibrated Model.....	61
22. Southern Profile Calibrated Model.....	62
23. Northern Profile: Sensitivity to Changes in the Hydraulic Conductivities of the Unconfined Aquifer.....	66
24. Southern Profile: Sensitivity to Changes in the Hydraulic Conductivities of the Unconfined Aquifer.....	67
25. Northern Profile: Sensitivity to Changes in the Transmissivities of the Confined Aquifer.....	68
26. Southern Profile: Sensitivity to Changes in the Transmissivities of the Confined Aquifer.....	69
27. Northern Profile: Sensitivity to Changes in the Hydraulic Properties of Both Aquifers.....	71
28. Southern Profile: Sensitivity to Changes in the Hydraulic Properties of Both Aquifers.....	72
29. Northern Profile: Sensitivity to the Position of the Interface Between High and Low Transmissivity Units.....	73
30. Southern Profile: Sensitivity to the Position of the Interface Between High and Low Transmissivity Units.....	74
31. Northern Profile: Sensitivity to the Permeability Barrier.....	76
32. Northern Profile: Sensitivity to Recharge.....	77
33. Southern Profile: Sensitivity to Recharge.....	78
34. Northern Profile: Sensitivity to the Leakance of the Confining Layer.....	80
35. Southern Profile: Sensitivity to the Leakance of the Confining Layer.....	81

TABLES

	Page
1. Calibrated Model Hydraulic Parameters.....	56
2. Water Balance Comparison.....	63
3. Sensitivity Analysis Summary.....	83

INTRODUCTION

The population of Washoe Valley, located in western Nevada between Carson City and Reno (Figure 1), has been steadily increasing along with the rest of the region for the last 25 years. With this growth will come additional demands for water. Limited water supplies will be further strained by any future droughts coupled with water quality problems brought on by the rural lifestyle of the valley, namely high nitrate concentrations generated by a large animal population (mostly horses) and a large number of individual septic tanks. The problem is complicated by the fact that most residences also have their own supply wells very near the sources of the nitrates (i.e. in the most sensitive areas). During the drought years of the early 1990's many residents of New Washoe City had to deepen their wells by 30 to 60 meters, or more.

The three main population centers of the valley are Washoe City near the northern end of the valley, New Washoe City near the east-central flank of the valley and the northeastern edge of Washoe Lake, and the community of Bellevue in the southwestern section of the valley near Lakeview Summit (Figure 2). Additionally, population is spread out along the entire western side of the valley. Two new developments are either under way or proposed. These are the Lightning W to the southwest near Lakeview Summit, and the Serpa development immediately south of Jumo Grade on the east side of the valley.

Washoe Valley lies near the transition between two climatic regimes. Because it lies in the rain shadow of the Sierra Nevada Mountains to the west, the floor of the valley receives relatively little precipitation and can be characterized as primarily a sagebrush environment. In the Carson range immediately to the west, the Pinyon pine/mountain mahogany environment begins only a slight distance above the valley floor, reflecting a significant increase in precipitation. As global climate changes, the

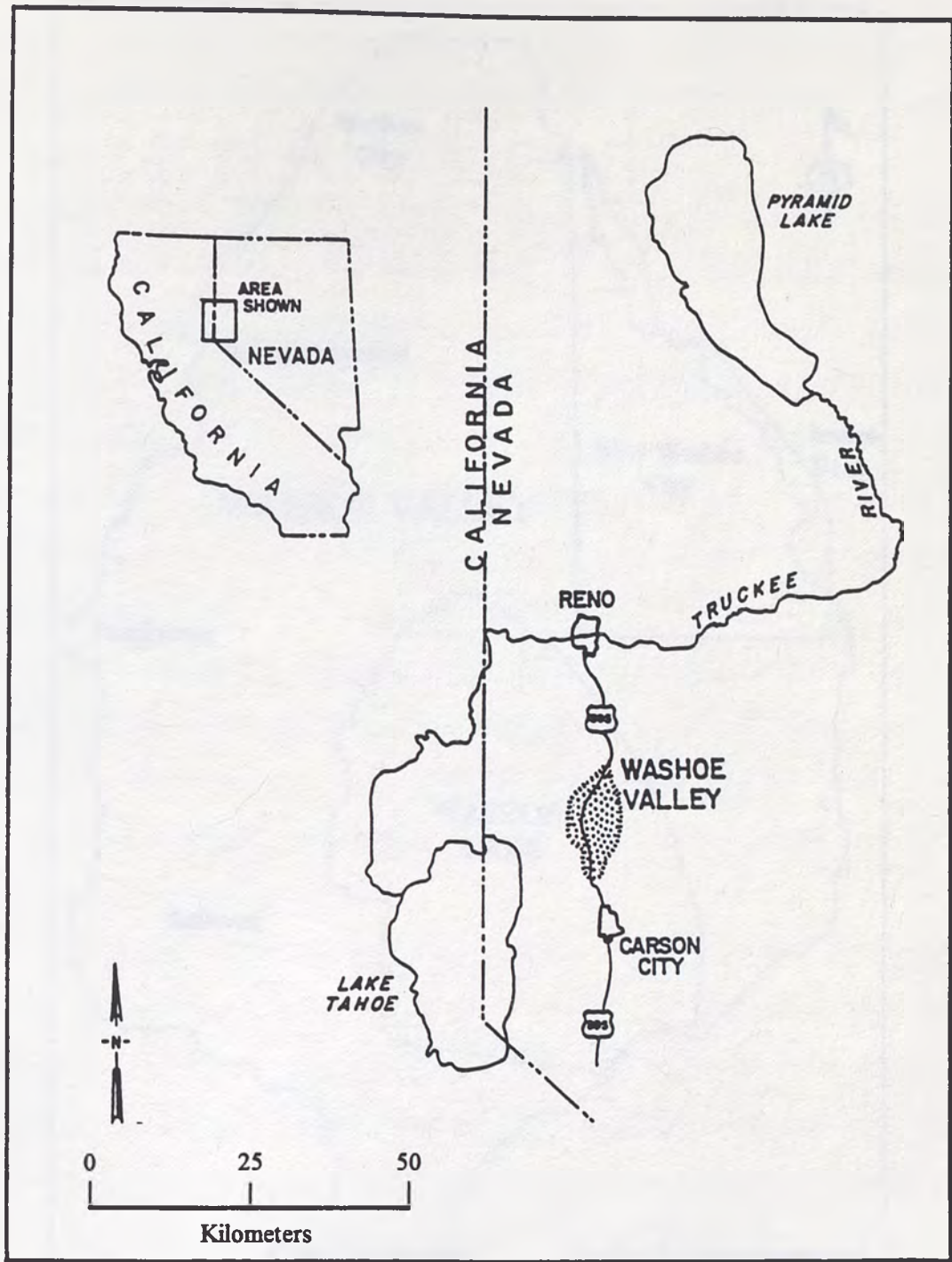


Figure 1. Regional Location Map of Washoe Valley.

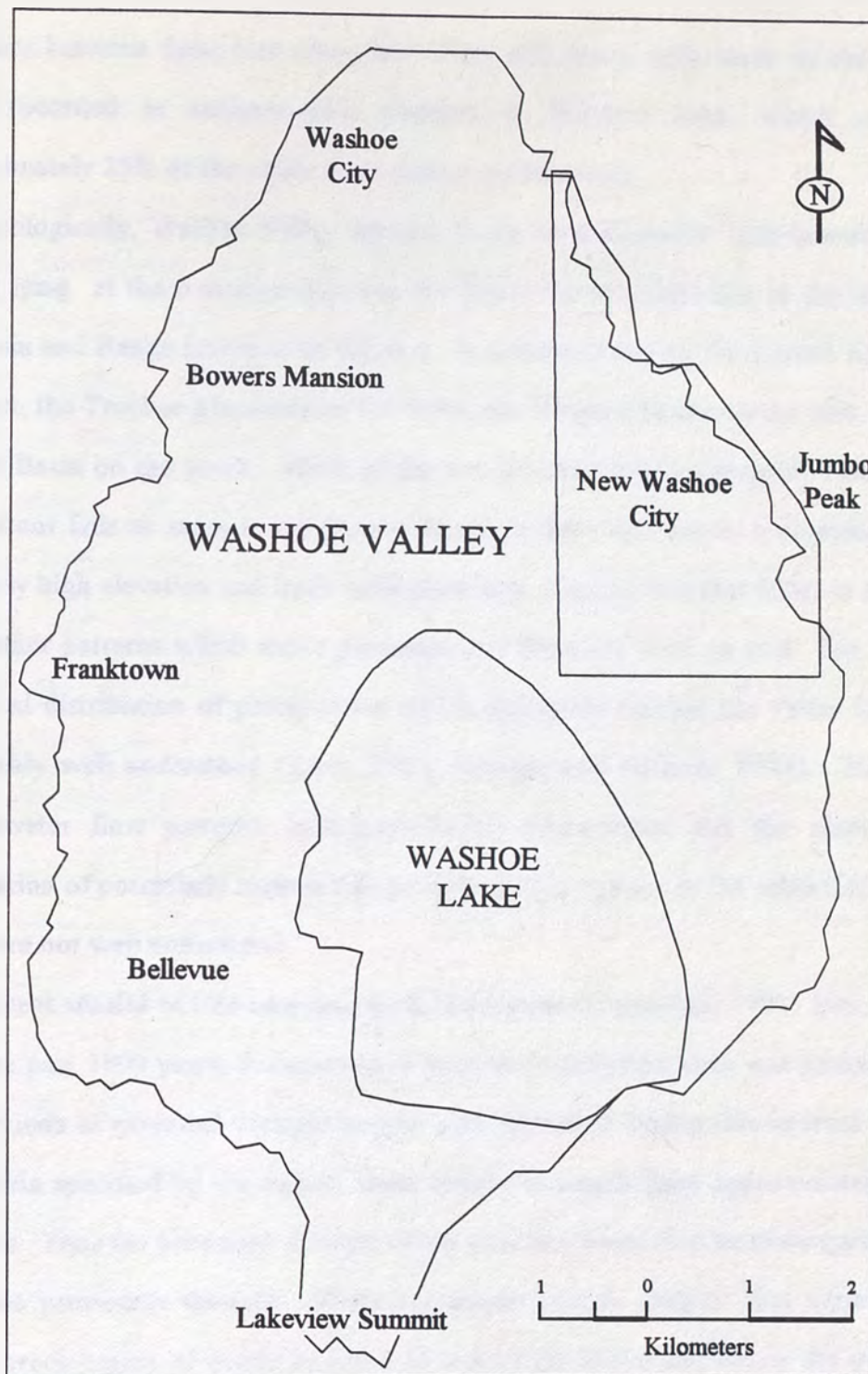


Figure 2. Local Features of Washoe Valley.

boundary between these two zones moves up and down, with much of the change being recorded in sedimentation patterns in Washoe Lake, which occupies approximately 25% of the valley floor during normal years.

Geologically, Washoe Valley appears to be an asymmetric fault-bounded half-graben lying at the transition between the Sierra Nevada Batholith to the west and the Basin and Range province to the east. It is surrounded by the Carson Range on the west, the Truckee Meadows on the north, the Virginia Range on the east, and the Carson Basin on the south. Much of the precipitation which ultimately reaches the valley floor falls as snow in the Carson Range to the west, due to a combination of relatively high elevation and large catchment area, plus the fact that it lies in the path of weather patterns which move predominantly from the west to east. The amount and areal distribution of precipitation which ultimately reaches the valley floor are reasonably well understood (Rush, 1967, Arteaga and Nichols, 1984). However, groundwater flow patterns, lake-groundwater interactions, and the amount and distribution of potentially recoverable groundwater in storage in the subsurface of the valley are not well understood.

Recent studies of tree ring data from the Sierras (Graumlich, 1992) indicate that over the past 1000 years, droughts have been more prevalent than wet periods, with nine periods of extended drought having been identified during this interval. Based on criteria specified by the author, these ranged in length from approximately 15 to 60 years. Thus the persistent drought of the past few years may be more typical than had been previously thought. There are ample data to suggest that variations in annual precipitation of nearly an order of magnitude above and below the norm are common (Houghton, et al, 1975, Nichols, 1989, USGS, 1992). Any decrease in surface water input to Washoe Valley will necessitate a greater reliance on tenuous

groundwater supplies, making it imperative to develop an understanding of available groundwater and its distribution throughout the subsurface of Washoe Valley.

SCOPE AND OBJECTIVES

Site specific data with which to develop groundwater models, particularly data on the subsurface distribution of hydraulic conductivities and transmissivities, are typically sparse. Usually, only limited, widely distributed, and often poorly determined physical property measurements are available from which to begin constructing a groundwater model. Assignment of hydraulic properties to model nodes is most often done by sediment grain size analysis from available boreholes (Winter, 1981, Thomas, et al., 1989), followed by some statistical interpolation scheme, such as kriging (Anderson and Woessner, 1992) to assign areal distributions. Because the number of available boreholes is seldom adequate, other means, such as electrical resistivity, magnetics, or gravity, can often map physical properties, stratigraphic thicknesses, and lateral boundaries of subsurface hydrostratigraphic units for input to a groundwater model. Washoe Valley is particularly well suited to this type of study, because it is a small basin where a substantial amount of hydrologic and geologic data has already been compiled. Additionally, numerous wells exist from which to construct potentiometric surface maps and make transmissivity estimates from specific capacity tests.

The objectives of this thesis are 1) to use various geophysical methods to define the overall basin structure of Washoe Valley as well as inter-basin variations in hydraulic properties, 2) to demonstrate the viability of geophysics as a means of obtaining subsurface distributions of hydraulic properties when other data are sparse or absent, 3) to establish methodologies and guidelines for incorporating geophysical data directly into groundwater models of other basins or areas and 4) to develop this

information into a groundwater model of Washoe Valley. Although numerous geophysical studies have been applied to hydrogeologic problems, most of them result in the mapping of hydrostratigraphic units followed by the suggestion that anyone who needs to can further apply this information to whatever problem is at hand. This thesis takes the additional step of actually using geophysical results to estimate values of hydraulic properties and their spatial distribution as inputs to the groundwater model.

In the summer of 1991, Washoe Lake dried up completely for the first time since the 1930's, providing a unique opportunity to conduct scientific studies. Gravity, ground magnetic, and terrain conductivity surveys were run on the dry lake bed and in the surrounding valley between October of 1991 and April of 1993 to gain a better understanding of the subsurface geology of Washoe Valley. Approximately 1475 ground magnetic stations, 84 gravity stations, and two traverses with an EM-34 terrain conductivity meter were occupied. Survey control on the lake bed was achieved through the collection of Global Positioning (GPS) co-ordinates along a north-south base line and two east-west cross lines. Additionally, GPS elevations were used in the gravity data reduction.

The various geophysical data were used to determine hydrologically important subsurface lithology and the overall structure of the basin. The geophysically determined structural and stratigraphic models were then used to help constrain models of the groundwater flow of the basin. In some areas, the geophysical data corroborated the available geologic and hydrologic data, in other areas it helped to fill in gaps in the data.

The 1965 potentiometric surface data (Rush, 1967) were also gridded, contoured, and plotted. Transmissivity estimates were obtained from specific capacity tests which were made on several wells. Additional sources of data used

include U.S. Geological Survey data bases and logs filed with the State Engineer's office. These results were used to assign hydraulic properties to the groundwater model. The water balance of the model was based on the recharge and discharge data from Rush (1967) and Arteaga and Nichols (1984). Finally, two cross-valley profiles were extracted from the potentiometric surface contours to establish the standard against which the groundwater model was calibrated.

Sensitivity analysis of the groundwater model of Washoe Valley to the parameters defined by the magnetic and electromagnetic data suggest that the model is indeed sensitive to these parameters. This supports the efficacy of using geophysical results as input to groundwater models of other areas.

GEOLOGIC SETTING

The oldest rock unit exposed in both the Carson and Virginia ranges is a Cretaceous granodiorite, which cooled about 80 million years ago when the Sierra Nevada batholith formed (Tabor et al., 1983). Based on its presence on both sides of the valley as well as the densities required by their gravity model, Thompson and Sandberg (1958) also assumed the granodiorite to be the basement underlying Washoe Valley. While volcanic rocks are absent in the Carson range to the west, numerous volcanic units are exposed in the Virginia range to the east, where volcanism began about 22 million years ago and continued until about 1 million years ago. These rocks are described in detail by Whitebread (1976). Additionally, density measurements were made on several of these units by Thompson and Sandberg (1958).

The boundary contacts of Washoe Valley with both the Carson and Virginia ranges are defined by high angle Holocene faults scarps. As the ranges rose rapidly relative to the valley floor, sediments poured into the valley, mostly from the west.

Nearer the north-south axis of the valley, they interfinger with younger, finer-grained lake sediments (Tabor, et al., 1983). The exact age of Washoe Lake has not been determined, but is estimated by Karlin et al. to have been present for at least 2.5 million years.

HYDROLOGIC SETTING

Washoe Valley is located approximately 30 kilometers south of Reno (Figure 1). The total area of the watershed is about 220 sq. km., with the valley occupying about 75 sq. km. During most years, Washoe Lake occupies about one fourth of the valley floor. At full stand, the elevation of Washoe Lake is 1533 meters above mean sea level (AMSL). Bathymetric data indicate the maximum depth of the lake is on the order of 3 to 4 meters (Tabor et al. 1983). The size and position of Washoe Lake has probably varied considerably during its existence. During the Pleistocene, it was much larger than it is now, with a depth of approximately 12 meters. (Tabor et al. 1983).

Natural recharge to Washoe Valley is primarily from runoff of snowmelt from the Carson range, and from intermittent precipitation on Washoe Lake and the valley floor over the entire year. The primary controls on the distribution of precipitation are climatic and orographic. The Carson range is higher in elevation and receives more snow fall. Additionally, the catchment area to the west is much greater. The Virginia range is much lower in elevation and smaller in area, and lies in the rain shadow of the Carson range. Such an imbalance of recharge (>90% from the west) is atypical of Basin and Range valleys farther to the east. The recharge from direct precipitation on the lake and the valley floor are seasonal, and on an annual basis, losses from these surfaces due to evaporation and evapotranspiration are three to four greater than recharge from precipitation.

The only surface discharge from the basin floor is from Little Washoe Lake into Steamboat Creek near Washoe City on the north at an elevation of about 1534 meters AMSL. Because this is slightly above maximum lake stage, outflow is intermittent, and in average years is an insignificant component in the water budget of the valley. Thus, most of the discharge is in the form of evapotranspiration from the valley floor and evaporation from Washoe Lake. Rush estimated consumptive use in 1965 to total only about 600 to 1000 m³/d for a population probably less than 250 households. Thus, 1965 is a reasonable representation of pre-development conditions. McKay (1991) estimates present consumptive use of at least 3500 m³/d for approximately 1000 households.

PREVIOUS WORK

Rush (1967) first summarized the general hydrology and water budget of Washoe Valley. He used the Maxey-Eakin formula, which relates greater precipitation to higher elevation, to derive estimates for annual recharge contributions from the various creeks feeding Washoe Valley from the Carson and Virginia ranges. According to his estimates, 96 percent of the recharge comes from the west, and only about 4 percent from the east. Of the recharge from the west, approximately half comes from Franktown Creek, and approximately half of the recharge from the east is from Jumbo Creek. He further summarized water level data, constructed a potentiometric surface map, tabulated specific capacity test data from wells where it was available, and estimated the amount of water in storage in the subsurface of Washoe Valley. These water level data are used here to reconstruct the potentiometric surface map for calibration of the groundwater model. His specific capacity data are used to help estimate the areal distribution of hydraulic properties in the model. He concluded that little, if any, of the surface water

recharge reaches the groundwater system in normal years. Rather, most of it flows directly into Washoe Lake where it is lost to evaporation during the summer months. Additionally, there is a large component of evapotranspiration from vegetated areas of the valley floor, particularly on the west side where the water level is normally within a few meters of the surface.

Although Tabor et al. (1983) were primarily interested in determining the seismic hazards of the valley, they also examined the overall basin configuration and made depth to bedrock estimates from seismic refraction data in the vicinity of New Washoe City. The bedrock depths provide a key constraint for magnetic modeling. Their report contains an extensive description of the geology and geologic history of Washoe Valley and the surrounding area.

Arteaga and Nichols (1984) used more extensive data on areal distribution of rainfall to modify Rush's recharge estimates, made more detailed estimates of evapotranspiration based on vegetation types, and further broke down the recharge and discharge data on a monthly basis. This helped to illustrate the temporal nature of the water balance, with recharge from snowmelt occurring in the spring and evaporation and evapotranspiration losses becoming more dominant as the summer progressed. They concluded that a delicate balance exists between inflow and outflow, with that balance being reflected largely in the level of Washoe Lake. In normal years, the volume of Washoe Lake (about 85,000 cubic meters) is approximately equal to the annual recharge/discharge to the valley.

McKay (1991) studied the groundwater quality of New Washoe City and additionally provided more detailed hydrostratigraphic information from local water wells. He found that water levels in the vicinity of New Washoe City have declined significantly since the beginning of the current drought period beginning in about 1987.

Karlin et al. (1993) provide areal distributions of sediment facies based on the results from five holes drilled on the dry bed of Washoe Lake between December of 1991 and August of 1992. They found significant differences in the spatial distribution of sediments in the drill cores. These differences are used here to help calibrate the magnetic and electromagnetic results.

GEOPHYSICS

Applications to Groundwater Investigations

The following discussions of the geophysical methods used in this work are oriented towards hydrogeologic applications. For the reader who is interested in further examining basic theory, introductory textbooks in geophysics such as Dobrin and Savit (1988) or Robinson and Coruh (1988) are highly recommended for discussions of the underlying principles of the gravity, magnetic and resistivity methods. Electromagnetic techniques, which measure conductivity (the reciprocal of resistivity) are relatively new, and good discussions have for the most part not yet found their way into textbooks. However, excellent discussions are available in several commercial publications (e.g. McNeill 1980b,c)

To be effective, all geophysical methods must be able to detect and map contrasts in physical properties between various earth materials. Ranges of physical properties of earth materials vary widely; from less than an order of magnitude for density contrasts to several orders of magnitude for magnetic properties (magnetization and susceptibility), and up to 15 orders of magnitude for resistivities. Gravity, magnetic (ground or aero-), and electrical resistivity or electromagnetic surveys are used to map each of these properties respectively. Instrumentation, field procedures, and data reduction techniques for all of these methods have been highly developed, primarily by the mineral and petroleum exploration industries. In the

short time since personal computers have come into common use, excellent data modeling and interpretation packages for these platforms have become readily available.

Physical property contrasts, mappable by these geophysical methods, occur in most hydrogeologic settings. Often more than one method is useful for a particular area or problem. Additional methods can substantiate the results of the original method, or different methods can be used to map other diagnostic properties.

For hydrogeologic applications, the physical property contrasts most often of interest is that between fine-grained sediments, primarily clays and silts, which form aquicludes or aquitards, and more coarse-grained sands and gravels which form aquifers. As discussed below, electrical resistivity and electromagnetic methods are the most definitive in mapping these contrasts. Neither gravity nor magnetics is particularly useful in such environments because significant density and magnetic contrasts seldom exist between these two sediment types. However, both density and magnetic contrasts can be used to map overall basin configuration when bedrock is both dense and magnetic, which it often is. Additionally, magnetics can be used to map magnetic units (e.g. volcanic flows) within an otherwise non-magnetic stratigraphic section.

The application of gravity surveys to groundwater investigations depends on the presence of density contrasts between saturated alluvial fill and bedrock. Typical density ranges are about 2.65 to 2.75 g/cm³ for bedrock and 2.1 to 2.4 g/cm³ for alluvial basin fill. Thus, density contrasts between basin fill and bedrock typically are on the order of 0.5 g/cm³, while those between different sediment are usually much smaller, on the order of 0.1 g/cm³ or less. The use of gravity data in groundwater models is well documented, particularly for the Basin and Range. Thomas et.al. (1989) and Burby and Prudic (1991) used gravity measurements to determine overall

basin configuration and made depth-to-bedrock interpretations to constrain transmissivity estimates. The contact between the aluvial basin fill and bedrock establishes the no-flow boundary in groundwater models.

Gravity surveying is probably the coarsest of all geophysical methods. However, gravity surveys are relatively inexpensive and easy to run. The resultant profiles usually mimic the configuration of the sediment-bedrock contact fairly closely, making first order interpretation very straightforward. Additionally, a large, easily accessible, public domain data base exists for the entire United States. One drawback, although not usually serious, is that densities of geologic units involved must often be estimated. However, the relatively narrow range densities for each rock type usually allows adequate estimates for modeling purposes. A more serious drawback is that interpreted models are non-unique, and other information is usually necessary to limit model alternatives.

The utility of the magnetic method lies in the fact that several rock types including volcanics, metamorphics, mafics, and granitic intrusives exhibit magnetic signatures. Except for volcanics, all of these commonly occur as bedrock. Thus, magnetics is often used in much the same manner as gravity to map overall bedrock configuration. When both gravity and magnetic data are available from an area, interpretations are often greatly improved by jointly modeling the two data sets to mutually constrain the range of possible solutions.

One advantages of the magnetic method is that airborne surveys can cover large areas very rapidly to map magnetic bedrock configuration. Also, corrections to the data are relatively few and simple. Disadvantages are the potentially higher costs, particularly of airborne surveys, and generally greater complexity of interpretation due to the dipolar nature of the Earth's field and the existence of different types of

magnetization. Moreover, remanent magnetization may not be aligned with the present day field.

Volcanic rocks are perhaps unique in that they exhibit the widest ranges of density, magnetization, and electrical resistivity of any single rock type. Furthermore, volcanic flows can lie anywhere within the stratigraphic section. Thus, interpretation of geophysical data where volcanic rocks are present can be quite complex. Tuffaceous rocks are often non-magnetic and usually very light, having densities comparable to sediments, or even less. Mafic volcanics can be very dense and highly magnetic, but may also exhibit relatively low magnetic signatures due to alteration. Electrically, tuffs can be highly conductive, as can be the clays which are often their alteration products. More mafic volcanics will usually be relatively resistive, particularly with respect to basin-fill sediments. Extrusive volcanics are usually magnetic, particularly those of more mafic composition.

When non-magnetic volcanic units lie within a stratigraphic section which is primarily alluvial, and thus also non-magnetic, it will normally not be possible to detect them with a magnetic survey. Such situations can be important in hydrogeological investigations because volcanics usually have significantly different hydraulic properties than the surrounding sediments. Unless they are fractured, volcanics will usually exhibit low transmissivities relative to the neighboring alluvium.

Relationships between electrical resistivity and hydraulic conductivity are well developed (Kelly and Reiter 1984, Mazac, et al. 1990, Urish 1981). Applications of electrical and electromagnetic methods to groundwater problems are relatively common. Electrical resistivity is probably the most diagnostic method for mapping interbasin variations in hydraulic properties due to the fact that saturated clays are ionic conductors, and thus highly conductive relative to saturated sands and gravels.

A commonly held misconception is that aquifers will appear as conductivity highs (resistivity lows) because water is such a good conductor. In reality, saturated aquifers are only good conductors relative to dry rocks and/or certain other rock types, but they are still poor conductors relative to saturated clays. Thus, in alluvial aquifers, high resistivities can almost always be interpreted to be reflecting more coarse-grained aquifer materials and low resistivities can be interpreted to be reflecting finer grained aquitards.

Which factors control the resistivity of a rock? While there are many, the two which are probably most applicable to groundwater investigations are water quality and degree of saturation. In general, electrical conductivity increases directly with degree of saturation and inversely with water quality. Two tacit assumptions almost always made in resistivity interpretations are that the water quality is the same in all formations, and that all formations (at least below the water table) are fully saturated. Thus any changes in resistivity are due to changes in lithology only. Frequent causes of conductive groundwater are high natural salinity and/or man-made pollutants. These assumptions probably hold in Washoe Valley, where the salinity is known to be unusually low for a closed basin (Lyons, 1993, pers. comm.) and any effects of anthropogenic nitrates on groundwater resistivity are likely to be minimal due to their relatively low electrical conductivity (McNeill, 1980a).

Tables of ranges of resistivities for the various earth materials are available in a number of sources (e.g. Palacky, 1990). Within any particular alluvial environment, the range of resistivities is likely to be relatively small, usually from about 5 to 50 ohm-meters. Resistivities of 5 to 10 ohm-meters will almost always reflect a unit which is predominantly clay, assuming the pore water is not saline. In most alluvial environments, resistivities from 10 to about 50 ohm-meters represent increasing amounts of coarser-grained sediments, with resistivities greater than 50 ohm-meters

reflecting predominantly coarse-grained sediments. Bedrock resistivities are typically much higher, with values in the low hundreds of ohm-meters.

Based on extensive field and laboratory measurements, several authors (Kelly and Reiter, 1984 , Mazac, et al., 1990, Urish, 1981) have developed equations of the following general form relating hydraulic conductivity to electrical resistivity:

$$K = a\rho^n$$

where:

K = hydraulic conductivity expressed in units of L/t

a = a proportionality constant which is a function of the particular earth materials involved and the system of units

ρ = the apparent resistivity, usually expressed in Ω-meters, and

n = an experimentally determined value ranging from 1 to 2.

Values of **n** and **a** are normally determined graphically from measurements on a specific suite of samples, with **n** being the slope and **a** being the x-intercept on a log-log plot. Researchers have typically attempted to relate values of **n** and **a** to site-specific or formation-specific characteristics such as porosity, degree of fracturing, or degree of saturation (Kelly and Reiter, 1984, Mazac, et al., 1990).

The electromagnetic measurements of this study were made with an EM-34 terrain conductivity meter. In recent years, due largely to the development of more sophisticated electronics and software interpretation routines, electromagnetic induction measurements have been replacing galvanic (ground contacting) resistivity measurements as the preferred means of obtaining resistivity data. The capability of electromagnetic methods to obtain measurements without ground contact offers significant improvements in survey efficiency in most situations. The EM-34 is called a terrain conductivity meter because it measures the conductivity of the ground, not the resistivity. This can be confusing since historically resistivity, not conductivity,

has been measured. Resistivity and conductivity are inversely related by $\sigma\rho = 1000$, where σ is the conductivity of the material and ρ is its resistivity. Thus, either quantity can be obtained from the other simply by dividing into 1000.

Electromagnetic induction systems consist of a transmitter which generates a primary magnetic field in a loop or coil. This magnetic field induces an electric current in the ground, which in turn regenerates a secondary magnetic field which is sensed by the receiver coil. The strength of the received signal is a function of the subsurface distribution of resistivities, the configuration of the transmitter and receiver coils, and the frequency of the signal.

Methods

Gravity data were collected with a LaCoste and Romberg Model G gravimeter. On the lakebed, gravity stations were occupied at nominal spacings of either 120 or 240 meters along a north-south base line and two east-west cross lines. Several regional stations were taken at points locatable on the 7 1/2 minute topographic maps of the area (Washoe City, Carson City). Gravity readings were taken at wider intervals than magnetic readings because they are much less sensitive to shallow variations and take more time than magnetic readings. Pre-established base stations were frequently re-occupied to allow drift corrections to be made (Appendix A). Free air, Bouguer, latitude, and terrain corrections were applied to reduce the data to complete Bouguer anomaly values (Appendix B). These data were subsequently merged with approximately 200 regional stations (Saltus, 1988). Figure 3 is the gravity station location map. Data quality for most of the gravity stations was excellent, particularly for those with GPS elevation control. Because the lakebed was so flat, a few gravity stations were taken without GPS elevation control. Elevations for these stations were interpolated from stations which had control.

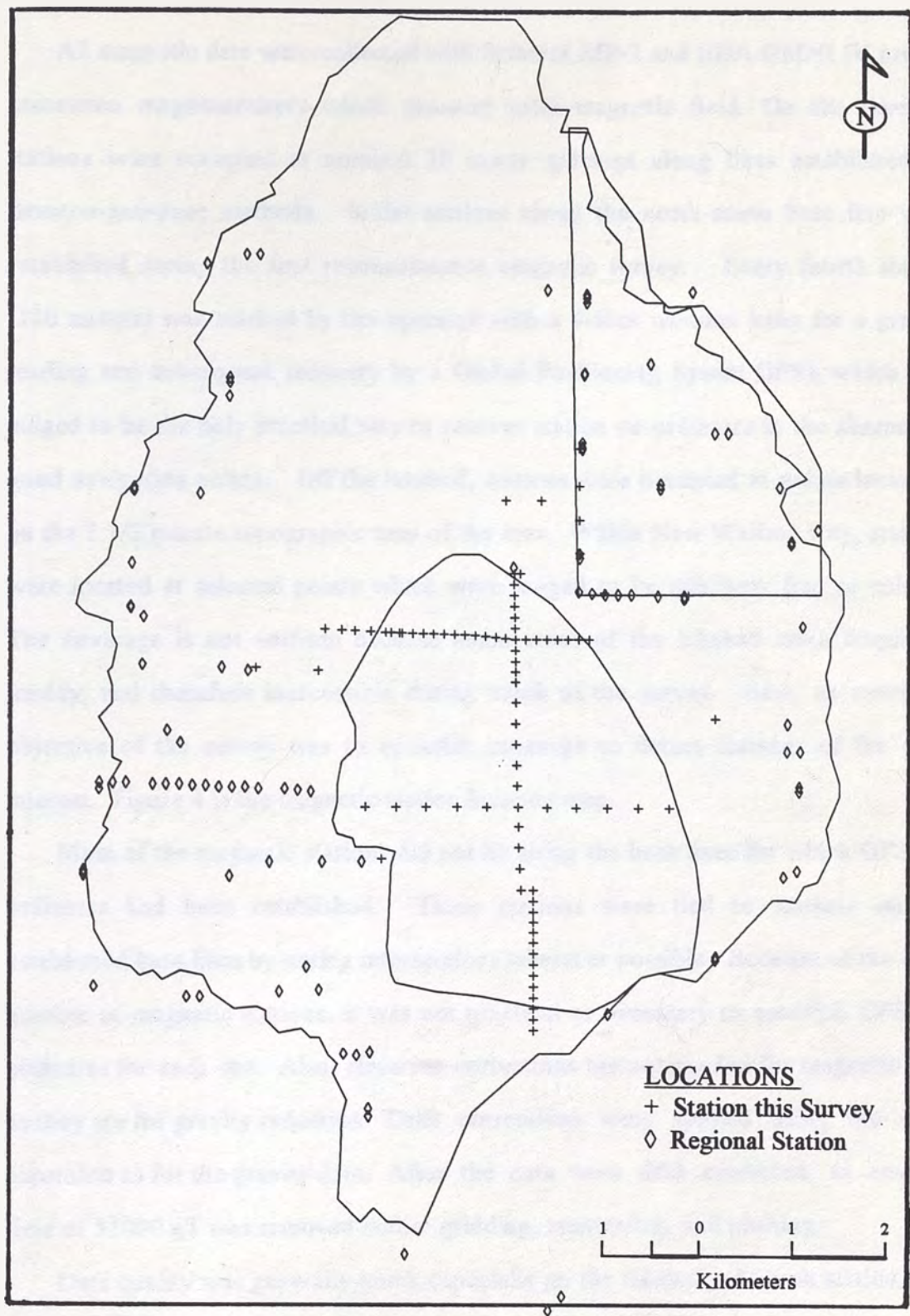


Figure 3. Gravity Station Locations.

All magnetic data were collected with Scintrex MP-2 and EDA OMNI IV proton precession magnetometers which measure total magnetic field. On the lakebed, stations were occupied at nominal 30 meter spacings along lines established by Brunton-and-pace methods. Initial stations along the north-south base line were established during the first reconnaissance magnetic survey. Every fourth station (120 meters) was marked by the operator with a 4-foot wooden lathe for a gravity reading and subsequent recovery by a Global Positioning System (GPS), which was judged to be the only practical way to recover station co-ordinates in the absence of good navigation points. Off the lakebed, stations were occupied at points locatable on the 7 1/2 minute topographic map of the area. Within New Washoe City, stations were located at selected points which were judged to be relatively free of culture. The coverage is not uniform because some areas of the lakebed were frequently muddy, and therefore inaccessible during much of the survey. Also, an overriding objective of the survey was to optimize coverage to detect features of the most interest. Figure 4 is the magnetic station location map.

Most of the magnetic stations did not lie along the base lines for which GPS co-ordinates had been established. These stations were tied to stations on the established base lines by noting intersections wherever possible. Because of the large number of magnetic stations, it was not practical or necessary to establish GPS co-ordinates for each one. Also, elevation corrections are not needed for magnetic data as they are for gravity reduction. Drift corrections were applied using the same algorithm as for the gravity data. After the data were drift corrected, an ambient field of 51000 nT was removed before gridding, contouring, and plotting.

Data quality was generally good, especially on the lakebed. At each station, two or three readings were taken to obtain a consistent value. Most stations were within 1-2 nanoteslas (nT). Due to cultural noise, data quality for the stations located

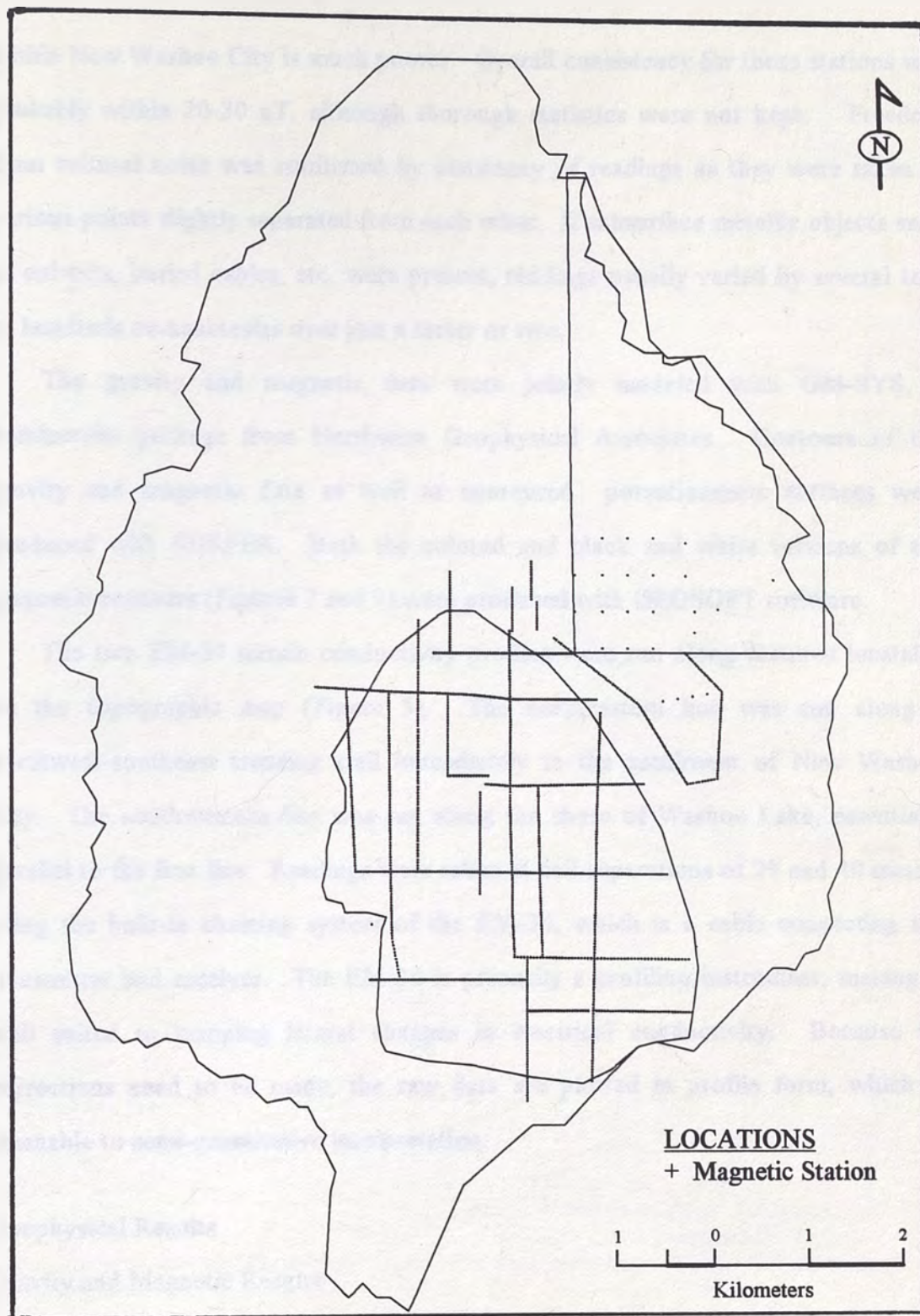


Figure 4. Magnetic Station Locations.

within New Washoe City is much poorer. Overall consistency for these stations was probably within 20-30 nT, although thorough statistics were not kept. Freedom from cultural noise was confirmed by constancy of readings as they were taken at various points slightly separated from each other. If subsurface metallic objects such as culverts, buried cables, etc. were present, readings usually varied by several tens to hundreds of nanoteslas over just a meter or two.

The gravity and magnetic data were jointly modeled with GM-SYS, a commercial package from Northwest Geophysical Associates. Contours of the gravity and magnetic data as well as contoured potentiometric surfaces were produced with SURFER. Both the colored and black and white versions of the magnetic contours (Figures 7 and 9) were produced with GEOSOFT software.

The two EM-34 terrain conductivity profiles were run along features locatable on the topographic map (Figure 5). The northeastern line was run along a northwest-southeast trending trail immediately to the southwest of New Washoe City. The southwestern line was run along the shore of Washoe Lake, essentially parallel to the first line. Readings were taken at coil separations of 20 and 40 meters using the built-in chaining system of the EM-34, which is a cable connecting the transmitter and receiver. The EM-34 is primarily a profiling instrument, making it well suited to mapping lateral changes in electrical conductivity. Because no corrections need to be made, the raw data are plotted in profile form, which is amenable to semi-quantitative interpretation.

Geophysical Results

Gravity and Magnetic Results

Figures 6 and 7 are the gravity and magnetic contour maps of Washoe Valley. The contour interval is 2 milligals (mg.) for the gravity map and 20 nanoteslas (nT)

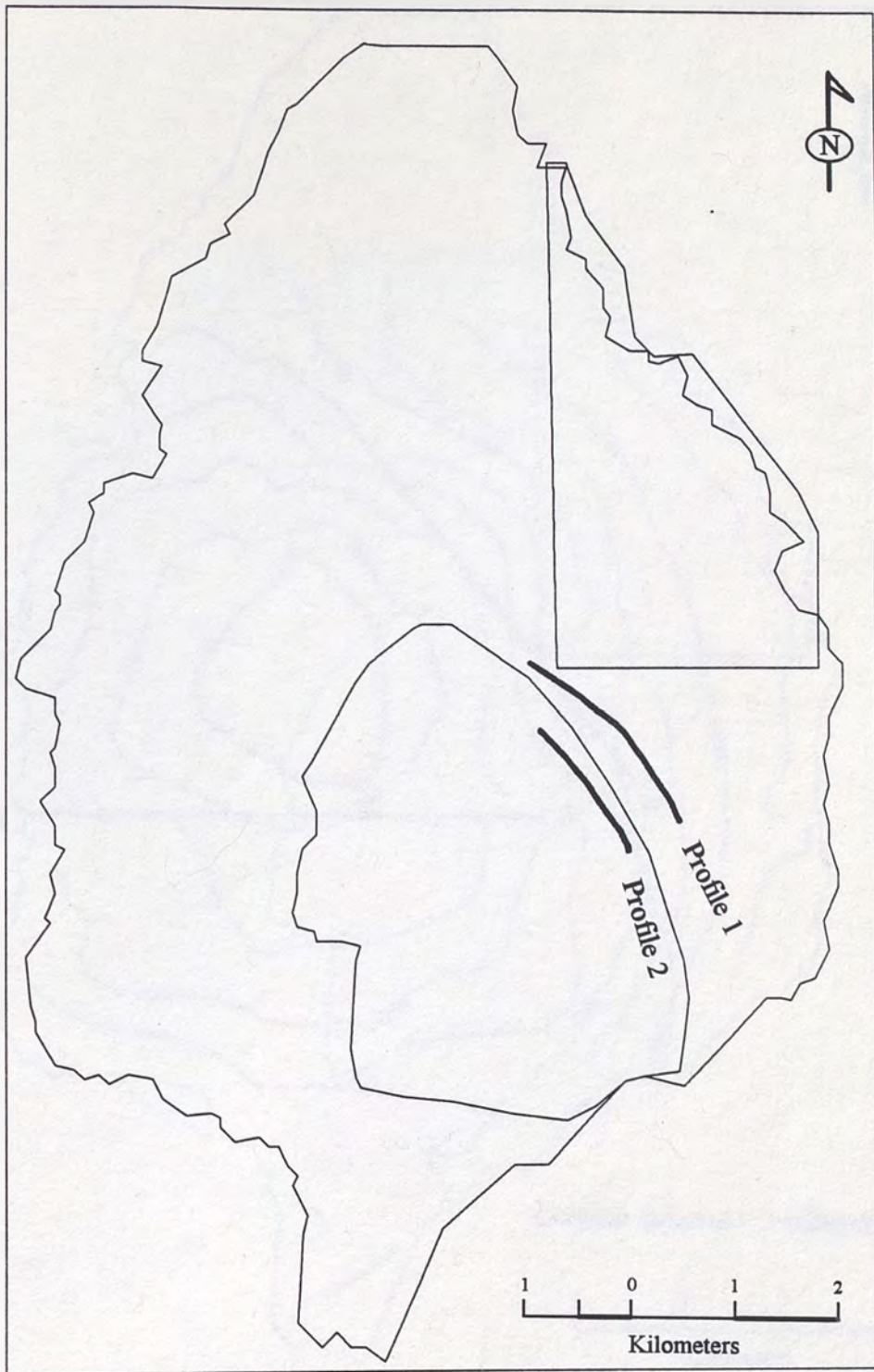


Figure 5. EM-34 Profile Locations.

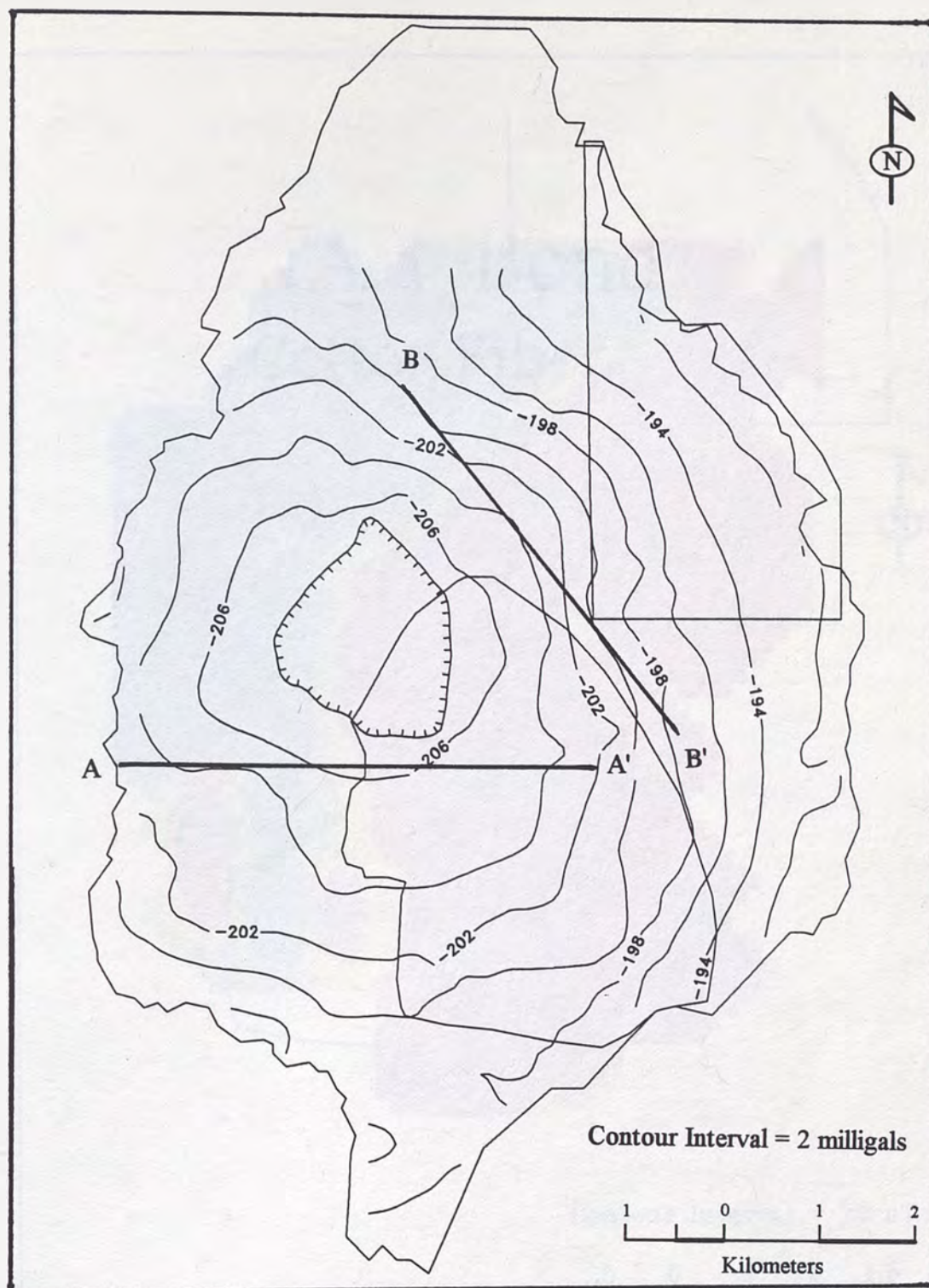


Figure 6. Gravity Contours with Interpreted Major Structures.

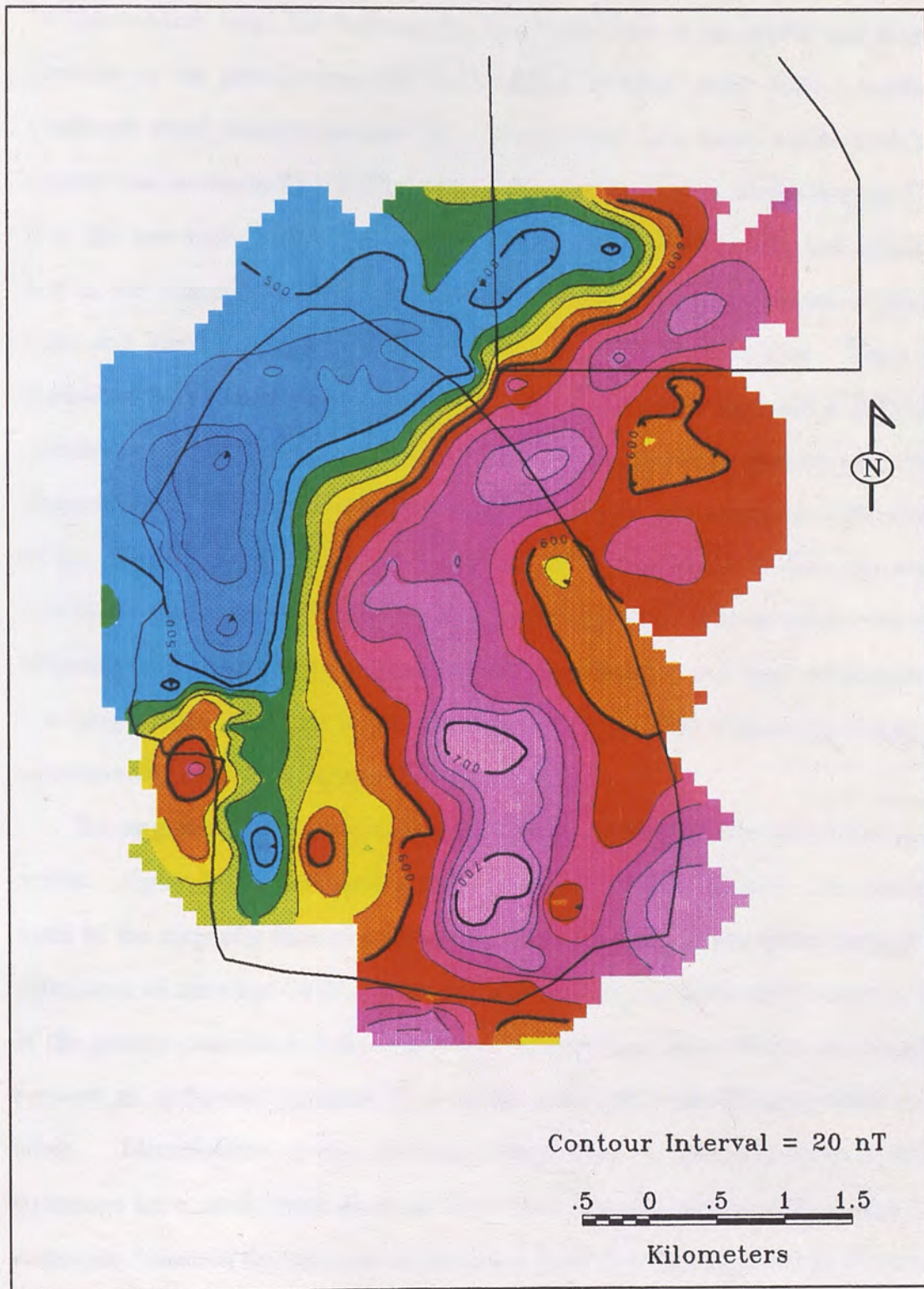


Figure 7. Magnetic Contours.

for the magnetic map. The most noteworthy feature seen in the gravity and magnetic contours is the arcuate magnetic high (Figure 7) which turns from a northeast-southwest trend beneath southern New Washoe City to a nearly north-south trend beneath the eastern half of Washoe Lake. This high appears to divide Washoe Valley into two sub-basins. The first is defined by the large (both in area and amplitude) low in the magnetic contours which lies immediately to the northwest of Washoe Lake and approximately one kilometer west of New Washoe City. There is a coincident low in the gravity contours (Figure 6), which suggests a substantial thickness of basin fill sediments. The second sub-basin is also defined by a low in the magnetic map. It is smaller and lies farther to the east, being cradled within the arc of the magnetic high. Unlike the larger low to the northwest, it does not have a coincident gravity low, rather it lies on a gravity gradient. This is interpreted to be reflecting the presence of volcanics with low density and high magnetization overlying shallow basement in the eastern subsurface. This observation is a key to understanding the hydrogeology of Washoe Valley.

The magnetic high is complex, with numerous northwest-southeast cross cutting trends. Figure 8 is a structural interpretation map of these features. An east-west trend in the magnetic data cuts across the central portion of the valley through the entire area of coverage (A-A', Figure 9) A coincident, but more subtle trend is seen in the gravity contours (A-A', Figure 6). It is interpreted to define the boundary between an upthrown structural block to the south and a downthrown block to the north. Identification of this structure is significant in that map scale east-west structures have rarely been observed in western Nevada, although they have been suspected, based on the exposure of numerous local east-west fault scarps (Cashman, 1993, pers. comm.).

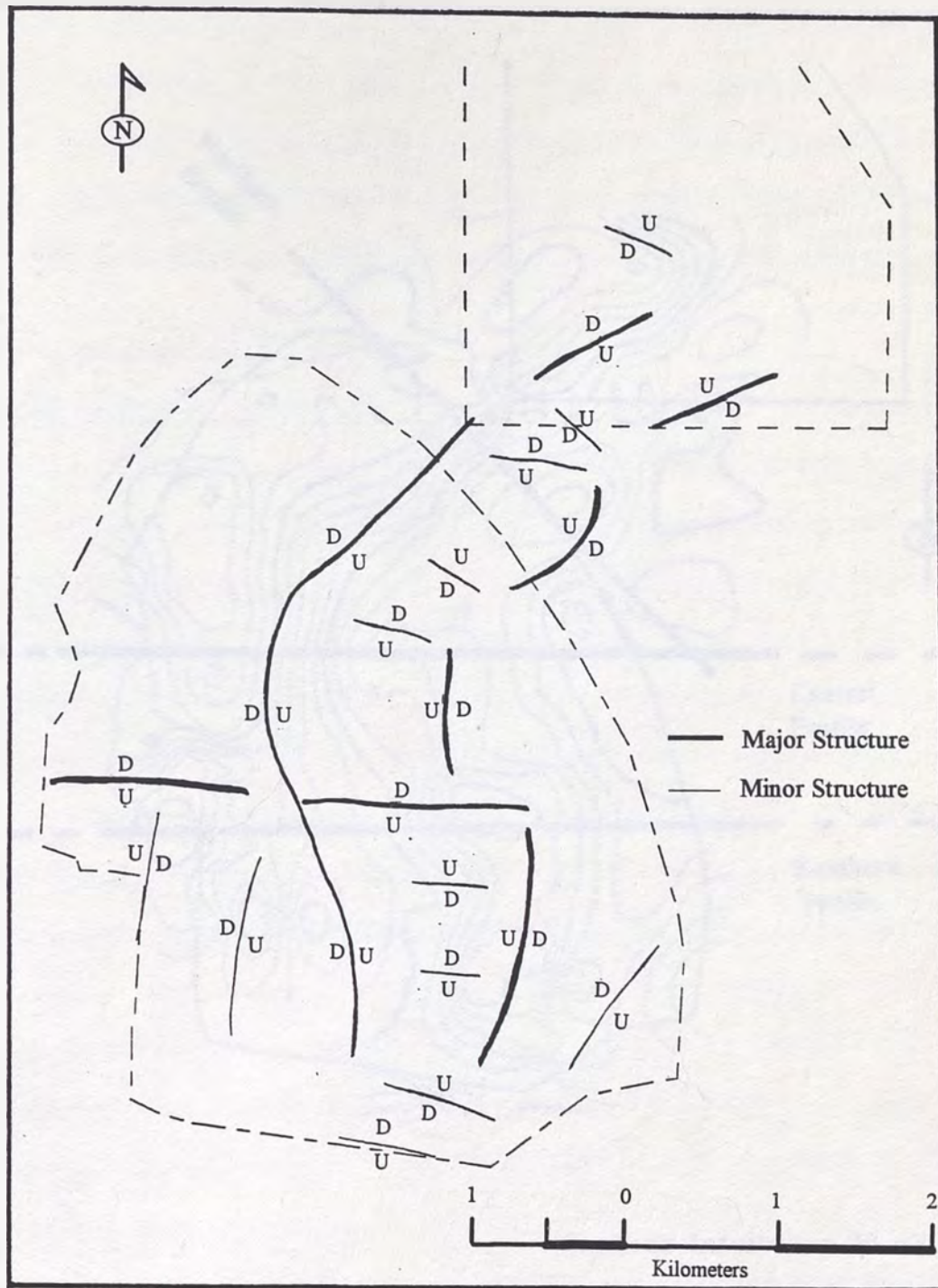


Figure 8. Structural Interpretation Map.

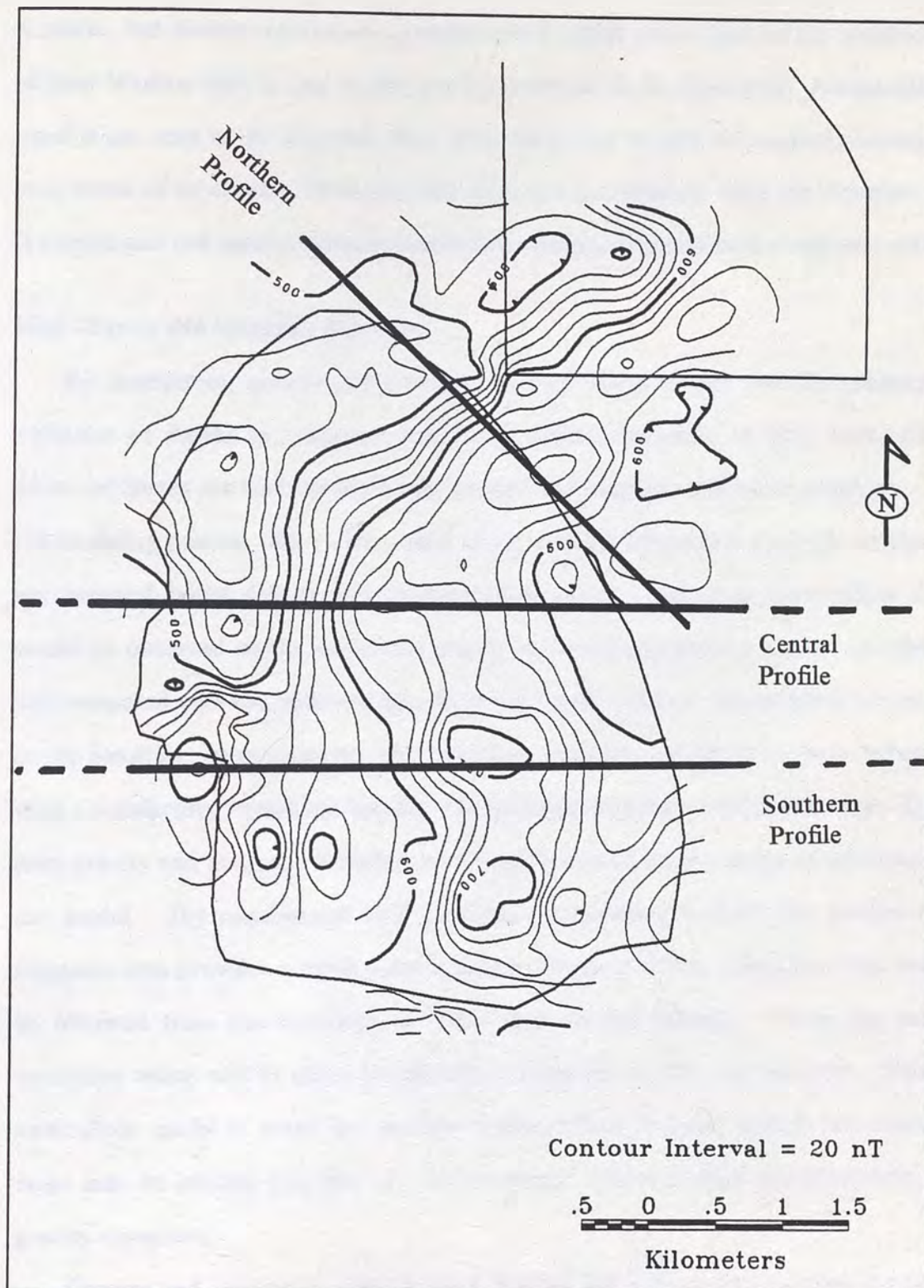


Figure 9. Magnetic Contours with Model Profile Locations.

A subtle, but definite northwest-southeast trend which passes just to the southwest of New Washoe City is seen in the gravity contours (B-B', Figure 6). A coincident trend is not seen in the magnetic data, most likely due to lack of magnetic coverage over much of its extent. However, this direction is consistent with the direction of the numerous and more prominent northwest-southeast trends in the magnetic data.

Joint Gravity and Magnetic Modeling

By themselves, gravity and magnetic contour maps do not provide quantitative estimates of depths to causative features or precise locations of their boundaries. These estimates are best obtained with gravity and magnetic modeling programs. In the modeling process, the various units of an assumed subsurface geologic structure are assigned initial density and magnetization values. The theoretical effect that would be observed on the surface by gravity and magnetic surveys is then calculated and compared with the observed data from the actual surveys. Adjustments are made in the densities, magnetizations, and boundary locations and the process is repeated until a satisfactory agreement between the field data and the model is obtained. The joint gravity and magnetic modeling significantly constrains the range of solutions to the model. The requirement that good fits be obtained to both the gravity and magnetic data provides a much more accurate definition of the subsurface than could be obtained from the modeling of either data set individually. There are many structures which will fit either the gravity or magnetic curves, but not both. This is particularly useful in areas like Washoe Valley, where features seen in the contour maps may be initially puzzling (i.e the prominent magnetic high has essentially no gravity signature).

Gravity and magnetics are modeled jointly along three cross-valley profiles, which are designated the southern, central, and northern profiles (Figure 9). The

modeled profiles are shown in Figures 10, 11, and 12 respectively. The profiles are selected to best resolve features of interest in the contour maps. Each profile model is based on an assumed two-dimensional structure. That is, all units seen on the profile are assumed to extend to infinity both into and out of the page, or plane of the profile. While this is not a totally accurate representation of true geology, it has been found to be a sufficiently accurate approximation for many geologic settings, particularly since more complex three-dimensional models are not usually practical.

Each profile shows three panels of information. The lower panel shows the assumed geologic cross section which produced the forward gravity and magnetic signatures. The fit between the gravity model curve and the observed gravity data are shown in the middle panel, and the fit between the magnetic model curve and the observed magnetic data are shown in the upper panel. For the gravity and magnetic panels, the closed circles are the data points (actually grid points from the contoured data) and the lines are the calculated effects from the assumed structure.

The model was kept as simple as possible. The same three major subsurface units are shown in each profile: 1) the granodioritic basement which has both high density and high magnetization, 2) the buried volcanic ridge which has low density but high magnetization, and 3) the basin fill sediments which have both low density and low magnetization. The granodiorite is assigned a model density of 2.67 g/cm^3 (the commonly accepted value for granitic rocks) and a magnetization of 0.001 cgs (emu/cm^3) units. The volcanic ridge is assigned a density of 2.17 g/cm^3 and a magnetization of 0.001 cgs units. The basin fill sediments are assigned a density of 2.17 g/cm^3 and a magnetization of 0.0 cgs units (non-magnetic). Thus the volcanic unit is seen to have the same low density as the sediments, but the same high magnetization as the basement rock. A density of 2.17 g/cm^3 may at first seem low for volcanics, but it is within the range of measured values of volcanic rocks in the

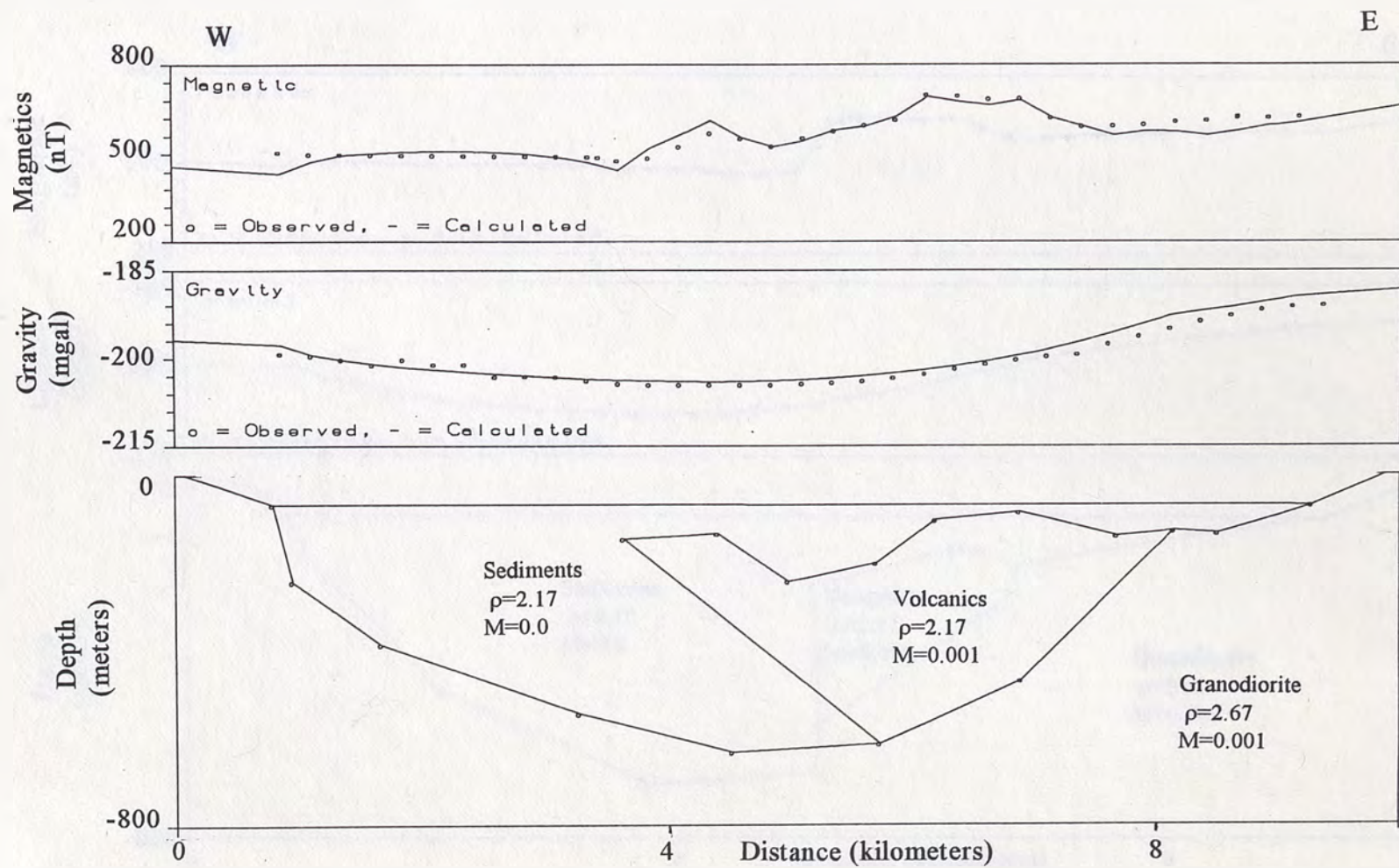


Figure 10. Southern Gravity-Magnetic Profile.

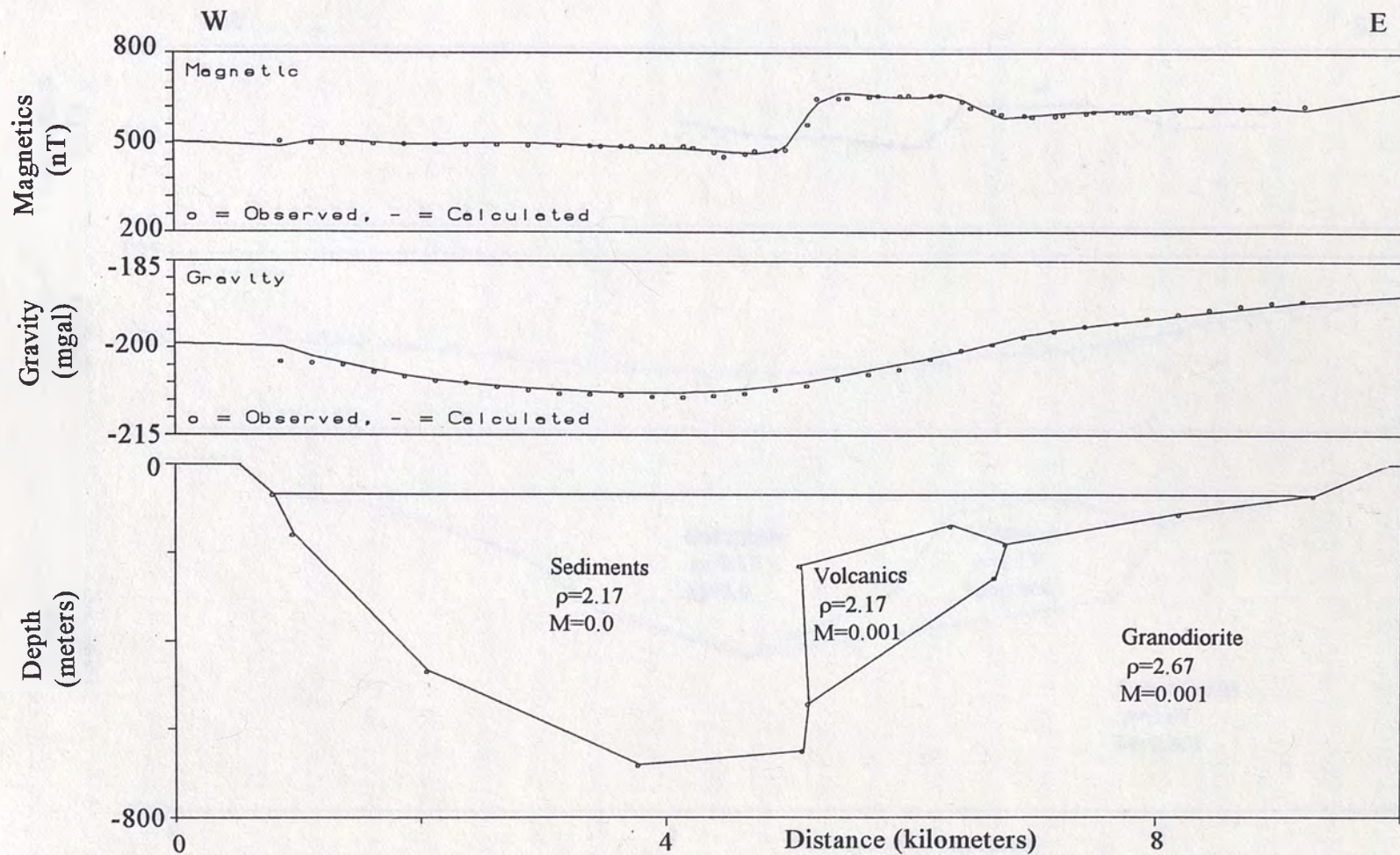


Figure 11. Central Gravity-Magnetic Profile.

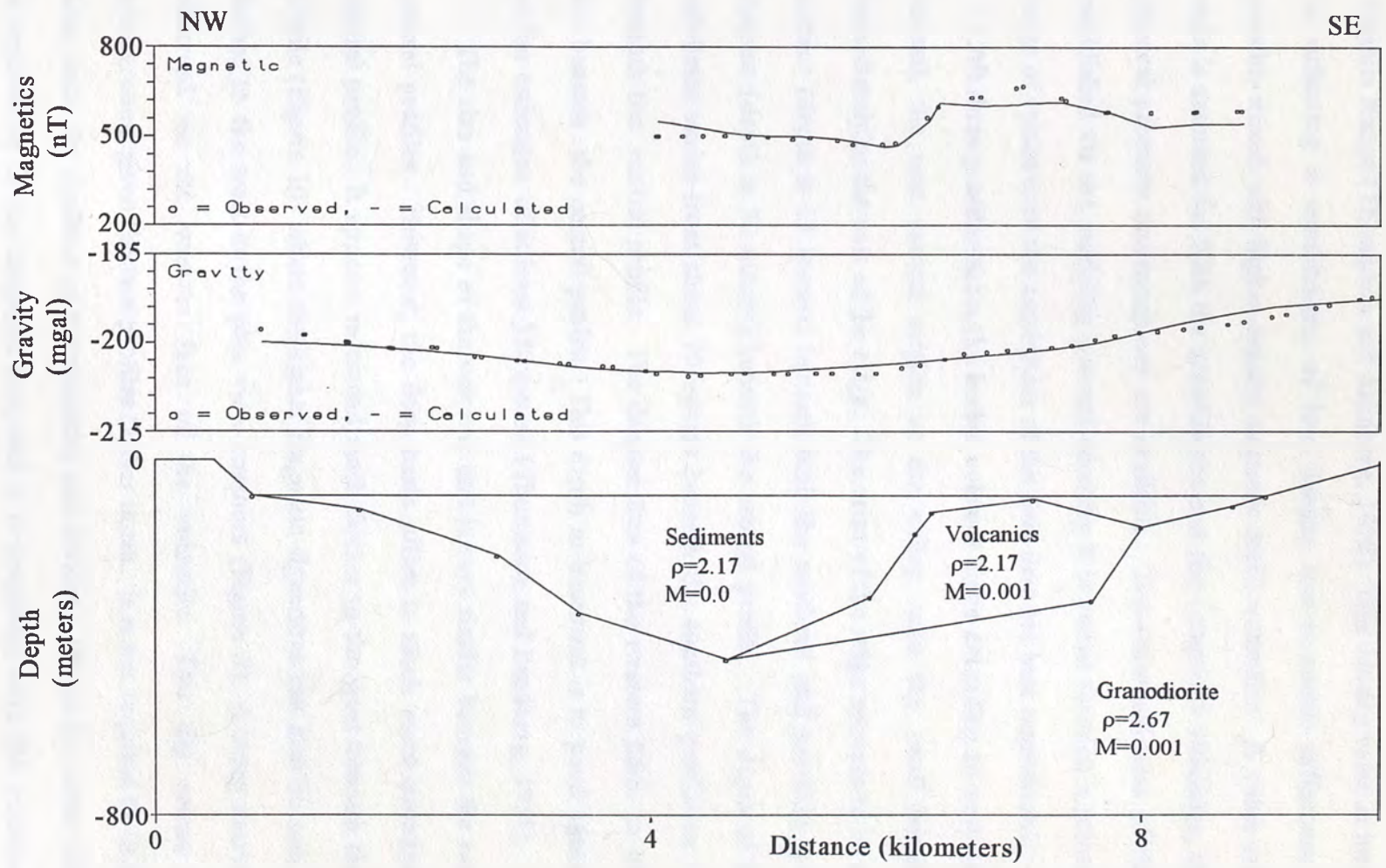


Figure 12. Northern Gravity-Magnetic Profile.

Virginia Range (Thompson and Sandberg, 1958). This density value is interpreted to be reflecting a combination of low density non-magnetic tuffaceous volcanics possibly mixed with higher density magnetic mafic volcanics. A value of 0.001 cgs units is assumed for both the granodiorite and the composite volcanics, although no physical property measurements are available. The reasonableness of this value is established via the modeling process whereby it is varied through a somewhat small range of values until the amplitudes of the field data are best reproduced.

All three profiles show the buried volcanic ridge extending to very near surface beneath the east central section of the valley, with the small sub-basin lying immediately to the east of the ridge. The crest of the ridge appears to lie nearest the surface (depth \cong 15 meters) beneath both the northern and southern profiles, and deepest (depth \cong 70 meters) beneath the central profile. The depth of the eastern sub-basin varies from about 70 meters beneath the southern profile to 110 meters beneath the central profile. The deepest axis of the western basin (\cong 600 meters) lies beneath the central profile. This depth to basement is in good agreement with earlier estimates of at least 550 meters (Thompson and Sandberg, 1958).

The size and shape of the volcanic unit is very similar beneath the northern and central profiles. However, the deep basin offset is much more prominent on the central profile. It appears to extend much farther to the west beneath the southern profile (Figure 10) where the higher magnetic signatures can also be seen to extend farther to the west in the plan view contours (Figure 7). A steep eastward dip is observed on the western face of the volcanics. This dip seems somewhat incongruous, given the two profiles farther north. It is not required to fit the gravity data, since the densities of the volcanics and the basin fill are the same. However, it is required to fit the magnetic data, and it is consistent with the presumed rotated half-graben structure of the basin.

The source of the magnetic high is assumed to be the mid Miocene Kate Peak andesite, which erupted approximately 12 million years ago near the end of the period of most rapid Basin and Range extension (Profett, 1977). This assumption is based on the following observations. First, the northeast trending limb of the subsurface magnetic high (Figure 7) trends toward Jumbo Peak (Figure 2), which is mapped by Tabor, et al. (1976) as Kate Peak formation, and hand drill core samples from Jumbo Peak exhibited high magnetization. Second, the fact that the unit exhibits a magnetic high suggests that it is unaltered. According to Whitebread (1976), the Kate Peak exposed in the Virginia range is essentially unaltered, whereas the Alta formation, the next higher volcanic unit in the stratigraphic sequence, is extensively altered, and should be less magnetic. Whitebread also mapped other volcanic units lower in the stratigraphic sequence in the Virginia range, but from the present data, it cannot be ascertained with certainty whether or not they might underlie the Kate Peak in the subsurface of eastern Washoe Lake.

The gravity model is complicated by the location of Washoe Valley at the transition of the Sierra Nevada batholith to the west and the Basin and Range province to the east. Thompson and Sandberg observe the lowest point in their regional gravity map to lie along the eastern edge of the Carson range, and not beneath the crest of the Sierras, as would be expected if isostatic equilibrium was being maintained. Thus they interpret a regional gravity gradient of approximately 8 milligals across Washoe Valley, with the high to the east. In this model, a deeper density contrast of about $+0.12 \text{ g/cm}^3$ beneath the western half of the model and $+0.20 \text{ g/cm}^3$ beneath the eastern half were needed to compensate for the regional gradient. These density differences likely reflect the relative densities of granitic and mafic rocks which are more prevalent in the deeper western and eastern subsurfaces respectively (Thompson and Sandberg 1958). It is further noted that this gradient

was adequately modeled using density contrasts within the upper 5 km. of the crust only. It was not possible to match the gradient when using a crustal model of approximately 40 km. thickness beneath the Sierras and 29 to 33 km. beneath the Basin and Range, as proposed by Martinelli (1989).

While the thickness of Washoe Valley which is obtained from gravity models is a function of the density chosen for the sediments, the effects of the regional structures discussed above have a much greater impact on the modeled depths and the overall basin geometry. Fortunately, these uncertainties are not particularly detrimental to the groundwater model. First, magnetic modeling provides additional constraints on basin geometry, particularly beneath the eastern subsurface. Secondly, because a two-layer quasi-three-dimensional groundwater model is being used, only transmissivities need be specified for the confined aquifer. Thicknesses, and thus exact depths, are not specifically required. Errors in estimating the basin depth from the gravity model are probably at most on the order of 20 to 30%. These are likely small relative to errors in estimating hydraulic conductivity of the basin fill.

Electrical Conductivity Survey

The limited number of resistivities measured at Washoe Lake range from about 20 to 50 ohm-meters, which is typical of sedimentary environments. It was assumed that the pore water is of the same quality (resistivity) everywhere and that no saline water is present because the observed resistivities are too high. Moreover, Washoe Lake is somewhat anomalous for a closed basin lake in that its waters appear to be non-saline (Lyons, pers. comm. 1993). If saline waters were present in any significant concentration, observed resistivities would likely be well below 10 ohm-meters. The fact that Washoe Lake appears to be so non-saline suggests a much larger

throughflow (flushing) of water than can be accounted for by presently observed discharges. Flow along deep fractures or faults may be one explanation.

The key to interpreting the conductivity data lies in noting the difference in sediment character between Paleoclimate drill holes 2 and 3 (Figure 13) in terms of their positions relative to the magnetic high (Figure 7). Both holes were drilled to depths of approximately 25 meters. Through most of their depth range, drill hole 3, which lies directly above the magnetic high, contains a higher ratio of fine-grained sediments than drill hole 2, which lies over the magnetic low some 1400 meters to the north. Is this apparent difference in shallow depositional character more than just a spatial coincidence, or is it somehow related to the deeper magnetic feature? A conductivity profile between the two drill holes should be able to answer this question, since the fine-grained sediments to the south should be more electrically conductive. Unfortunately, by the time this correlation was recognized, Washoe Lake had refilled, making it impossible to run a profile between the two drill holes. However, the trend of the magnetic high was observed to continue to the northeast beneath dry ground in the vicinity of New Washoe City, where the two parallel EM-34 profiles (Figure 5) were occupied perpendicular to the magnetic trend to map differences in electrical conductivity across it.

Figure 14 shows a clear spatial relationship of the conductivity high with the magnetic high for the northeastern profile. The penetration depth of the EM-34 is approximately 30 meters, which is also roughly the depth of drill holes 2 and 3. Thus, the conductivity high is interpreted to be reflecting the presence of fine grained sediments lying above the volcanics. This strongly suggests that shallower depositional patterns may be controlled by deeper structures in the subsurface of Washoe Valley. Although it is not shown, a similar conductivity high was observed on the southwestern profile.

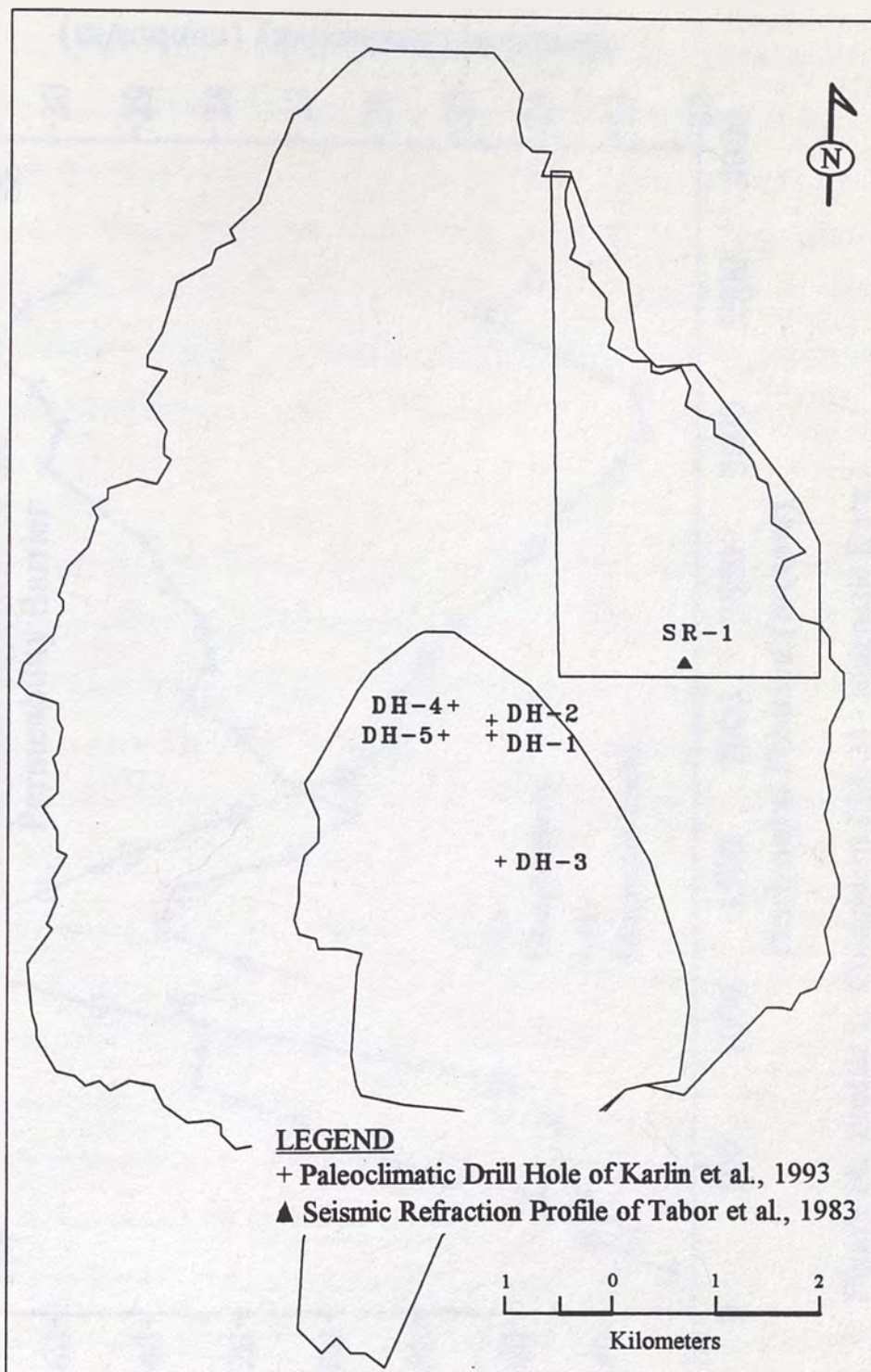


Figure 13. Location of Paleoclimate Drill Holes.

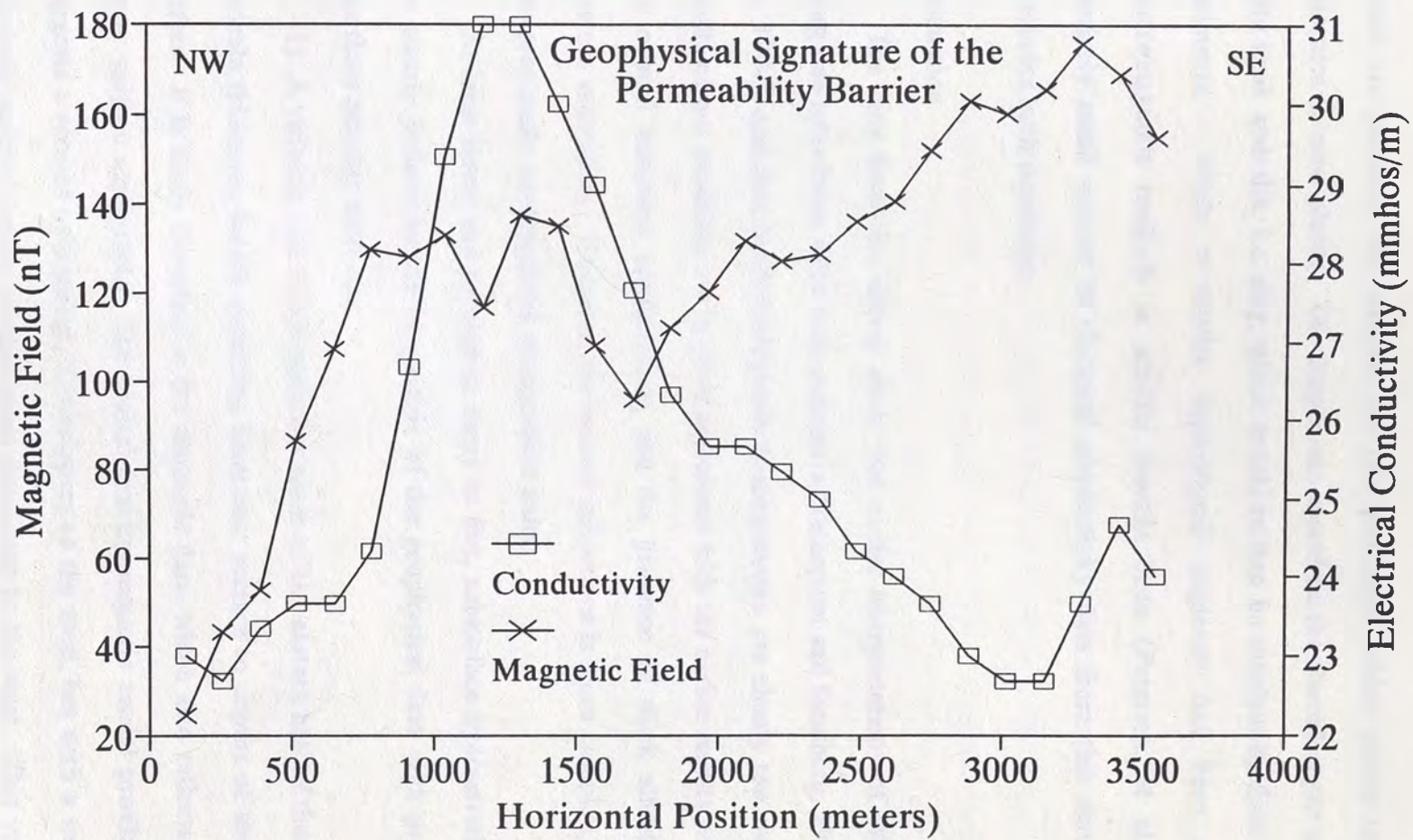


Figure 14. Profile 1: Coincident EM-34 - Magnetic Data.

There are possibly two sources for this conductor which seems to overlie the volcanics in most places. The deeper one would be the altered upper section of the Kate Peak andesite, i.e. clay, which would in turn be overlain by finer grained lake sediments. While a similar depositional sequence has been resolved by electromagnetic methods in another Nevada basin (Petersen, et al. 1989), the relatively small amount of electrical conductivity data from this survey presently precludes such resolution.

Discussion

The data from this survey show that earlier interpretations of Washoe Valley being one large basin filled with sediments (Thompson and Sandberg, 1958, Tabor, et al., 1984), and thus hydrogeologically homogeneous, are clearly too simplistic. The results of our modeling are in good agreement with the earlier results with respect to the overall basement configuration and the presence of thick alluvial fill in the western subsurface. However, the eastern subsurface is more complex, with at least two previously unrecognized stratigraphic units.

At least three, and perhaps as many as five, subsurface hydrostratigraphic units are clearly defined by the integration of the geophysical data with previous work. The three primary units are:

- 1) A volcanic unit which underlies much of the eastern half of the basin. It has variable thickness, locally extending from near surface to depths of several hundred meters. It is easily identified in the magnetic data, which also reflects the irregular upper surface topography. The central gravity-magnetic model profile (Figure 11) suggests a rotated half-graben, downsloping to the west, but with a western margin relatively uplifted before another steep downdrop to the west. This volcanic unit is interpreted to have a relatively low transmissivity, based on data from other studies

and requirements of the groundwater model. Initial estimates of transmissivity (1-3 meters/day) are based on similar values for volcanics of the Alta formation in a groundwater model of the Spanish Springs Valley (Hadiaris, 1988). She attributed the observed transmissivities mostly to fracture porosity, and the same mechanism is assumed for this model.

2) A fine-grained unit which locally overlies the volcanics. Where present, it is distinctly identified as a unit of low electrical resistivity (20-30 ohm-meters), and thus fine grain size and low transmissivity. Thickness estimates are constrained by the magnetic modeling of this survey and the seismic refraction results of Tabor et al. (1983). This is interpreted to be the same fine-grained unit logged in drill hole 3, which is located over the magnetic high.

3) The third unit is primarily coarse-grained valley fill to the west, but may consist of two or three sub-units. It is most readily identified spatially as correlating with the large gravity and magnetic lows to the west and northwest. Near the range front to the far west, well logs and high measured transmissivities suggest that relatively coarse-grained alluvial fan materials interfinger to the east with finer-grained lake sediments. In drill holes 1 and 2 (Figure 13), medium to coarse-grained sediments were encountered from surface to depths of approximately 25 meters. In drill holes 4 and 5 to the west and northwest, mostly coarse sands were encountered to depths of 10-12 meters, before they were abandoned due to sand heave. While it is unlikely that sand of this purity persists through the entire depth section, it does indicate that coarser-grained materials may be widespread and make up a large portion of the unconfined aquifer in this region.

Rush (1967) discusses the presence of an extensive confining layer at a depth of approximately 30 meters in most of the western subsurface, although well logs suggest that it may be locally absent. Based on the evidence from drill hole 1 and the

Rasmussen flowing well about two kilometers to the west, it may be only 2-3 meters thick. It is problematic as to whether or not this confining unit extends to the east. Electrically, one would expect it to be a conductor, but it appears to be too thin to resolve, particularly to the east where it would be expected to blend with the other conductive materials.

The deeper, confined western aquifer is likely to be locally heterogeneous, although it may have quite uniform hydraulic properties on basin scale. Typical of alluvial fans, it appears to be more coarse-grained to the west, and becomes more fine-grained towards the north-south axis of the valley, where it interfingers with lake sediments which are also fine-grained.

THE GROUNDWATER MODEL SIMULATION

The Conceptual Model

The conceptual groundwater flow model of Washoe Valley integrates our geophysical results with the known hydrology and subsurface geology of the basin as the first step in constructing the mathematical model. Hydraulic conductivities and transmissivities input to the mathematical model are derived from physical property estimates of the conceptual model. An alluvial fan model is probably applicable to the western subsurface, with more coarse-grained sediments underlying the far western margin of the basin, and becoming progressively finer-grained toward the center of the valley. The confining layer at about 30 meters beneath the surface, forms a natural division between the upper unconfined and the lower confined aquifer.

Recharge to the model is assumed to come entirely from the margins of the basin as snowmelt runoff. Direction of groundwater flow is generally from the margins of the basin toward the center. Discharge is assumed to be entirely due to evaporation

from the surface of Washoe Lake and evapotranspiration from the rest of the valley floor. On an annual basis, discharge due to evaporation and evapotranspiration are three to four times greater than recharge due to precipitation (Arteaga and Nichols, 1984). The only other sources of groundwater loss in the system are a nearly negligible amount of surface outflow into Steamboat Creek through Little Washoe Lake to the north, and consumptive use. Although consumptive use is increasing, it was nearly negligible in 1965, the date to which the steady-state model is calibrated.

Washoe Lake, which covers about 25% of the valley floor, is a significant element of the flow system and the water budget. The volume of Washoe Lake at maximum stage is about 85,000 cubic meters, which is approximately the annual water balance for 1965. This suggests that the water budget for Washoe Valley is in a state of somewhat delicate balance. Under normal conditions where Washoe Lake is near maximum stage, the wetlands to the north remain at essentially the same head as the lake, and are also a significant element of the flow system. In drought years, as water is evaporated from the lake surface, it is initially replenished by groundwater. However, as the groundwater supply becomes inadequate to replenish the evaporation, the lake goes dry.

The Mathematical Model

The general equation for three-dimensional flow of groundwater of constant density through a heterogeneous porous media is given by McDonald and Harbaugh (1988, p. 2-1) as:

$$\frac{\partial}{\partial x} \left(K_{xx} \frac{\partial h}{\partial x} \right) + \frac{\partial}{\partial y} \left(K_{yy} \frac{\partial h}{\partial y} \right) + \frac{\partial}{\partial z} \left(K_{zz} \frac{\partial h}{\partial z} \right) - W = S_s \frac{\partial h}{\partial t}$$

where

K_{xx} , K_{yy} , and K_{zz} are values of hydraulic conductivity along the x,y, and z coordinate axes, which are assumed to be parallel to the major axes of hydraulic conductivity, in units of length per unit of time (L/t)

h is the potentiometric head in units of length (L)

W is a volumetric flux per unit volume of sources (+) and/or sinks (-) of water, in units of inverse time (1/t)

S_s is the specific storage of the porous media, in units of inverse length (1/L), and t is time.

This equation is solved by a finite difference approach using the computer program MODFLOW (McDonald and Harbaugh, 1988).

For steady-state simulations, there is no change in head with time, and the right hand side of the equation becomes zero. Solution of the equation for a particular groundwater flow regime requires a knowledge of the spatial distribution of transmissivities and hydraulic conductivities, boundary conditions, an initial configuration of heads, recharges and discharges, and for transient modeling, an estimate of initial conditions and specific storage. For this study, the conceptual model was transformed into the mathematical model in the following manner:

Model Layers

A quasi-three dimensional simulation is used in this study, with an upper unconfined aquifer of constant thickness of approximately 30 meters and variable hydraulic conductivities, a confining layer, and a confined aquifer of variable transmissivities. In a quasi-three dimensional simulation, confining beds and the heads within them are not explicitly modeled. Rather, vertical flow through the confining layer is defined by a leakance term which adds or extracts water from the aquifers above or below (Anderson and Woessner, 1992). The advantage of a quasi-

three dimensional approach is in the simplification of the model and reduction of computer time. Due to the well documented existence of the confining layer beneath the west side of the valley, a quasi-three dimensional model seems appropriate here.

The Unconfined Aquifer

Most evidence suggests that the unconfined aquifer is present beneath much of the western valley floor, and has a thickness of about 30 meters. The magnetic and electrical conductivity data of this thesis suggest that it probably becomes more heterogeneous in the east. It appears to be present, at least locally, beneath southern New Washoe City (Figure 15, and McKay, 1991).

The Confining Layer

The existence of artesian heads (Arteaga and Nichols, 1984) over much of the western side of the valley suggests the presence of a confining layer. Additionally, artesian water was encountered at a depth of about 30 meters in drill hole 1 (Figure 13), where finer grained sediments were encountered in the 1-2 meter interval immediately above the artesian water, thus providing a thickness estimate for the confining layer. The Rasmussen flowing well, about a mile to the west, bottoms at 47 meters, substantiating the depth estimates for the confining layer. Artesian heads exist in the eastern subsurface, although they are less prevalent. This suggests that the confining layer may become less distinct as it blends with other fine-grained sediments in the complex eastern subsurface.

The Confined Aquifer

For purposes of this model, essentially all of the valley fill below 33 meters is treated as a confined unit, although local variations within the subsurface of Washoe Valley must certainly exist. As with the unconfined aquifer, the western half

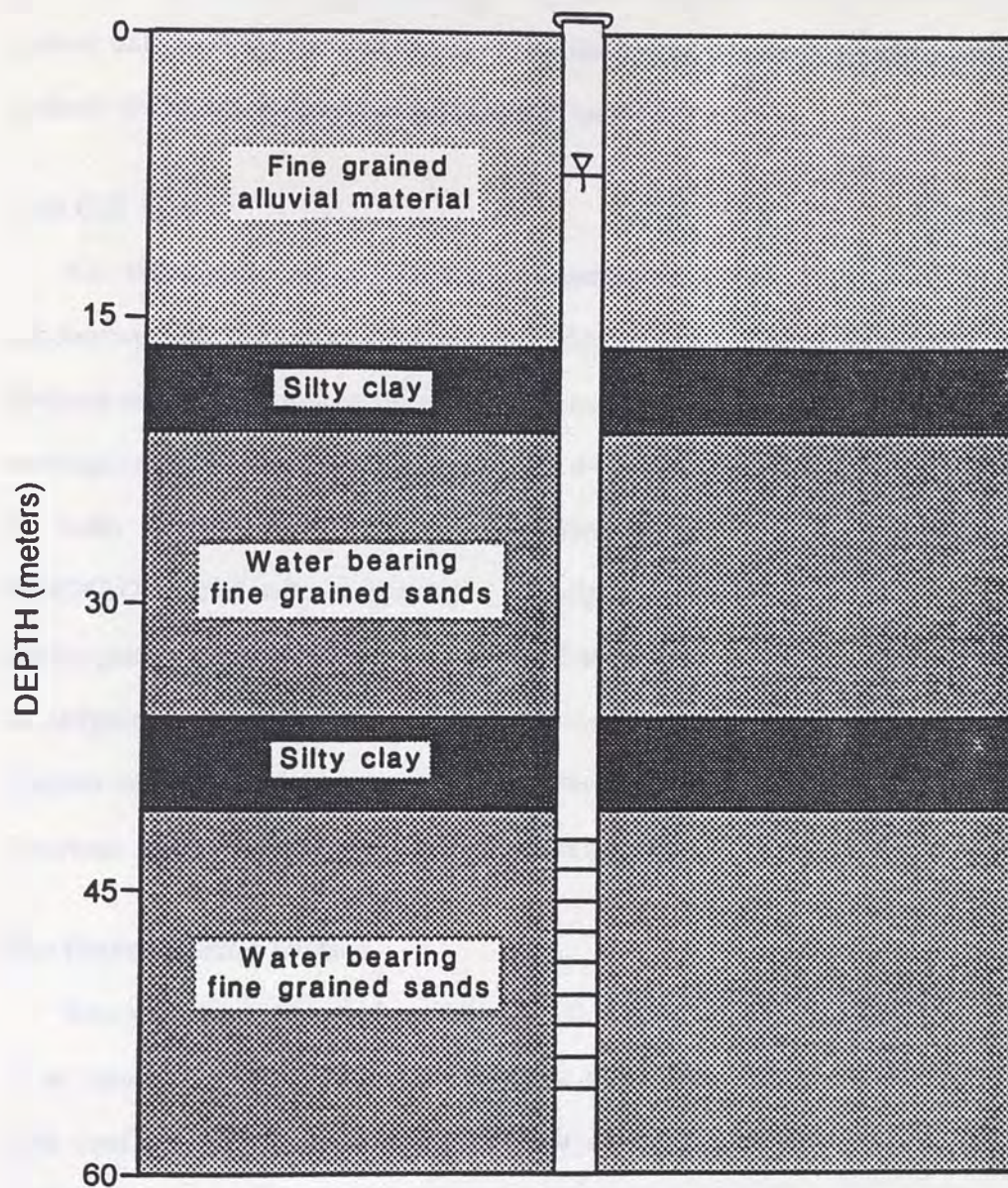


Figure 15. Generalized Stratigraphic Section of New Washoe City (after McKay, 1991).

probably represents a combination of alluvial and lacustrine sediments, while the eastern half includes the volcanic unit defined by the magnetic anomaly and the finer-grained sediments defined by the electrical conductivity data.

Grid Cell Size

For this simulation, a grid cell 200 meters on a side (Figure 16) was assumed appropriate for both model layers in order to adequately approximate all of the features seen in the surface topographic maps and the geophysical data. The overall rectangular dimensions of the model were 44 cells in the east-west (x) direction, and 70 cells in the north-south (y) direction, giving a total of 3080 grid cells. MODFLOW arbitrarily assigns the grid origin to the lower left hand corner of the model grid, putting all of the cells in the first quadrant. These co-ordinates are used in assigning line numbers to the two cross-valley calibration profiles, with the line number referenced to the southern boundary of the model grid, and the horizontal locations referenced to the western (left) boundary.

The Potentiometric Surface

The potentiometric surface is the actual map of the hydraulic heads in an aquifer. In an unconfined aquifer, this is the water table (Freeze and Cherry, 1979). When both confined and unconfined aquifers exist in an area, as they do in Washoe Valley, problems can arise in distinguishing the two potentiometric surfaces. The potentiometric surface of Washoe Valley is reconstructed from 1965 data (Rush, 1967) and is shown on Figure 17. In the groundwater model of Washoe Valley, the base of the potentiometric surface is arbitrarily assigned to be the base of the unconfined aquifer, and all heads are computed relative to this level. The lake surface represents an area of equal head covering the central portion of the flow

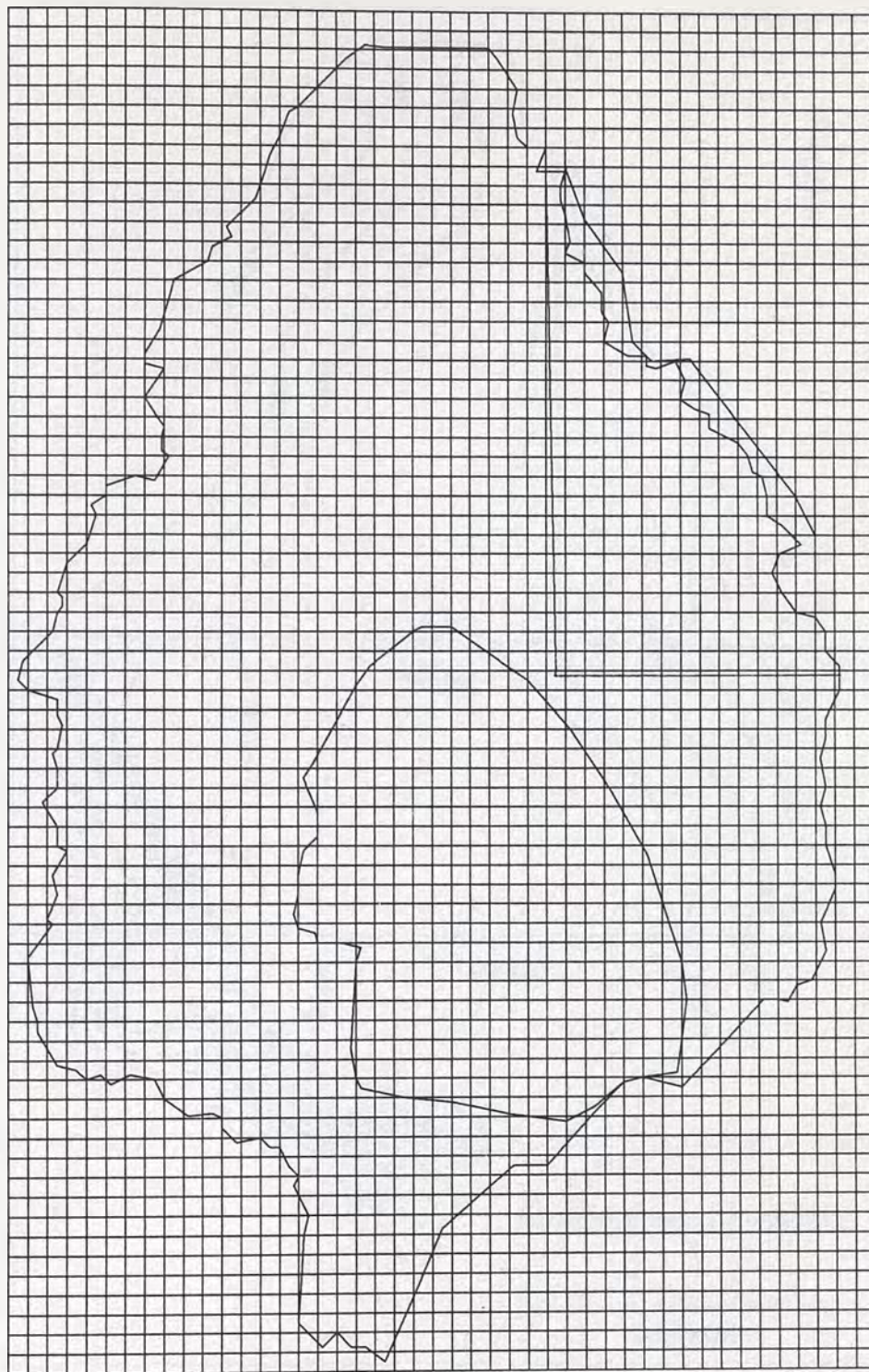


Figure 16. The Model Grid.

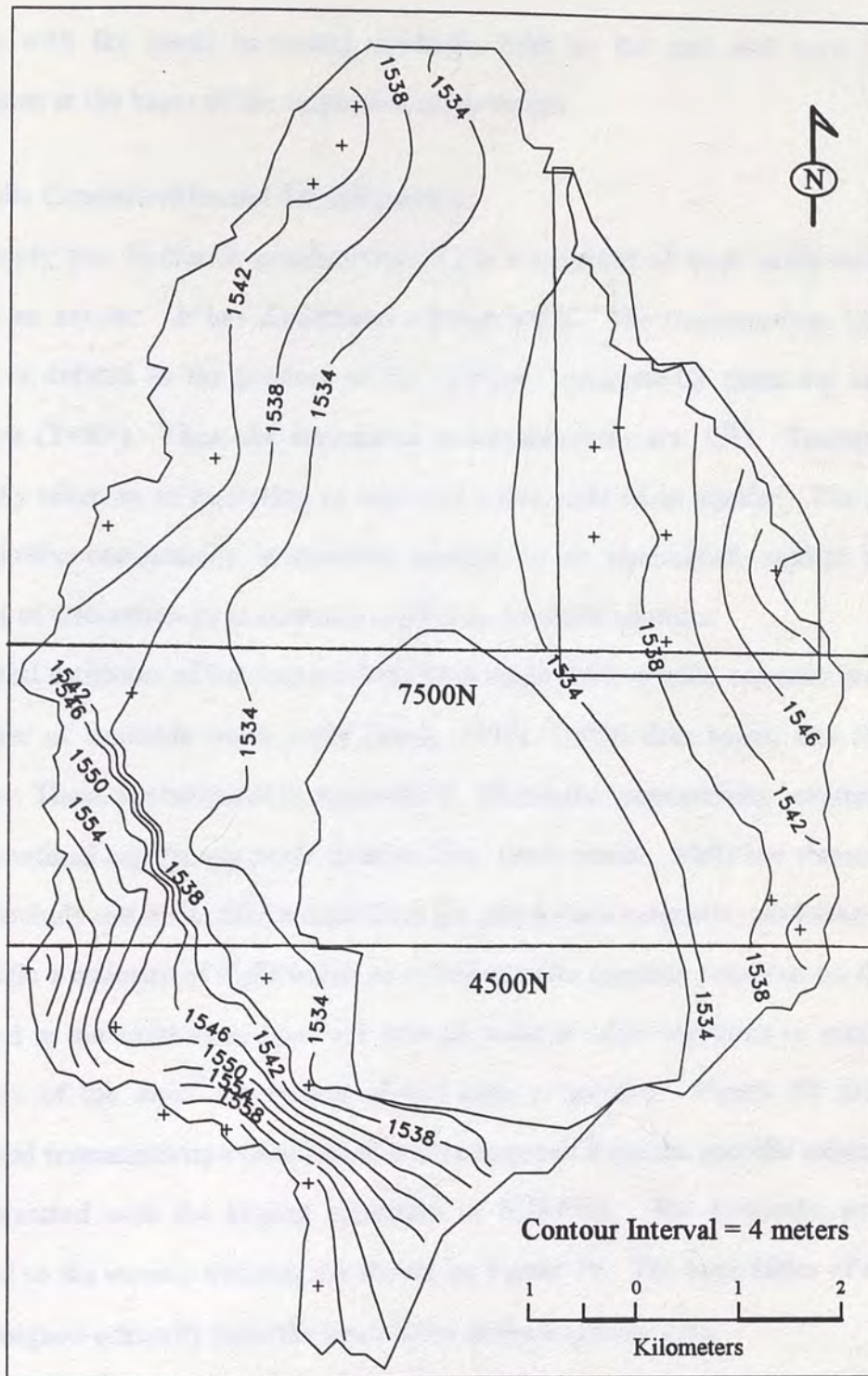


Figure 17. The 1965 Potentiometric Surface with Calibration Profiles.

regime, with the heads increasing gradually both to the east and west to their maximums at the bases of the respective range fronts.

Hydraulic Conductivities and Transmissivities

Simply put, hydraulic conductivity (K) is a measure of how easily water will flow in an aquifer. It has dimensions velocity (L/t). The transmissivity (T) of an aquifer is defined as the product of the hydraulic conductivity times the saturated thickness ($T=Kb$). Thus, the dimensions of transmissivity are L^2/t . Transmissivity is usually taken as an indication of expected water yield of an aquifer. The concept of hydraulic conductivity is normally applied to an unconfined aquifer and the concept of transmissivity is normally applied to confined aquifers.

Initial estimates of transmissivities were made from specific capacity tests from a number of available water wells (Rush, 1967), USGS data bases, and the state engineer. These are tabulated in Appendix F. Hydraulic conductivity estimates for the unconfined aquifer are made directly from these results, while the transmissivity values include estimated thicknesses from the gravity and magnetic modeling.

While a majority of wells which have had specific capacity tests run on them are clustered in the southwest, there are enough wells in other locations to make initial estimates of the areal distribution of hydraulic properties. Figure 18 shows the contoured transmissivity values which were computed from the specific capacity data and generated with the kriging algorithm of SURFER. The hydraulic properties assigned to the various domains are shown on Figure 19. The boundaries of domains were assigned primarily from the boundaries in the magnetic data.

The low values of hydraulic properties of Domains I and Ia to the north and northeast are assigned largely on the basis low hydraulic values from specific

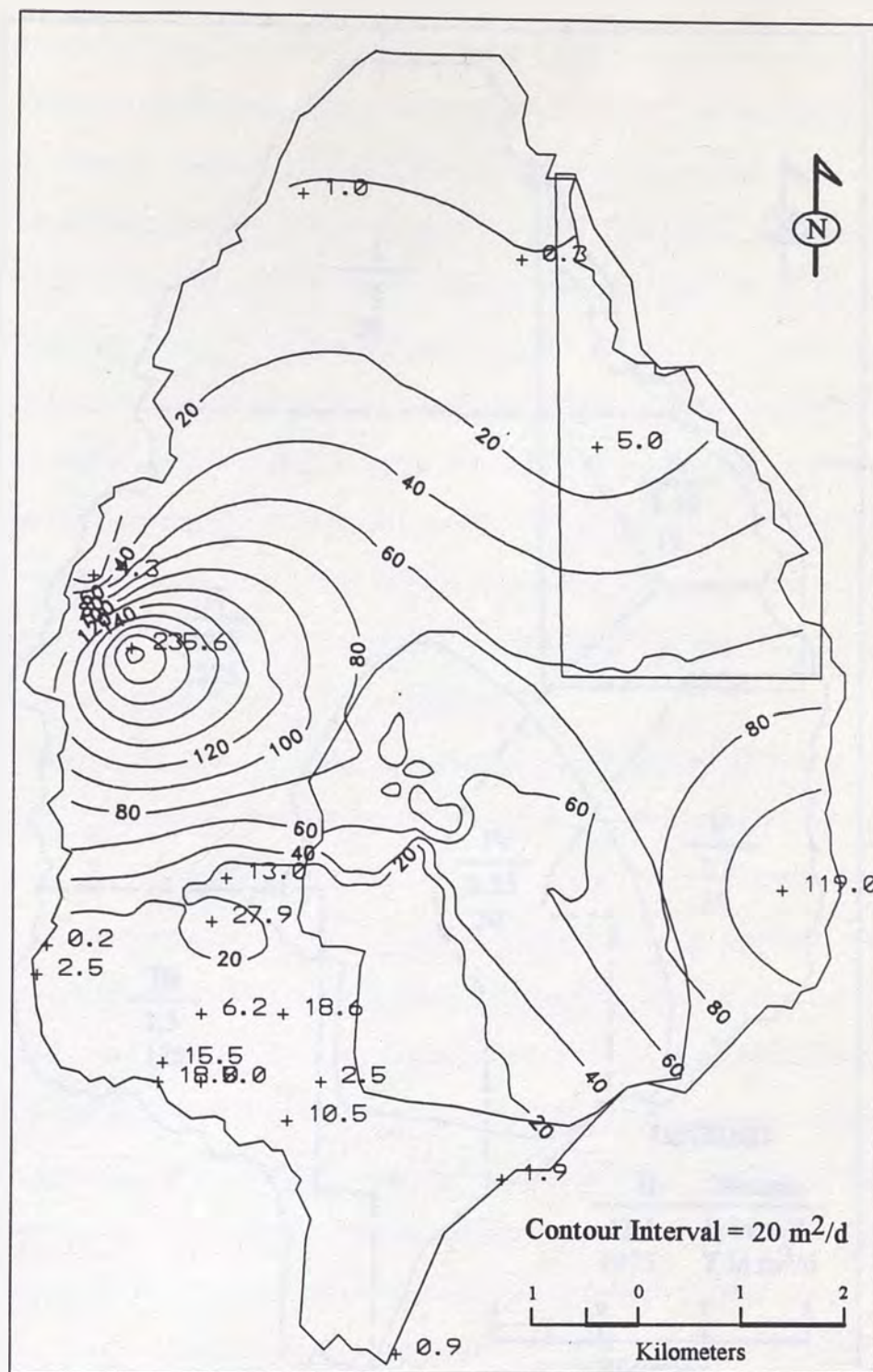


Figure 18. Contoured Transmissivities from Specific Capacity Data.

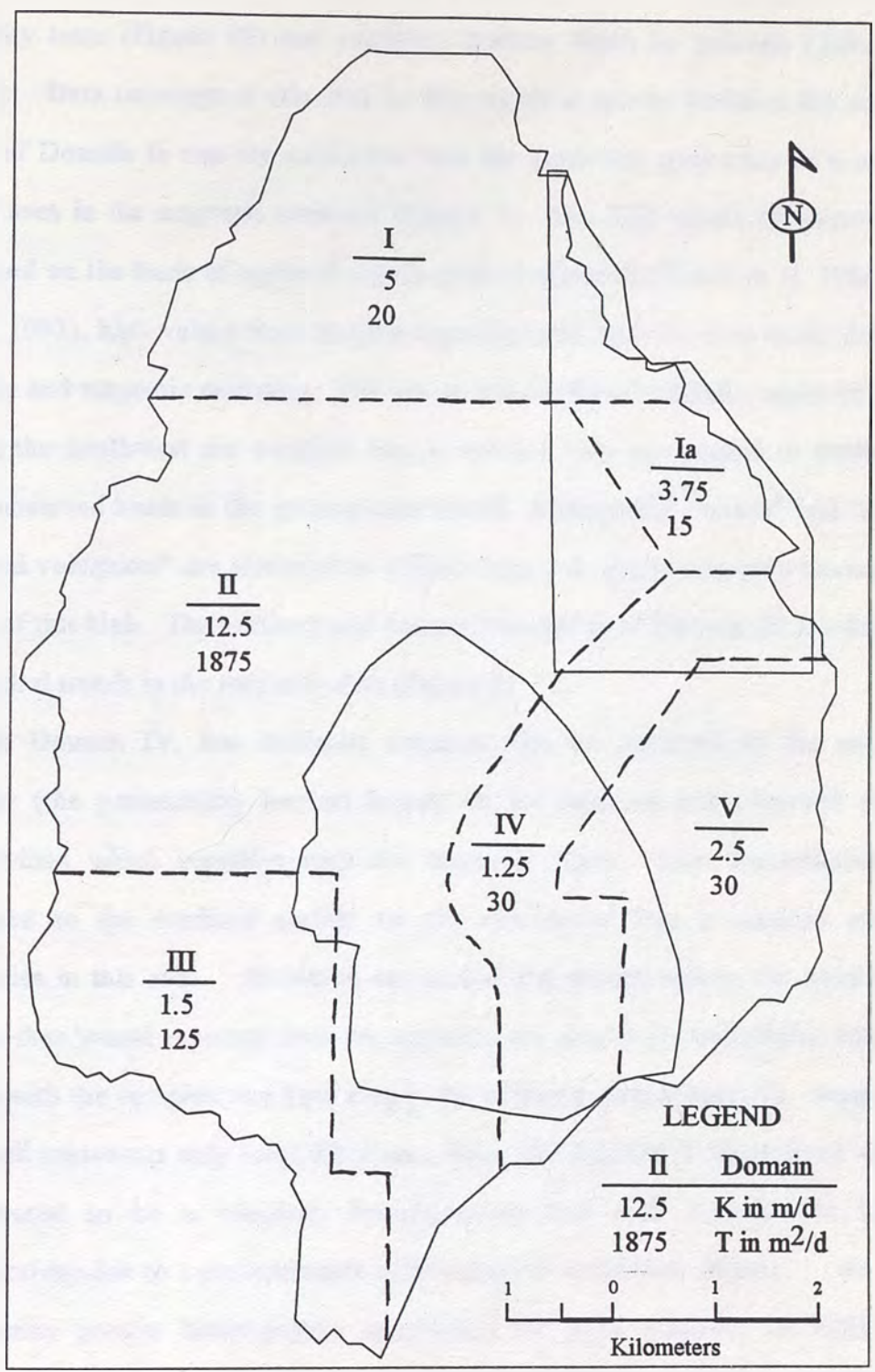


Figure 19. Domains I thru V of Similar Hydraulic Properties.

capacity tests (Figure 18) and relatively shallow depth to bedrock (Tabor et al. 1983). Data coverage in this area by this report is sparse, however the southwest edge of Domain Ia was set coincident with the northwest projection of a structural trend seen in the magnetic contours (Figure 7). The high values of Domain II are assigned on the basis of reported coarse-grained materials (Tabor et al. 1983, Karlin et al. 1993), high values from specific capacity tests, and the deep basin defined by gravity and magnetic modeling. The low to intermediate hydraulic values of Domain III to the southwest are assigned largely because they are needed to replicate the high observed heads in the groundwater model. Additionally, "basalt" and "blue clay (altered volcanics)" are identified in driller's logs and sparse magnetic coverage also hints of this high. The northern and eastern boundaries of Domain III are defined by structural trends in the magnetic data (Figure 8).

In Domain IV, low hydraulic conductivities are assigned to the unconfined aquifer (the permeability barrier) largely on the basis of low observed electrical resistivities which correlate with the magnetic highs. Low transmissivities are assigned to the confined aquifer on the assumption that it consists mostly of volcanics in this area. Measured transmissivities in the well to the southeast are higher than would be expected from the magnetic and electrical conductivity data. This, along with the complex structure seen in the magnetic data (Figure 7), suggests that the well represents only local lithology. Thus, the Domain V unconfined aquifer is interpreted to be a relatively heterogeneous unit with overall low hydraulic conductivity due to a predominance of fine-grained sediments. Based on this apparently greater heterogeneity suggesting the local presence of more coarse grained materials, the Domain V unconfined aquifer is assigned a slightly higher hydraulic conductivity than Domain IV. No distinction in transmissivity values is

made between Domains IV and V for the confined aquifer, where data are sparse and both are interpreted to be mostly volcanics.

Table 1. Calibrated Model Hydraulic Values.

DOMAIN	I	Ia	II	III	IV	V
Hydraulic Conductivities of the Unconfined Aquifer, in m/d	5	3.75	12.5	1.5	1.25	2.5
Transmissivities of the Confined Aquifer, in m ² /d	20	15	1875	125	30	30

Recharge

Recharge to the unconfined alluvial aquifer is simulated as a series of evenly distributed injection wells along both the west and east margins of the valley, except that a much higher single cell value was required on the east to simulate the recharge from Jumbo Creek. A total recharge of 85,600 m³/d was used for the calibrated model.

To construct the steady-state groundwater model, the 1965 recharge data are assumed to be representative of a normal year. Data from the USGS gauging station at an elevation of 2250 meters on Franktown Creek provide an additional control on this estimate (USGS, 1992). Data tabulated monthly for a 17 year period from 1974 to 1991 indicate fluctuations above and below a mean flow value of +/- one order of magnitude. Thus, adjustment of recharge values and/or distributions were varied within this range in the final flow model.

Discharge

Discharge is assumed to be primarily from evaporation from the lake surface and evapotranspiration from the valley floor. A uniform evaporation rate of 2.7×10^{-3}

m/d (1 meter per year) is used for the lake surface, based on data from Arteaga and Nichols (1984). This is certainly a more consistent number than the composite value of 4.2×10^{-4} m/d used for evapotranspiration from the valley floor. These are net numbers, with annual precipitation values subtracted. For example, precipitation is on the order of 1/3 meter/year, but lakebed evaporation is on the order of 11/3 meter/year, leaving a net evaporation of about 1 meter/year (Arteaga and Nichols, 1984).

Discharge was simulated in the steady-state groundwater model using the recharge package of MODFLOW, but with negative rates. While this is a somewhat different procedure from the usual one of simulating evapotranspiration as a head-dependent function, it can be justified by noting that for most of the valley floor, except on the far east side, water levels are less than 2 to 3 meters below land surface, and thus extinction depth (the depth of the water table below land surface at which evapotranspiration ceases to occur) is probably not a significant factor.

Outflow from Little Washoe Lake into Steamboat Creek to the north was not incorporated into the model, since in most years it is negligible. Neither was consumptive use considered, since in 1965 it was a relatively minor component of the water budget, and areal distribution was not well documented. However, for transient models incorporating present day as well as anticipated conditions, estimates of consumptive use must be incorporated.

Boundary Conditions and Initial Heads

All sides of Washoe Valley, which are surrounded by range fronts, are considered to be no flow boundaries in the flow simulation of Washoe Valley. Thus, there are 1267 inactive cells on the perimeter, with the remaining 1813 active cells defining the flow regime. The contact between the active and inactive cells is the

lateral no-flow boundary. Likewise, the bottom of the second layer of the model, representing Cretaceous granodiorite, is also considered to be a no-flow boundary. In general, the lateral margins of Washoe Valley are taken to be the 1585 meter (5200 foot elevation contour) level on the Washoe City 7 1/2 minute USGS quadrangle map.

A constant discharge rate representing evapotranspiration is applied to model nodes representing the land surfaces of Washoe Valley, excluding Washoe Lake, using the Recharge package of MODFLOW, but using a negative rate of recharge. The surface of Washoe Lake was simulated as a variable head boundary using the River package of MODFLOW. This in effect created a mixed boundary condition with both a constant head and a uniform flux rate across the lake surface.

Initial heads of 33 and 36 meters respectively for the unconfined and confined aquifers were specified in the model simulation. Head differences this small were difficult, at best, to distinguish in the real data. These values resulted from an effort to separate artesian heads from the water table based on sketchy well log data, and thus should be considered very tentative.

The Steady-State Simulation

Calibration

The model was calibrated to the potentiometric surface of late 1965 because there is a substantial set of water level data available. Furthermore, these data represent essentially pre-development condition (Rush, 1967). The model was assumed to be calibrated when the following conditions were met for each of two cross-valley profiles:

- 1) the mean absolute error (MAE) of the differences in head between Rush's 1965 data and the model was less than one meter. Stated mathematically,

$$M = \frac{\sum |R - H|}{N} \leq 1$$

where:

M is the computed mean absolute error

R is Rush's 1965 head value for each point

H is the model head value for each point, and

N is the number of comparison points

2) a water balance within 1% was attained.

A steady-state calibration was achieved with the conditions shown in Tables 1 and 2. The values for recharge and discharge are based on the estimates of Rush (1967) and Arteaga and Nichols (1984), although some adjustments were necessary. Hydraulic conductivities and transmissivities were then adjusted until a suitable fit to the two cross-valley potentiometric surface profiles (Figure 20) was obtained. The northernmost profile was selected because it is near the north-south center of the valley and it cuts across the major features of interest; the deeper part of the basin on the west, the complex hydrostratigraphy on the east near New Washoe City, and the east-side recharge from Jumbo Creek. The southern profile was selected because it is relatively distant from both the northern profile and the EW structure identified in the magnetic and gravity data.

Figures 21 and 22 compare heads of the calibrated models with the potentiometric surface of 1965 for the two cross-valley. A mean absolute error considerably less than one meter was achieved for the northern profile. The mean head difference of the southern profile was about one meter, which appears to be

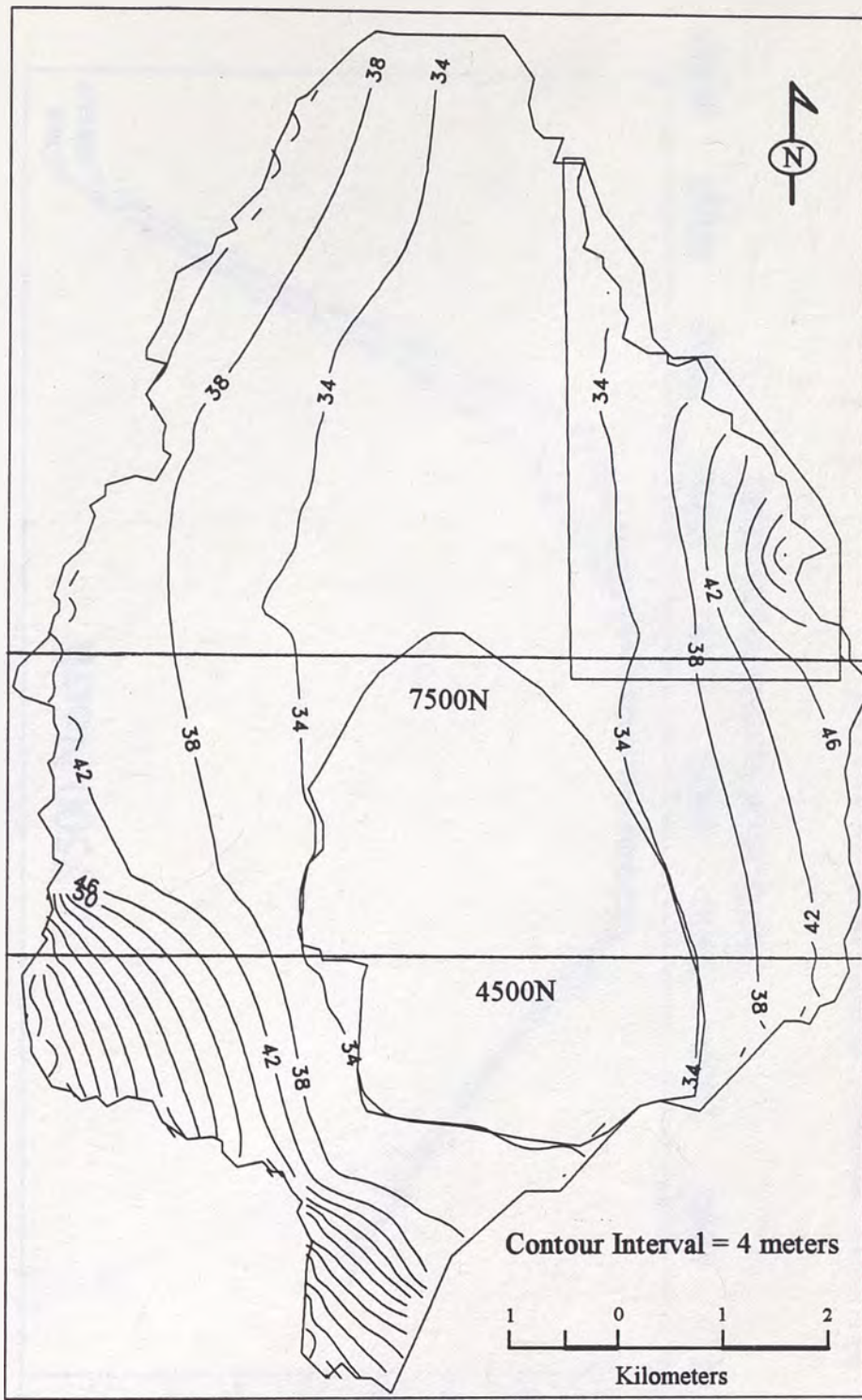


Figure 20. Calibrated Model Potentiometric Surface of the Unconfined Aquifer.

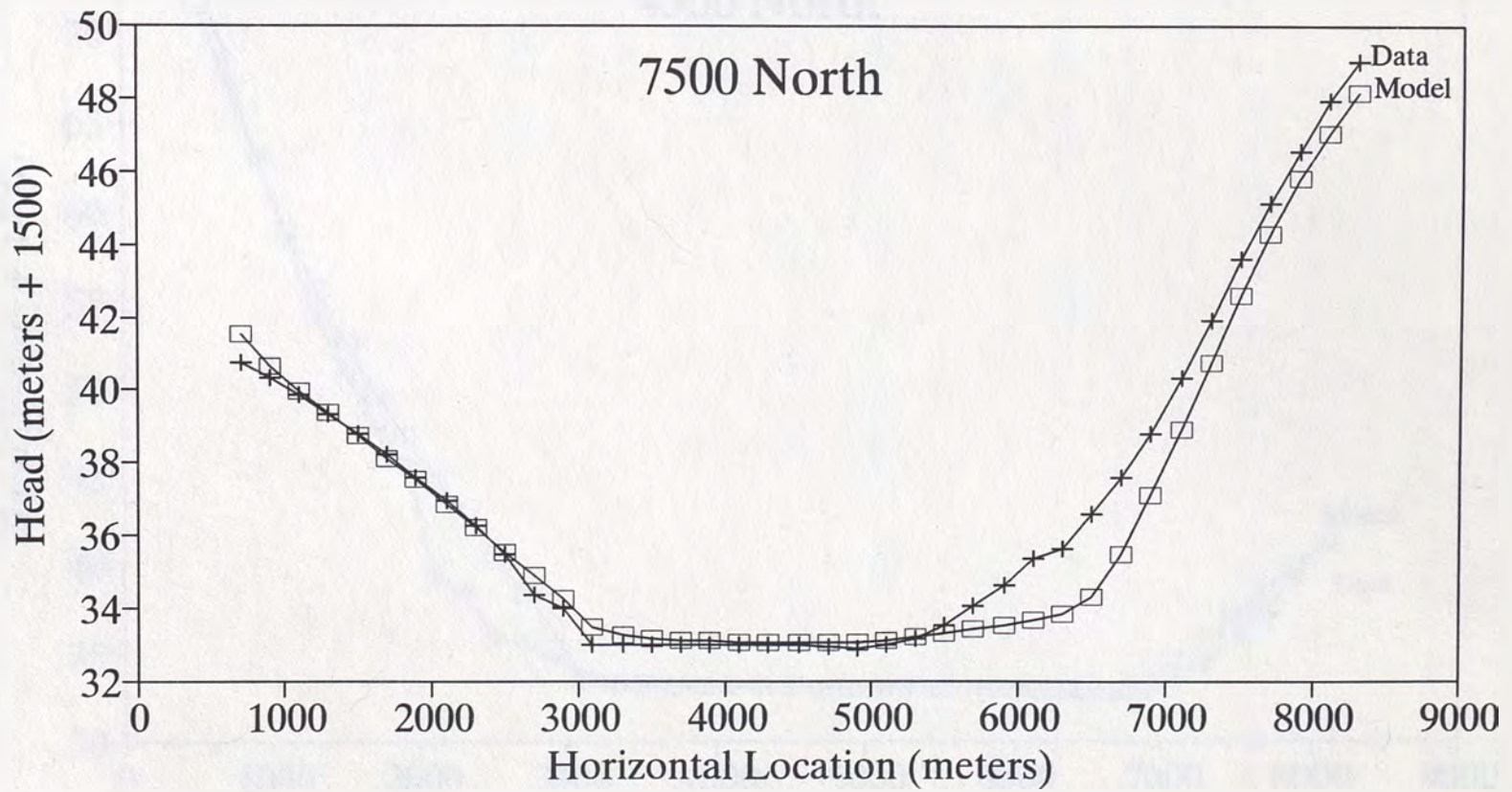


Figure 21. Northern Profile Calibrated Model.

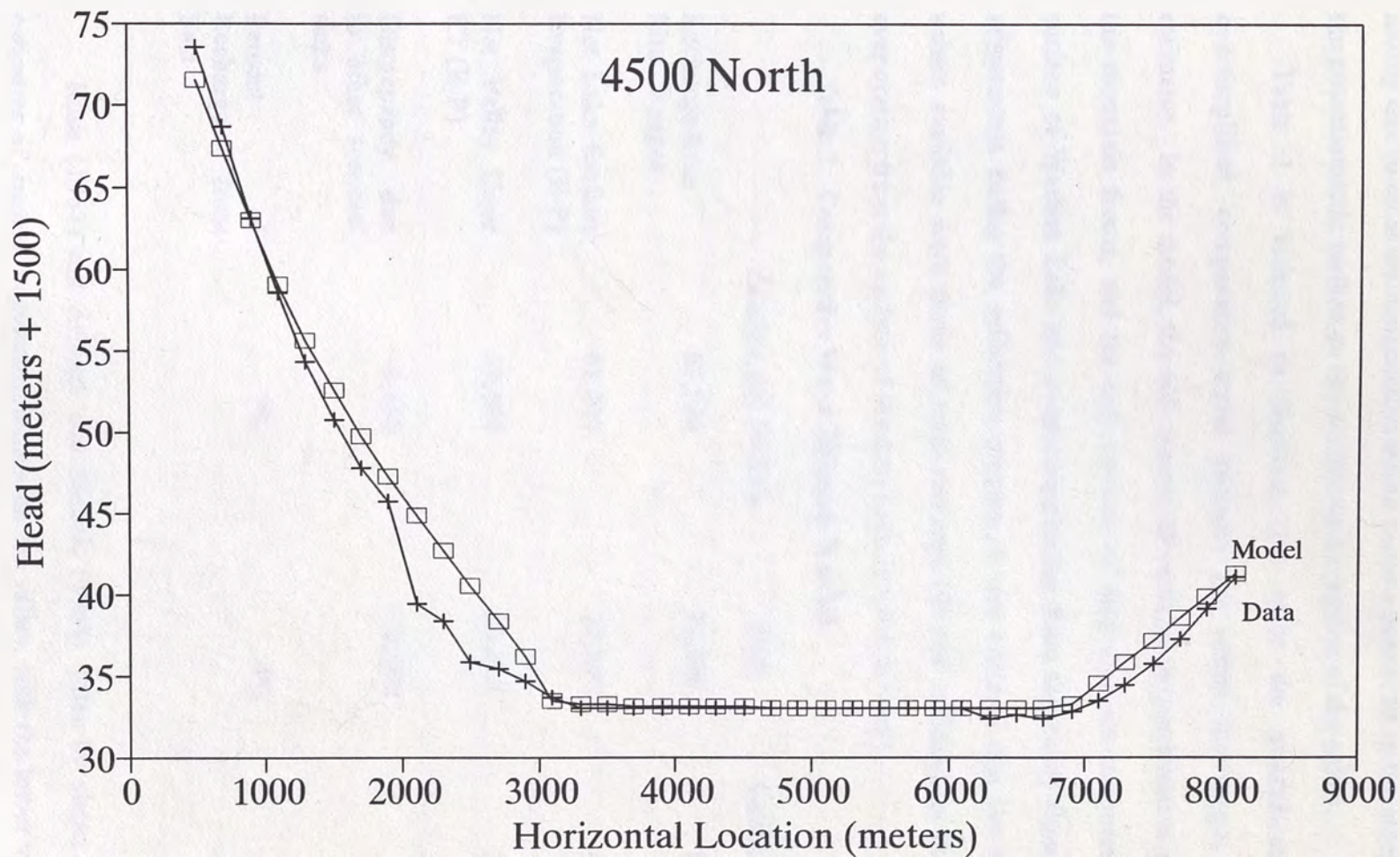


Figure 22. Southern Profile Calibrated Model.

mostly due to local inhomogeneities which cause a poorer fit to the steep gradients in the potentiometric surface on the southwestern portion of the valley.

Table 2 is included to illustrate that while the groundwater model is oversimplified, comparative water balances are within the ranges of previous estimates. In the model, the only source of recharge is precipitation entering from the mountain fronts, and the only sources of discharge are evaporation from the surface of Washoe Lake and evapotranspiration from the valley floor. In making adjustments during the calibration process, it was assumed that the most accurate values available were those of total recharge (85,600 m³/day) to the valley, and evaporation from the surface of Washoe Lake (61,800 m³/day).

Table 2. Comparative Water Balances in m³/d.

	<u>Arteaga and Nichols</u>	<u>Rush</u>	<u>Calibrated Model</u>
Recharge from Mtn. Ranges	87,900	77,700	85,600
Net Lake Surface Evaporation (E-P)	61,200	33,800	62,200
Net Valley Floor ET (E-P)	33,100	25,200	24,300
Discrepancy, due to other sources/ sinks	-6,400	+18,900	-900
Percent of Recharge from East	7%	4%	18%

Rush (1967) and Arteaga and Nichols (1984) differ by about 30% in their estimates of surface evapotranspiration for the valley, with the lower values of Rush seeming to provide a better fit to the model. To fit the 1965 potentiometric surface,

it was necessary to increase the percentage of recharge from the east side of the valley to about 18%. This recharge is considerably higher than earlier estimates for the east side of the valley of 7% and 4% respectively by Arteaga and Nichol (1984) and Rush (1967). It is undoubtedly too high since it implies that as much as 2 to 4 times more water is being recharged to the east side of the valley than previously estimated. This ratio was necessary because it was not possible to get model heads comparable to observed heads on the east using the lower recharge rates only. Without the added recharge, the model heads could not be made to fit the observed heads, even if extremely low transmissivities were used. If the lower recharge rates were used, this would necessitate reducing the average annual recharge for the entire valley to $\frac{1}{2}$ to $\frac{1}{4}$ of the original estimates. This is an unrealistic scenario, since it implies that Washoe Lake should have gone dry much more frequently in the past. The total water balance of 85,600 m³/day is approximately equal to the volume of water in Washoe Lake at full stand. The single value used for evapotranspiration over the entire valley probably underestimates evapotranspiration on the west side, and over estimates it on the east. This has the effect of requiring higher recharge ratios on the east in the model. Using a more representative areal distribution of evapotranspiration would bring the recharge ratios in the model more in line with earlier estimates.

Sensitivity Analysis

Sensitivity analyses were performed by varying the following parameters separately: 1) hydraulic conductivity of the unconfined aquifer, 2) transmissivity of the confined aquifer, 3) combined hydraulic parameters of the two aquifers, 4) position of the contact between the high and low transmissivity units, 5) effects of

the permeability barrier, 6) total recharge, and 7) vertical hydraulic conductance of the confining layer between the two aquifers.

Sensitivity to Changes in the Unconfined Aquifer

The hydraulic conductivities of all domains in the unconfined aquifer were reduced to one tenth, halved, doubled, and multiplied by ten. The results are shown in Figures 23 and 24 for the northern and southern profiles respectively. For the northern profile, heads on the west side of the valley change little with changes in the hydraulic conductivity of the unconfined aquifer, except when a very low hydraulic conductivity is used. Conversely, the eastern side of the valley is much more sensitive to changes in the hydraulic conductivities of the unconfined aquifer. For the southern profile, the western side of the valley exhibits a much greater sensitivity to changes in hydraulic conductivities of the shallow aquifer, more comparable to those on the east.

Sensitivity to Changes in the Confined Aquifer

In this analysis, the transmissivities of all domains of the confined aquifer were reduced by one tenth, halved, doubled, and multiplied by ten. The northern profile (Figure 25) exhibits a relatively high sensitivity in the west due to changes in transmissivities of the confined aquifer, unlike the situation for the unconfined aquifer. Much less sensitivity is exhibited to the east, except when transmissivity is decreased tenfold. Much of this dominance can be explained by noting that the confined aquifer on the west is by far the single most prevalent unit in the valley. It is much thicker and more porous to the west, and thus contains most of the water. The southern profile (Figure 26) shows a high sensitivity on the west to changing transmissivities of the confined aquifer, but little sensitivity on the east. Again, this reflects the relatively small volume of confined aquifer in the eastern subsurface.

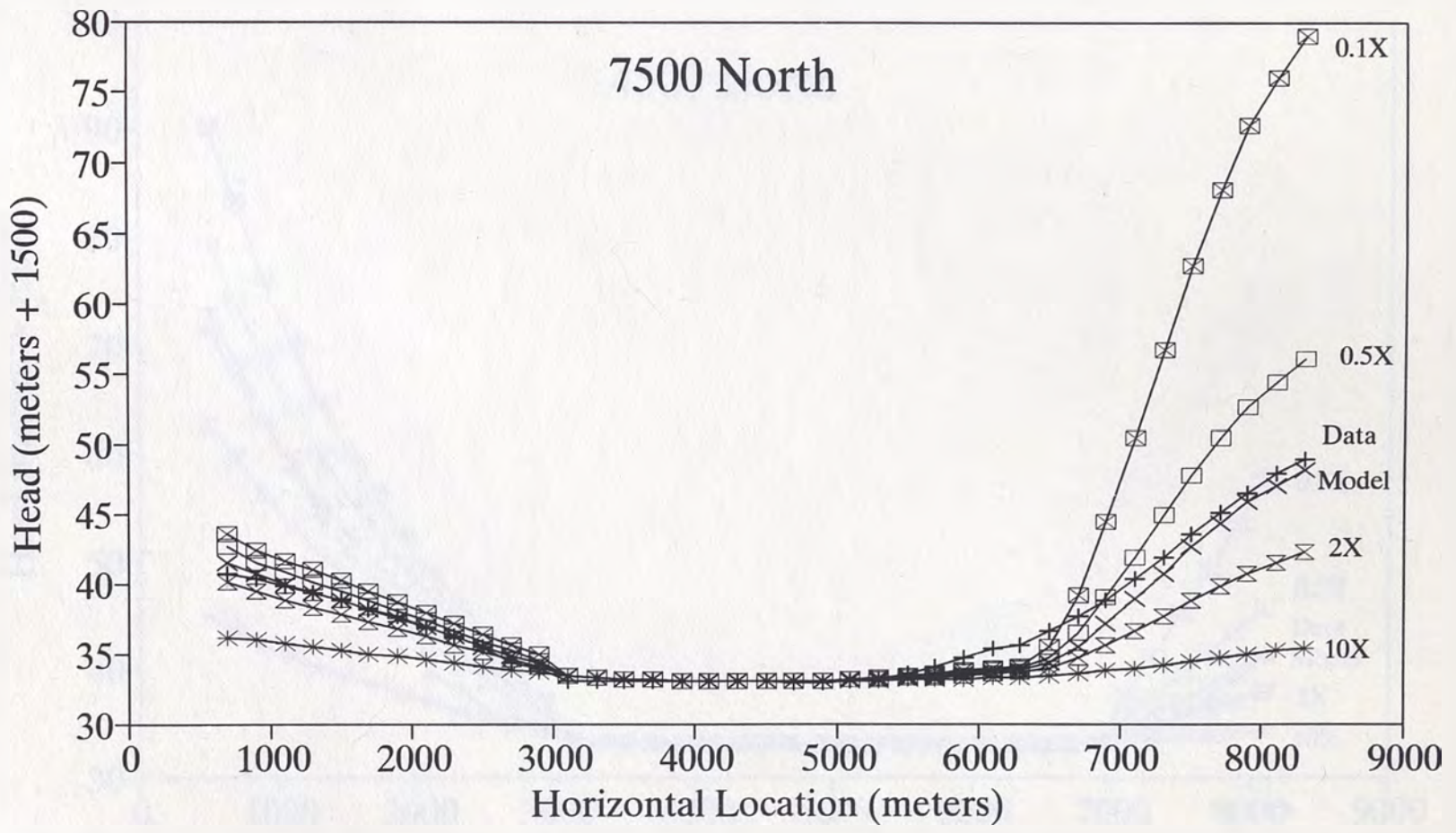


Figure 23. Northern Profile: Sensitivity to Changes in the Hydraulic Conductivities of the Unconfined Aquifer.

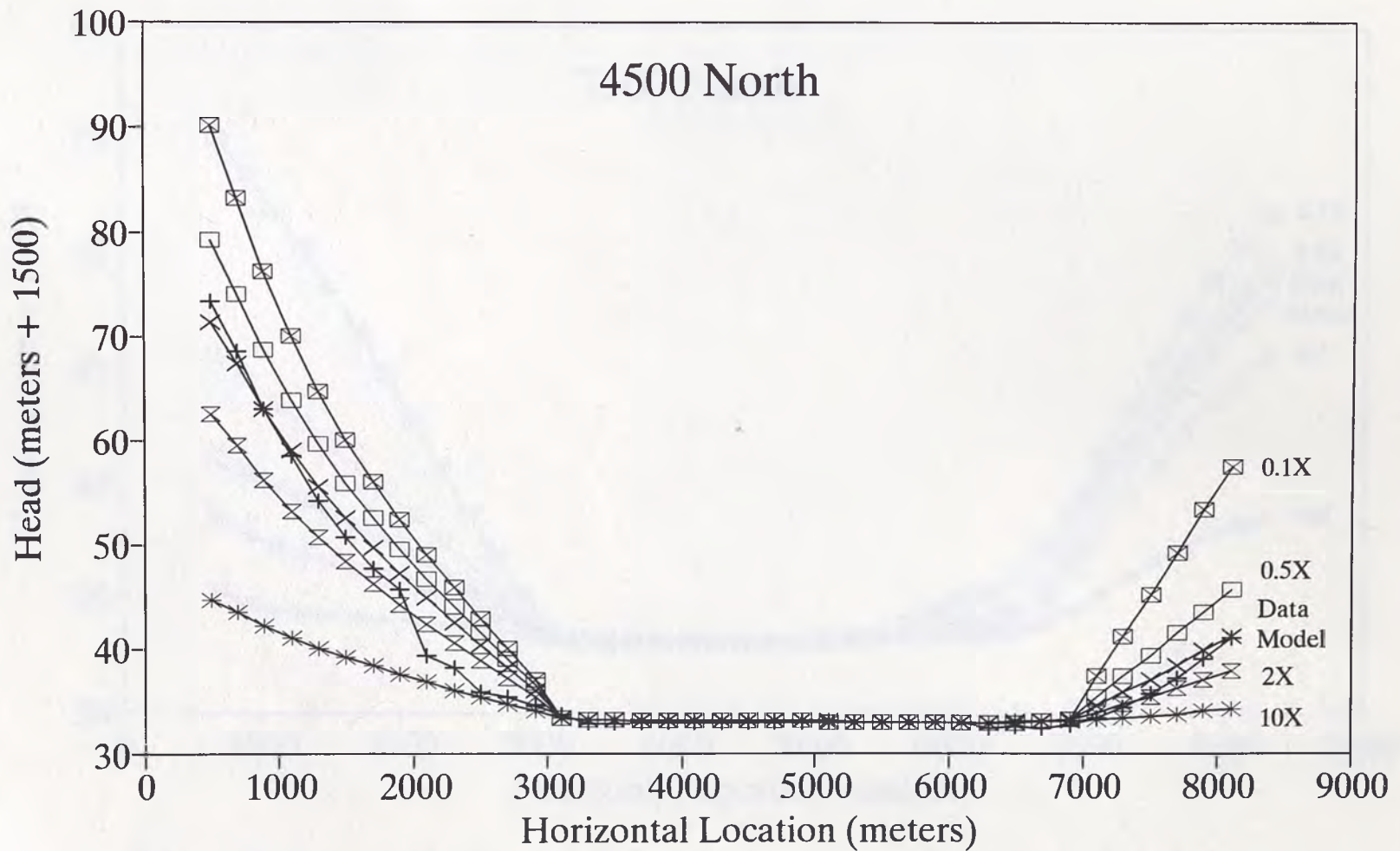


Figure 24. Southern Profile: Sensitivity to Changes in the Hydraulic Conductivities of the Unconfined Aquifer.

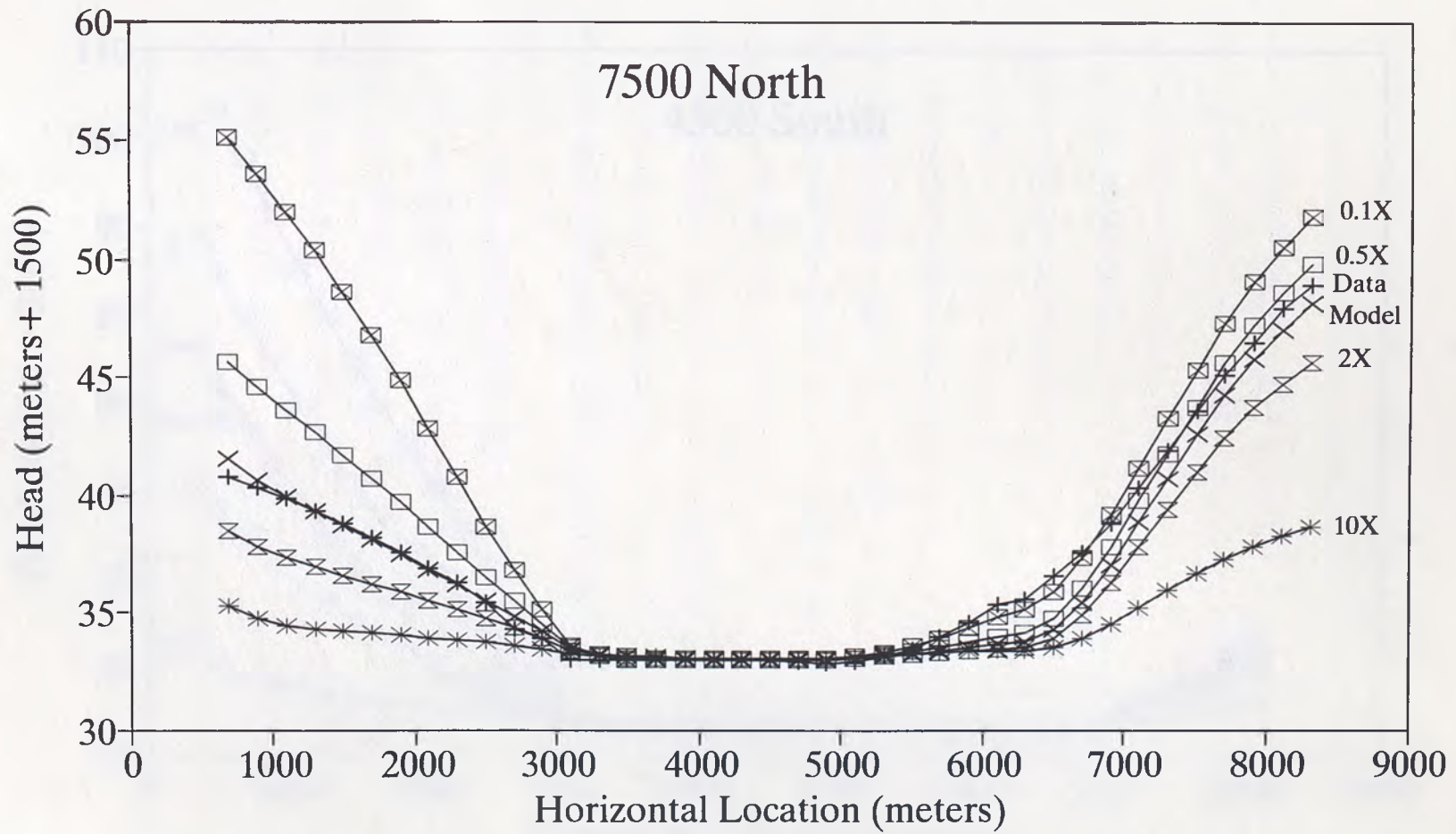


Figure 25. Northern Profile: Sensitivity to Changes in the Transmissivities of the Confined Aquifer.

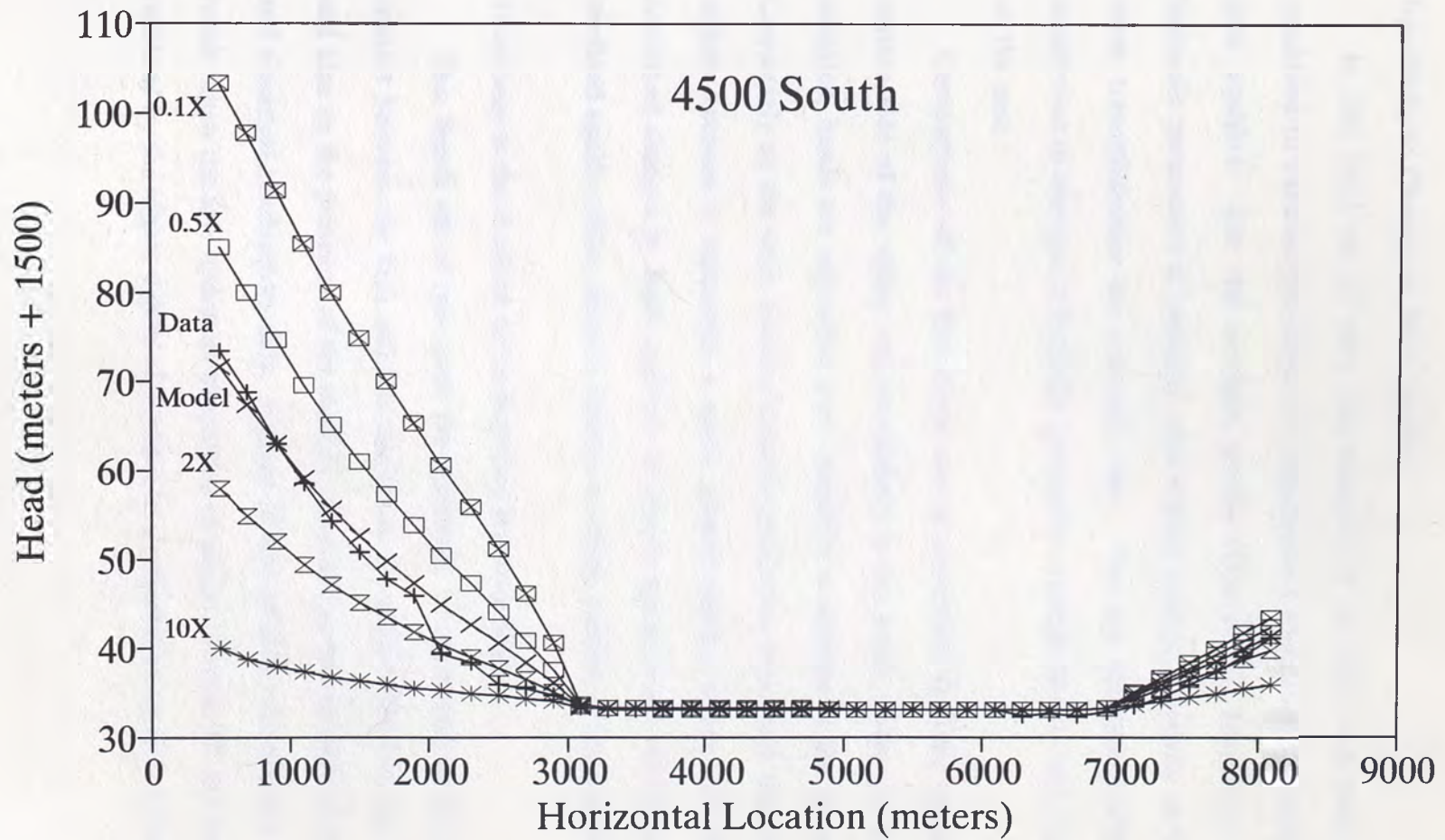


Figure 26. Southern Profile: Sensitivity to Changes in the Transmissivities of the Confined Aquifer.

Sensitivity to Changes in Both Aquifers

In this third set of runs, the changes of the first two runs are essentially combined to examine the effects of simultaneous changes in hydraulic properties of both aquifers. For the northern profile (Figure 27), sensitivity to changes in hydraulic parameters is moderate with slightly greater sensitivity on the east, except when transmissivities are extremely low. For the southern profile (Figure 28), sensitivities to changes in hydraulic properties are high on the west, but little changed on the east.

Comparisons of the first three sets of sensitivity analyses suggest that on the eastern side of the valley, and particularly to the north where the geology is more complex, heads are somewhat more sensitive to changes in the unconfined aquifer. Conversely on the west, heads are more sensitive to changes in the confined aquifer, largely because it represents a much greater relative volume of water. For the combined changes in both aquifers, the results appear more consistent with those of confined aquifer alone, since its volume is a large portion of the combined volume.

Sensitivity to the Position of the Interface Between Units

This fourth set of runs tests the sensitivity of the model to the position of the contact between the high and low transmissivity units defined by the magnetic data, and also to the presence of the shallow permeability barrier defined by the magnetic and electrical conductivity data. Figures 29 and 30 show the changes in heads which result when the low hydraulic properties of model Domain IV for both aquifers are replaced by the higher values of Domain II, in effect moving the contact between the

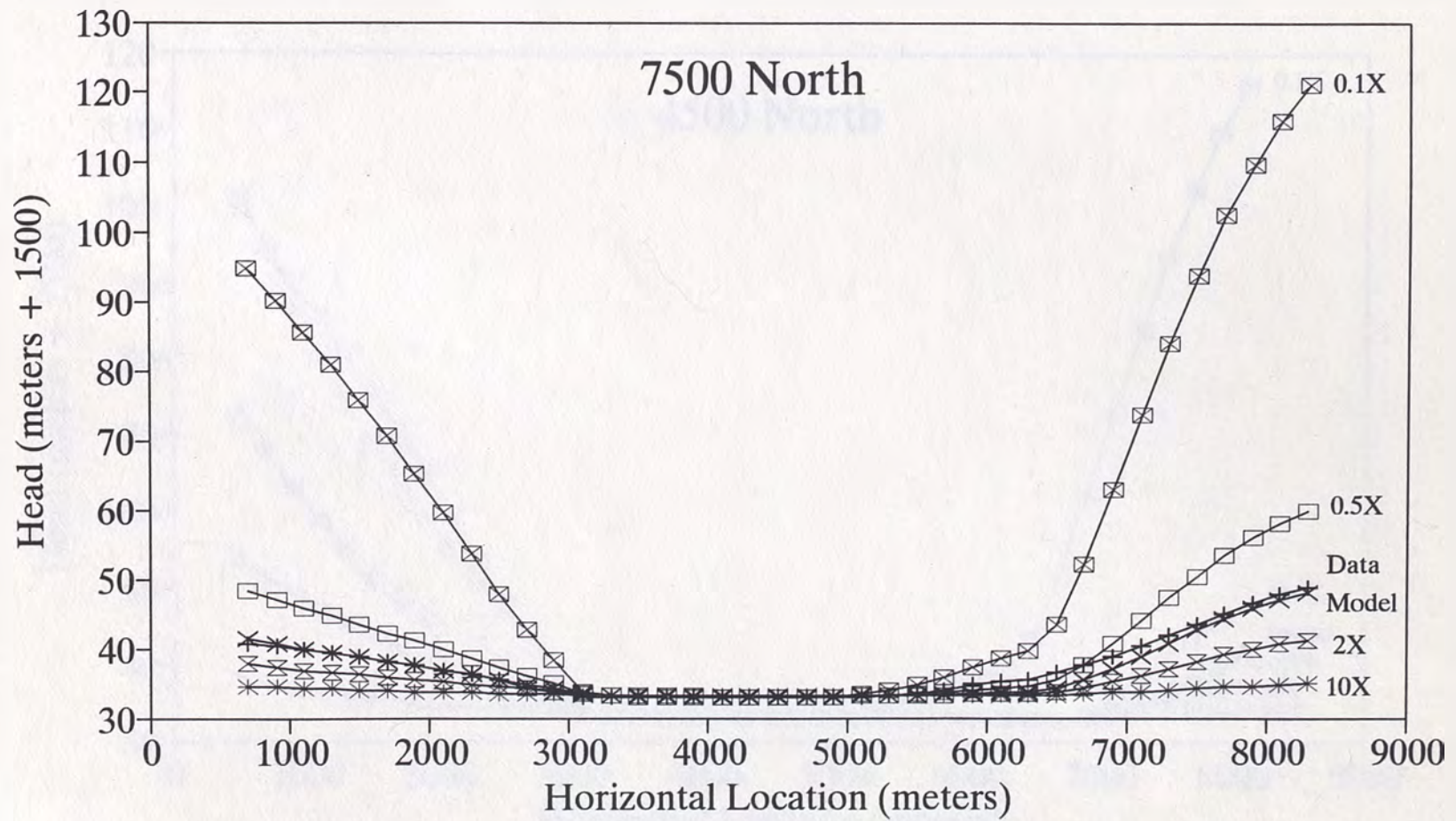


Figure 27. Northern Profile: Sensitivity to Changes in the Hydraulic Properties of Both Aquifers.

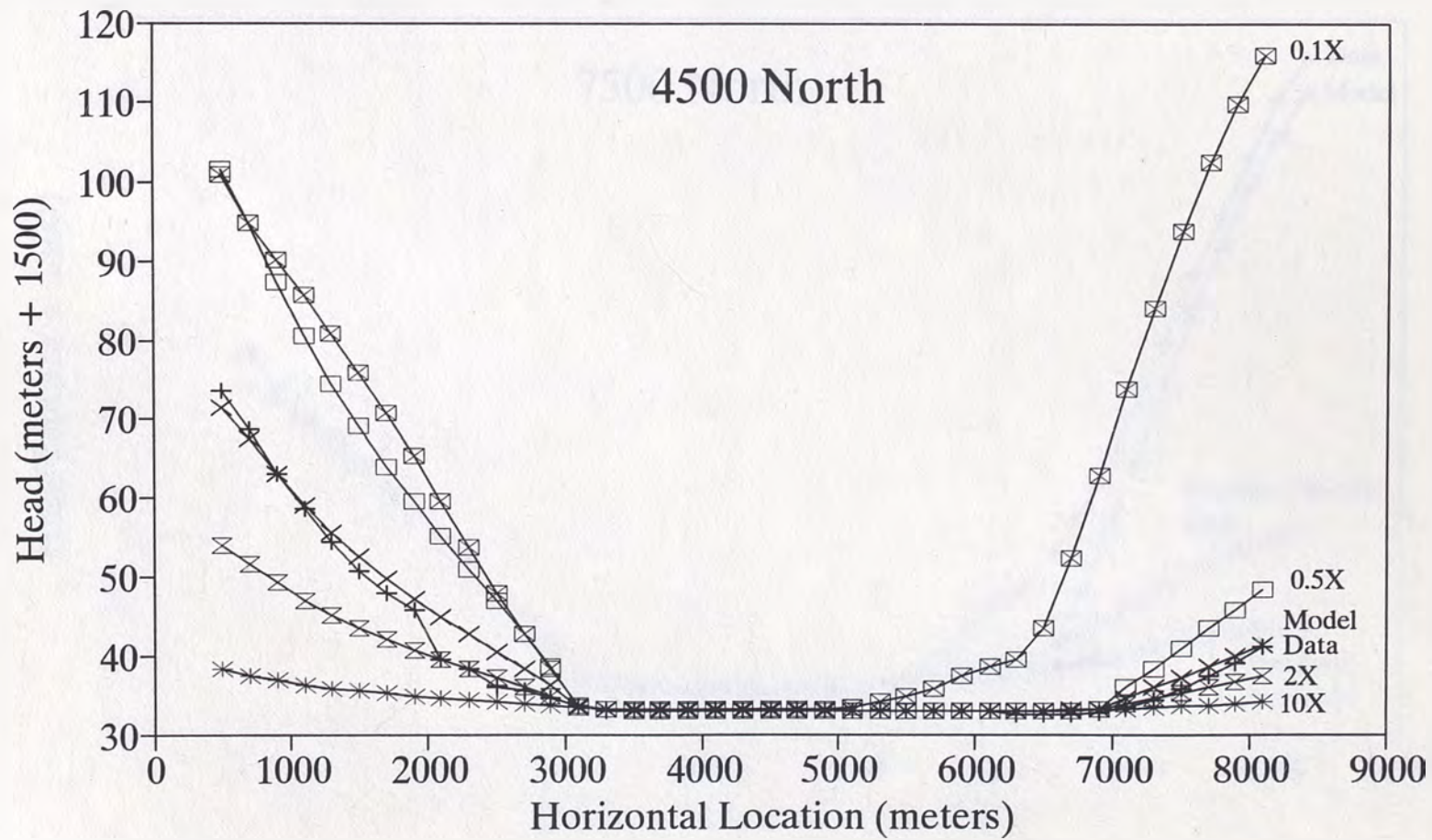


Figure 28. Souther Profile: Sensitivity to Changes in the Hydraulic Properties of Both Aquifers.

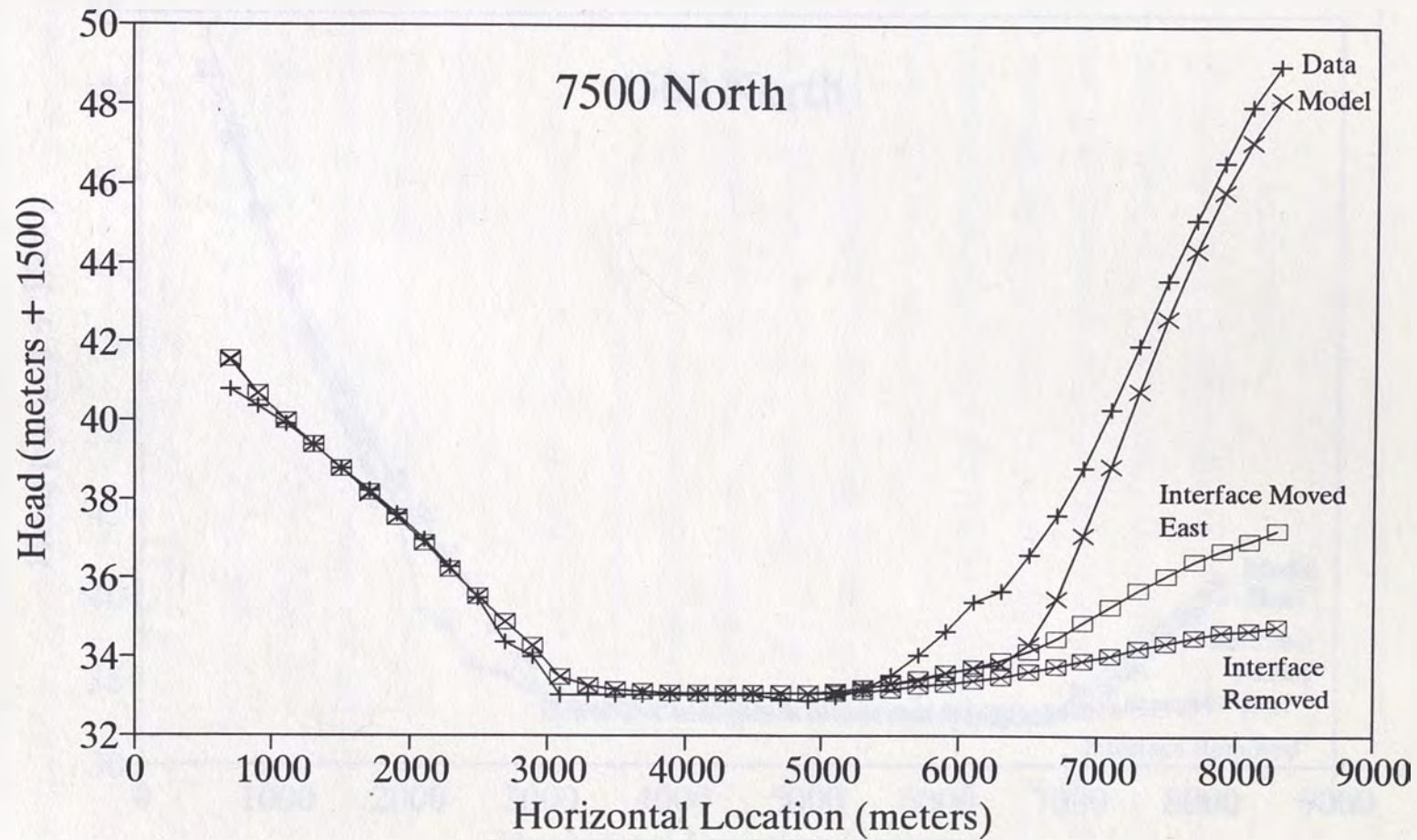


Figure 29. Northern Profile: Sensitivity to the Position of the Interface Between High and Low Transmissivity Units.

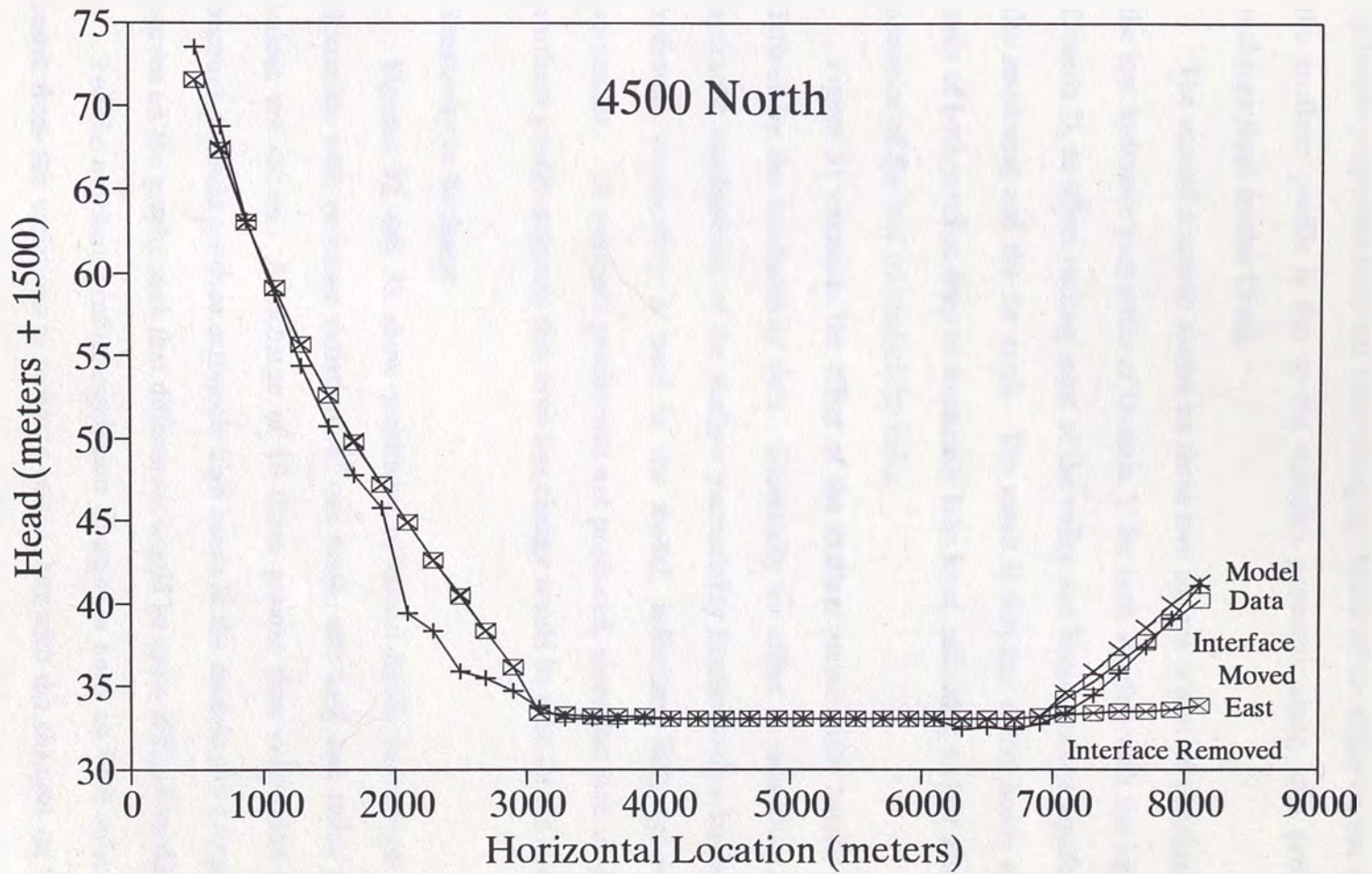


Figure 30. Southern Profile: Sensitivity to the Position of the Interface Between High and Low Transmissivity Units.

expected, no effect is observed on the western end of either profile, where the hydraulic properties have not been changed. Much of the effect on the eastern end of the northern profile is due to the complex geometry along with proximity to the recharge from Jumbo Creek.

The second scenario shown on these two figures is that of additionally replacing the low hydraulic properties of Domain V for both aquifers with the higher values of Domain II, in effect making most of the valley one homogeneous aquifer, except for the southwest and the far north. The result is that the model heads on the eastern ends of both profiles drop to essentially lake level, reflecting a clear sensitivity to the presence of the low transmissivity units.

Figure 31 examines the effect of the shallow permeability barrier (Domain IV) defined by the conductivity data. Essentially no effect is seen from changing the hydraulic conductivity of the shallow permeability barrier until a tenfold increase in hydraulic conductivity is used in the model, indicating little sensitivity to this parameter. A southern profile was not produced, since the lack of change on the northern profile suggests that even less change would be seen on the south.

Sensitivity to Recharge

Figures 32 and 33 show sensitivity of model heads to changes in recharge. Scenarios with recharge variations of one tenth, one half, and twice the calibrated values are shown. A recharge of 10 times greater than calibration is not shown because it would produce extremely high heads in the models and compress the other curves on the graphs such that differences would be more difficult to distinguish.

For the northern profile, significant changes in head on both sides of the valley result from the variations in recharge tested, but with the changes on the east being somewhat greater. For the southern profile, significant changes are also seen on both

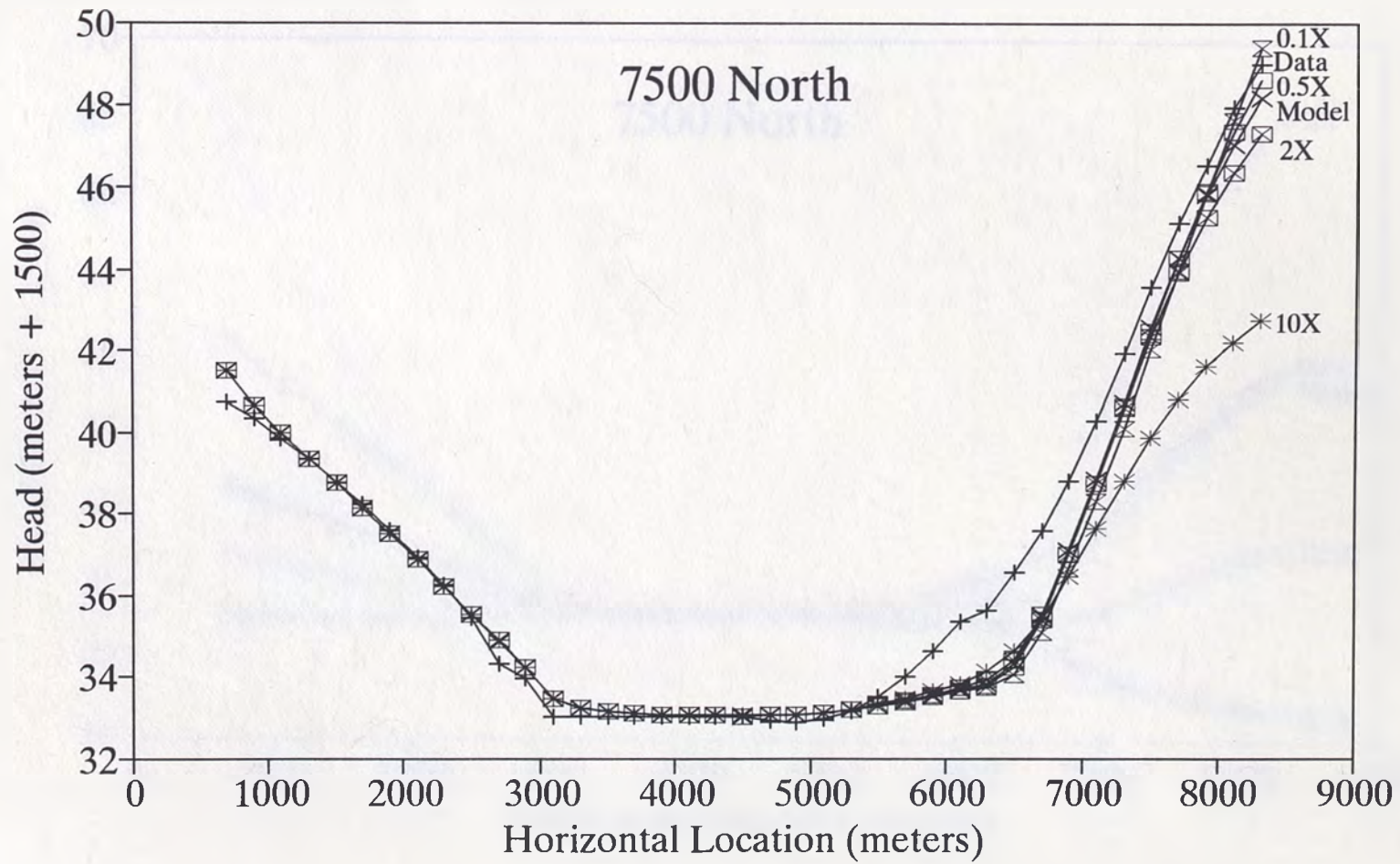


Figure 31. Northern Profile: Sensitivity to the Permeability Barrier.

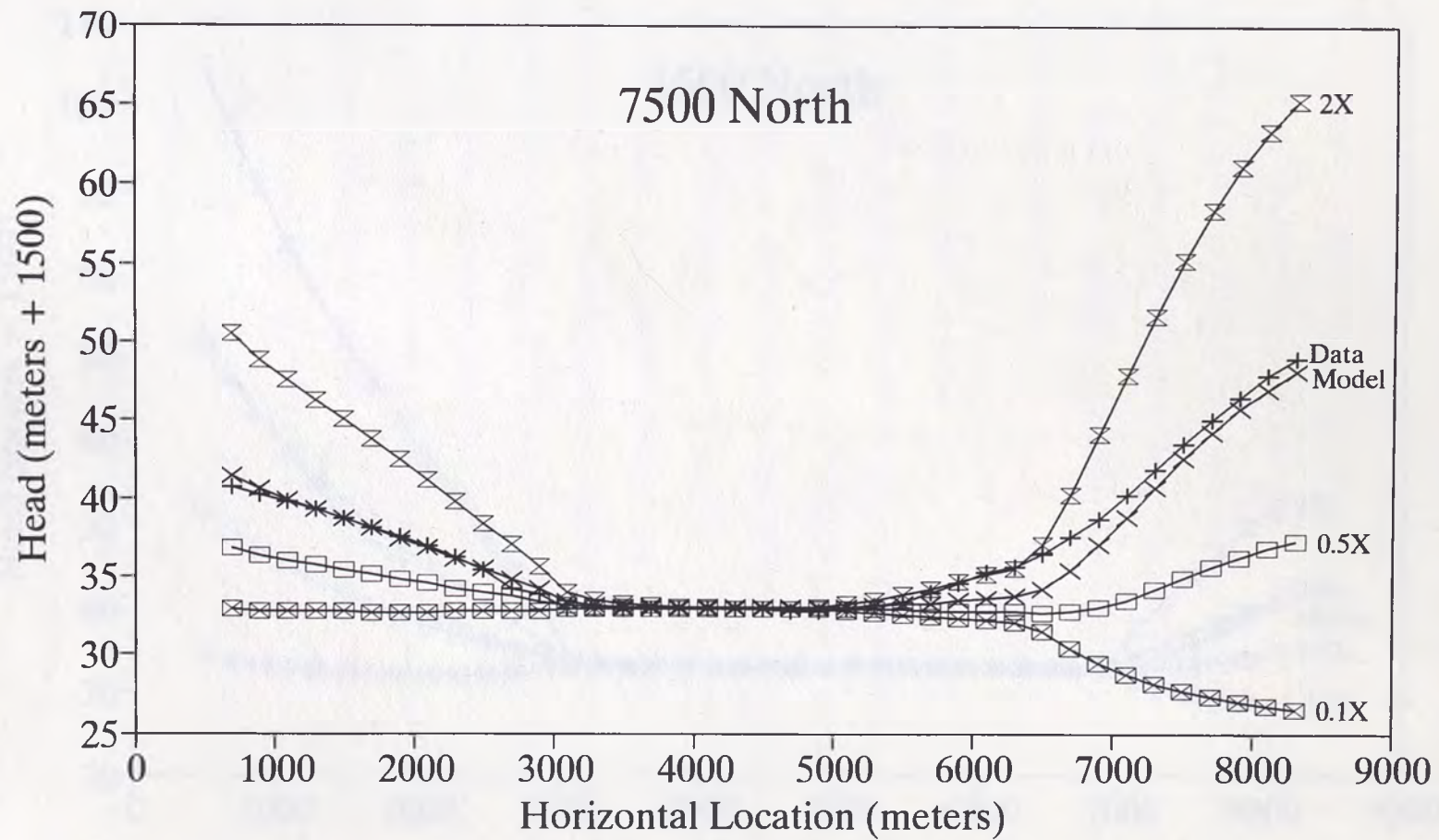


Figure 32. Northern Profile: Sensitivity to Recharge.

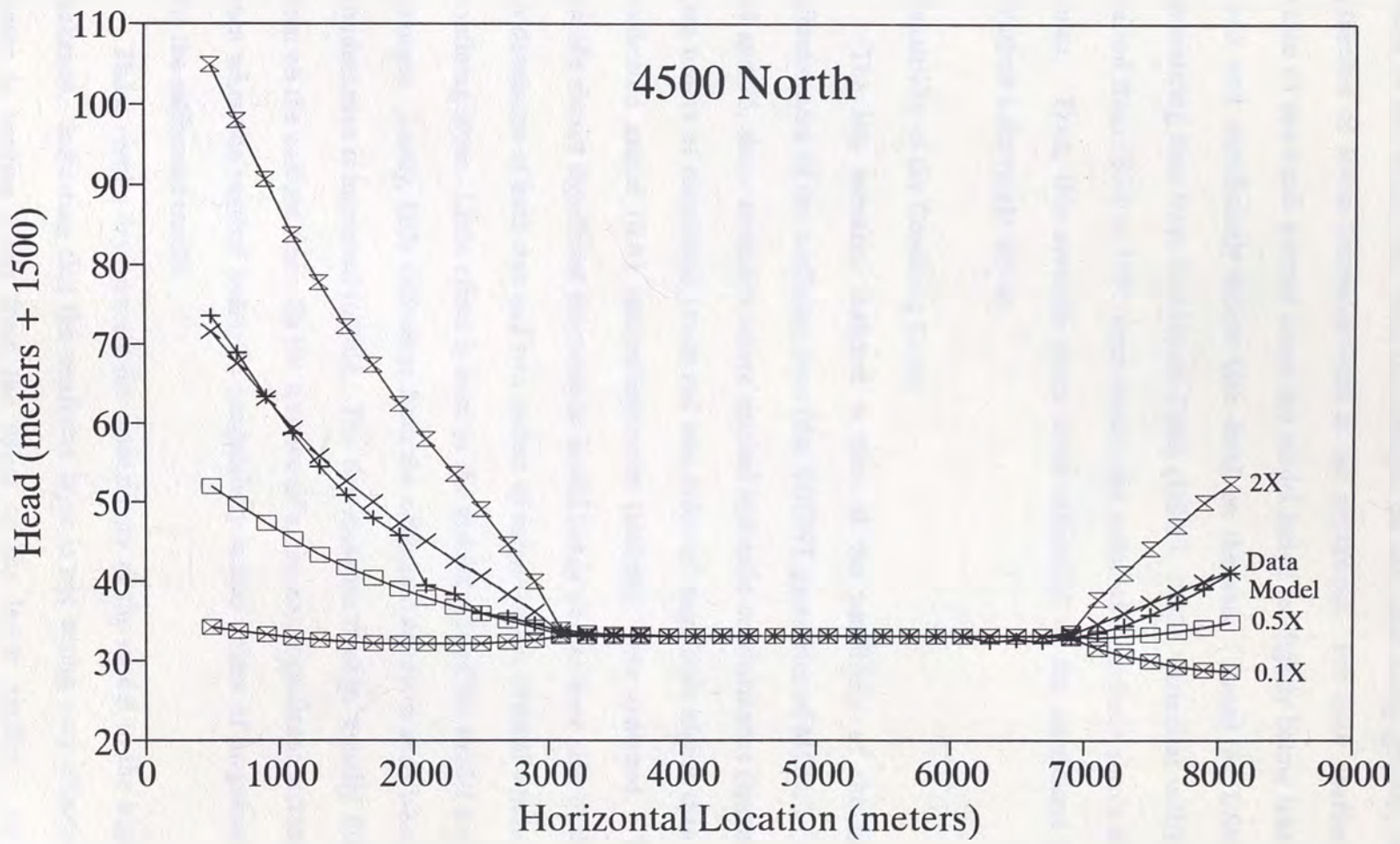


Figure 33. Southern Profile: Sensitivity to Recharge.

sides of the valley, but with the changes on the west being greater, reflecting the presence of lower transmissivities in the southwest. For both profiles, a recharge value of one tenth normal drops the model heads to slightly below lake level on the west and significantly below lake level on the east. Based on USGS long-term monitoring data from Franktown Creek (USGS, 1992), variations within the 17 year period from 1974 to 1991 were about one order of magnitude above and below the mean. Thus, this scenario gives some indication of the conditions under which Washoe Lake might dry up.

Sensitivity to the Confining Layer

The last scenario analyzed is that of the sensitivity of the model to the effectiveness of the confining layer (the VCONT parameter of MODFLOW). Figures 34 and 35, show scenarios where vertical hydraulic conductances (leakance) one and two orders of magnitude lower and one order of magnitude higher than those of the calibrated model (0.01 meters/day/meter (m/d/m)) were analyzed. The northern profile shows significant increases in model heads on the west side of the valley due to decreases of both one and two orders of magnitude in vertical conductance of the confining layer. Little effect is seen on the eastern side of the model due to the same changes. Lastly, little difference from the calibrated model is seen when the vertical conductance is increased tenfold. For the southern profile, equally little change is seen on the eastern side. On the western side, the only significant increase in heads is seen when the vertical hydraulic conductivity is two orders of magnitude lower than for the calibrated model.

These results demonstrate the insensitivity of the model to the higher values of leakance, indicating that the confining layer is not acting very effectively. That is, water is moving freely from the upper to the lower aquifer. As the vertical

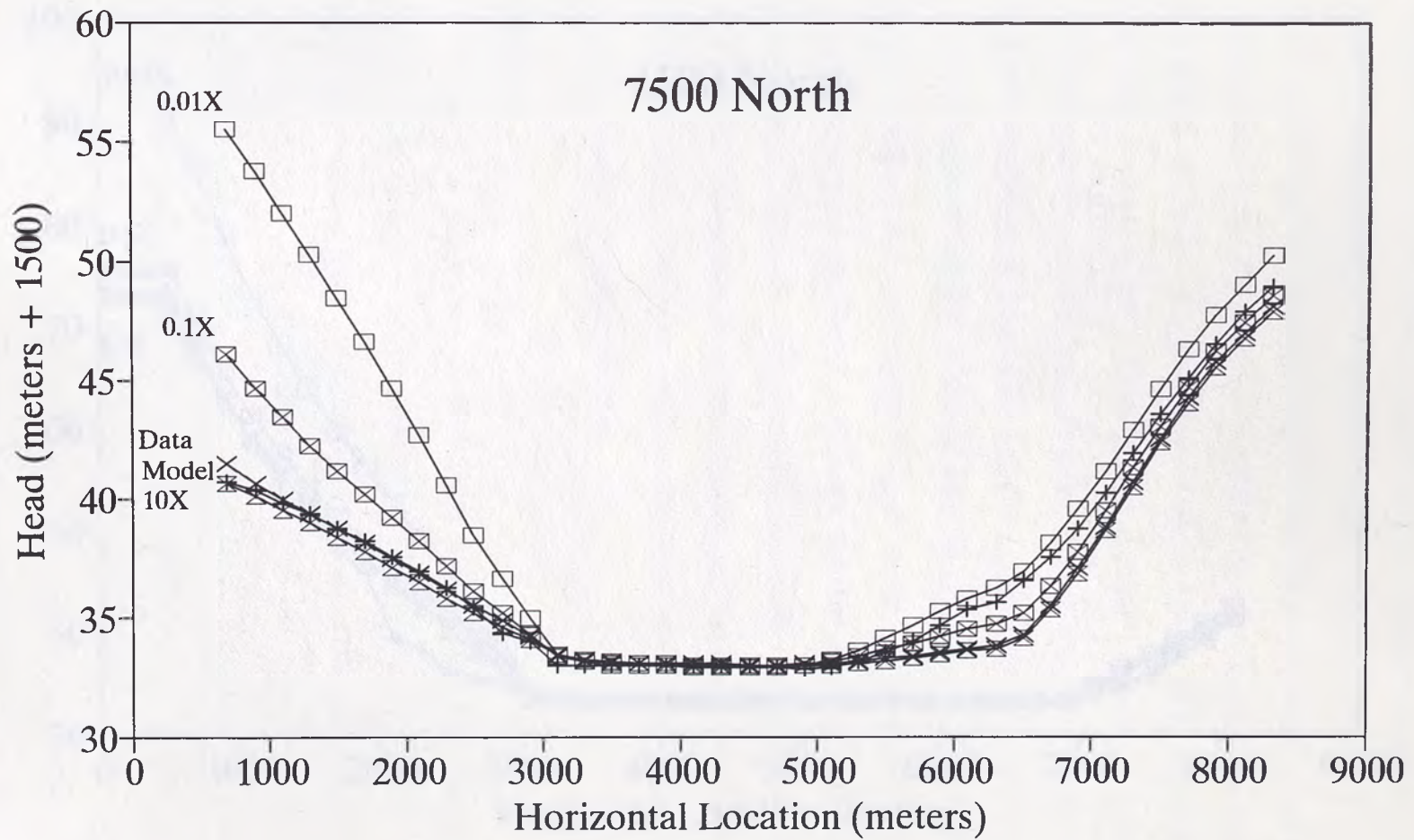


Figure 34. Sensitivity to the Leakance of the Confining Layer.

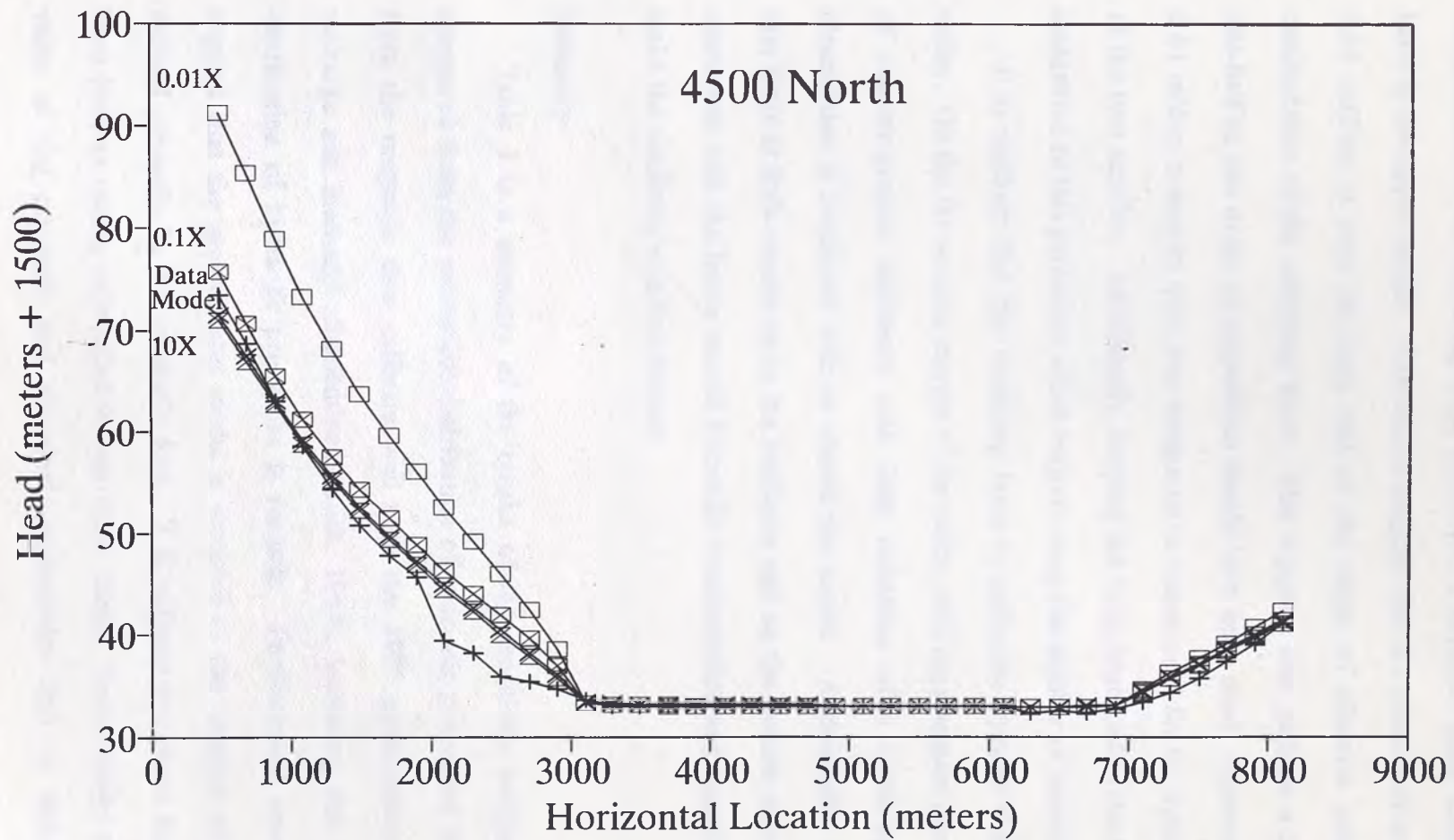


Figure 35. Southern Profile. Sensitivity to the Leakance of the Confining Layer.

conductance of the confining layer decreases, it becomes more effective and heads build in the upper aquifer. The models suggest that the value used in the calibration, 0.01 m/d/m, is near the high end of the range of effective values of vertical conductance of the confining layer. This suggests that perhaps a lower value (by one-half to one order of magnitude) should have been used. However, the value of 0.01 m/d/m is already quite low compared to values used for the hydraulic properties of the two aquifers. Additionally, keeping the value high makes the model relatively insensitive to this parameter which helps to keep the number of variables down.

It is unlikely that the confining layer is uniformly present beneath the entire valley. On the far western margin of the valley, drill logs suggest greater thicknesses of coarser-grained sediments with little indication of a confining layer. This observation is consistent with an alluvial fan model. Additionally, the observation that there is little sensitivity to the confining unit on the eastern side of the valley is consistent with the lower overall hydraulic conductivities and transmissivities which make the confining unit less distinct.

Summary

Table 3 is a summary of the results of the sensitivity analyses. The heads computed from the subsurface distribution of hydraulic properties defined primarily from the magnetic data calibrate well with the 1965 potentiometric surface and recharge and discharge distributions (Rush, 1967), indicating that this subsurface distribution of hydraulic properties is realistic. Furthermore, sensitivity analyses suggest that the groundwater model is sensitive to the location of the boundaries defined primarily by the magnetic data. It is unlikely that these boundaries would have been as readily indentified by any other means. These results clearly show the value of the magnetic and electrical conductivity data in defining inter-basin

variations in hydraulic properties for input to the groundwater flow model. The geologic sources of the lower transmissivity units required by the model for the eastern subsurface have distinct geophysical signatures.

Table 3. Summary of Sensitivity analyses.

<u>Parameter</u>	<u>Sensitivity</u>
K's of unconfined aquifer	Higher on east
T's of confined aquifer	Slightly higher on west
Combined effect of both aquifers	Slightly higher on west
Recharge	Higher where Transmissivities are low
Boundary location	Moderate to high
Presence of the permeability barrier	Generally low
Leakance	Low to moderate

Aquifer properties normally varied by factors of 0.1, 0.5, 2.0 and 10X.

Limitations of the Model

The model represents a simplification of the flow system of Washoe Valley. Estimates based on sparse data and/or regional values were made for many of the parameters, partly because better information was not available, and partly because of an effort to minimize the number of other variables so that the effects due to the features identified in the geophysical results could be isolated and examined. While the degree to which the model was simplified may be acceptable here, more accurate values for most parameters are needed to analyze the long term effects of projected increases in consumptive use, coupled with a high likelihood of being exacerbated by

one or more periods of extended drought. The model was only calibrated to a steady-state scenario, but transient calibration is clearly needed.

The River package of MODFLOW was used to simulate the effects of flow between Washoe Lake and the groundwater system. In the model, this package limits the amount of simulated flow between the surface water body and the aquifer by limiting range of head differences which control this flow. For this study, the limiting head value was set at the average surface elevation of Washoe Lake (1533 meters). This puts an arbitrary and perhaps unrealistic constraint on the system, particularly under extreme values in recharge or discharge. The other option for modeling a surface water body in a groundwater system is to not limit the amount of flow into and out of the system due to head differences between the surface water body and the aquifer. In effect, this makes the lake a part of the problem domain instead of a boundary. The lake level in the model is allowed to build until the size of the model lake equals the size of the real lake. This option was not used initially because calibration is more difficult to achieve and it was felt that the more limiting nature of the River package would better constrain the model such that the effects of the variations in hydraulic properties defined by the magnetic and electromagnetic surveys could be more readily isolated and examined. Whenever a lake is incorporated into a groundwater model, setting its head to a constant value is a common practice because the calibration is easier. Furthermore, the software to handle variable lake heads has not been available (Cheng and Anderson, 1993). Using a constant head for the lake surface is particularly expeditious when one's objective is to obtain an initial sense of the effects of a particular parameter, as it is here.

Use of the River package requires the specification of a conductance term which defines how readily water passes between the aquifer and the surface water body.

Because no field data were available from which to estimate values for this term, it was set to a high value such that in the model water could flow freely from the aquifer to the lake. Possible effects of variations in this parameter were not evaluated. Setting this parameter to a lower value might have been more geologically realistic, but it would have added another degree of complexity to the model.

Clearly, re-evaluation of the areal distribution of recharge and discharge are also needed. The model assumes all recharge is at the margins of the basin. Almost certainly there is some recharge along the courses of streams on the valley floor, but little data were available from which to make reasonable estimates of this parameter. The model was calibrated with a uniform recharge rate along the western side of the basin, although earlier data (Rush, 1967) suggest that half the west side recharge comes from Franktown Creek. When this distribution of recharge was used in the model, the 1965 potentiometric surface could not be duplicated.

Data on the spatial distribution of hydraulic properties within the basin, particularly of the complex eastern subsurface, are still quite limited. Due to the limited recharge from the east, groundwater flow in the model is extremely sensitive to the spatial positions of subsurface heterogeneities relative to the recharge points.

In numerous wells in the 1965 data set (Rush, 1967), it is difficult at best to distinguish heads in the confined aquifer from the water table. This was particularly true when available driller's logs indicated multiple screening of a well. Thus, "mixing" of the two potentiometric surfaces may have occurred in some areas.

The effects of seasonality are not addressed. Recharges and discharges were treated as annual net numbers whereas in reality most of the recharge in the form of runoff from snowmelt occurs in the spring and most of the discharge in the form of evaporation and evapotranspiration occurs in the summer.

CONCLUSIONS AND RECOMMENDATIONS

From the combined geophysical and groundwater modeling efforts in Washoe Valley, the following conclusions can be drawn:

- 1) Transmissivities of the eastern subsurface of Washoe valley are generally much lower than those of the western subsurface, by as much as one to two orders of magnitude.
- 2) The eastern subsurface is much more geologically and hydrologically complex, particularly in the shallow subsurface.
- 3) This complexity results in a much greater sensitivity of the east side of the valley to changes in recharge/discharge conditions.

The geophysical data play a key role in developing the groundwater model by identifying several lithologic units for which hydraulic parameters can be estimated, and by defining the boundaries of these units. Lower transmissivity units in the eastern subsurface have distinct magnetic and electrical signatures. The groundwater model does not show a particularly strong sensitivity to the edge of the volcanic unit beneath Washoe Lake, whereas the magnetic model does. Knowledge of the location of the edge of the volcanic unit is critical for locating future water wells.

The unit of intermediate transmissivities to the southwest is clearly needed in the groundwater model. Its hydraulic properties are well defined in the specific capacity data and supported by other observations in the driller's logs. Owing largely to a lack of coverage, the hydraulic properties of this unit are not well defined in any of the geophysical data sets, however, its boundaries are well defined by the magnetic data (Figures 7 and 8). Thus the groundwater and the geophysical data supplement each other in this region.

The spatial coincidence of the shallow resistivity low, indicating finer-grained sediments, with the edge of the buried magnetic high is strong evidence for a genetic relationship between deep structure and shallow sediment depositional patterns. While postulation of a specific mechanism for such a relationship is beyond the scope of this work, such a relationship does suggest that deeper tectonic features in this and similar basins may exert strong control on shallower groundwater movement and sediment deposition patterns. The eastern subsurface of Washoe valley has a clearly different depositional character than in the west. Thus, there were probably two ancient Washoe Lakes, one lying in the deeper basin to the west (Figure 11), similar in character to the present-day Washoe Lake, and the other a much smaller and probably more marshy lake, with a locus much farther east.

The present study suggests several directions for future work, including:

- 1) A more detailed mapping of heterogeneities in the eastern subsurface, using a combination of magnetic/electromagnetic surveys.
- 2) A re-evaluation of recharge estimates from both sides of the valley using updated precipitation and stream flow data. This is particularly important in the east, where a more precise knowledge of recharge distribution in relationship to aquifer heterogeneities is critical.
- 3) A better evaluation of the true areal distribution of evapotranspiration based on updated maps of vegetation, land use, and the water table, particularly from the western side of the valley, where it is perhaps underestimated by the present model. Using a higher ET rate on the west side of the valley would effectively reduce the percentage of eastern side recharge to ratios more in line with those of earlier estimates.
- 4) Inclusion of available data on seasonal relationships of recharge and

discharge and seasonal and long-term fluctuations in well levels in the transient model. These will lead to a better understanding of overall flow patterns in the valley and a further refinement of the water balance.

- 5) Transient modeling with no controls on the lake surface elevation would provide a better understanding of lake-groundwater interactions and the long term effects of potential drought conditions and/or increased consumptive use.

In summary, geophysical data provide important constraints on groundwater models. Gravity can be used to define overall basin structure. Magnetics is useful in evaluating detailed stratigraphy within the basin. Joint modeling of gravity and magnetics provides much better constraints on overall basin configuration and interbasin lithology than is possible from modeling either individually. Electromagnetic measurements provide excellent definition of shallow variations in hydraulic properties. Limits of possible models can be further constrained by known geology and data from borehole logs.

Groundwater modeling is important because it helps us understand the subsurface groundwater flow of a particular area or basin. However, groundwater models are only as good as the data on which they are built. This work demonstrates that geophysical surveys, particularly magnetic and electromagnetic data, provide important information on the subsurface distribution of hydraulic properties that are essential to understanding the groundwater flow regime of Washoe Valley.

REFERENCES

- Anderson, M.P., and W. Woessner, 1992, *Applied Groundwater Modeling-simulation of Flow and Advective Transport*, Academic Press, 381 p.
- Arteaga, F.E., and W.D. Nichols, 1984, *Hydrology of Washoe Valley, Washoe County, Nevada*, U.S. Geological Survey Open File Report 84-465.
- Burbey, T.J., and D.E. Prudic, 1991, *Conceptual evaluation of regional ground-water flow in the carbonate rock province of the Great Basin, Nevada, Utah, and adjacent states*. U.S. Geological Survey Professional Paper 1409-D.
- Cashman, P.H., 1993, *Personal communication*.
- Cheng, X., and M.P. Anderson, 1993, *Numerical simulation of ground-water interaction with lakes allowing for fluctuating lake levels*, *Groundwater*, v. 31, no. 6, pp. 929-933.
- Dobrin, M.B., and C.H. Savit, 1988, *Introduction to Geophysical Prospecting*, McGraw-Hill, Inc., 867 p.
- Freeze, R.A., and J.M. Cherry, 1979, *Groundwater*, Prentice-Hall, 604 p.
- Graumlich, L.J., 1992, *A 1000-year record of climatic variability in the Sierra Nevada, USA.*, abs., American Quaternary Assoc. biennial meeting, Univ. of Calif., Davis.
- Hadiaris, A.K., 1988, *Quantitative analysis of groundwater flow in Spanish Springs Valley, Washoe County, Nevada*, unpublished Master's thesis, University of Nevada, Reno.
- Houghton, J.G., C.M. Sakamoto, and R.O. Gifford, 1975, *Nevada's Weather and Climate, Special Publication #2*, Nevada Bureau of Mines and Geology, University of Nevada Reno, 78p.
- Karlin, R., J. Trexler, and R. Petersen, 1993, *Initial results from paleoclimatic drilling and geophysical studies, Washoe Lake, Nevada*, abs.
- Kelly, W.E., and P.F. Reiter, 1984, *Influence of anisotropy on relations between electrical and hydraulic properties of aquifers.*, *J. Hydrol.*, 74, pp. 311-321.
- Lyons, W.B., 1993, *personal communication*.

- Martinelli, D.M., 1989, Geophysical investigations of the northern Sierra Nevada-Basin and Range boundary, west-central Nevada and east-central California, unpublished Master's thesis, University of Nevada, Reno.
- Mazac, O, M. Cislerova, W. E. Kelly, I. Landa, and D. Venodova, 1990, Determination of hydraulic conductivities by surface geoelectric methods, in *Geotechnical and Environmental Geophysics*, v. 2, pp. 125-131, Society of Exploration Geophysicists.
- McDonald, M.G., and A.W. Harbaugh, 1988, A modular three-dimensional finite-difference ground-water flow model, Book 6, Chapter A1, *Techniques of water resources investigations of the United States Geological Survey*.
- McKay, W.A., 1991, Analysis of groundwater quality in New Washoe City, Nevada, unpublished Master's thesis, University of Nevada, Reno.
- McNeill, J.D., 1980, Electrical conductivity of soils and rocks, Geonics, Ltd. Technical Note TN-5
- McNeill, J.D., 1980, Electromagnetic terrain conductivity measurements at low induction numbers, Geonics, Ltd. Technical Note TN-6
- McNeill, J.D., 1980, Applications of transient electromagnetic techniques, Geonics, Ltd. Technical Note TN-7.
- Nichols, W.D., 1989, Reconstructed drought history, north-central Great Basin: 1601-1982, in *Aspects of Climate Variability in the Pacific and Western Americas*, pp.61-68, *Geophysical Monograph 55*, The American Geophysical Union.
- Palacky, G. 1987, Resistivity characteristics of geologic targets, in *Electromagnetic Methods in Applied Geophysics*, p. 53-129, Society of Exploration Geophysicists.
- Petersen, R., J. Hild, and P. Hoekstra, 1989, Geophysical studies for the exploration of groundwater in the Basin and Range of northern Nevada, in *Proceedings of the Symposium on the Application of Geophysics to Engineering and Environmental Problems*, The Society of Engineering and Mineral Exploration Geophysicists, p. 425-435.
- Plume, R.W., 1987, Use of aeromagnetic data to define boundaries of a carbonate-rock aquifer in east-central Nevada, U.S. Geological Survey Water Supply Paper 2330, p. 1-10.
- Profett, J.M. Jr., 1977, Cenozoic geology of the Yerington district, Nevada, and implications for the nature and origin of Basin and Range faulting, *GSA Bulletin* v.88, pp. 247-266.

- Robinson, E.S., and C. Coruh, 1988, *Basic Exploration Geophysics*, John Wiley & Sons, 562 p.
- Rush, F. E., 1967, *Water-resources appraisal of Washoe Valley, Nevada*, U.S. Geological Survey Water Resources Reconnaissance Series Report 41.
- Saltus, R.W., 1988, *Gravity data set for the state of Nevada on magnetic tape*, EROS Data Center, Sioux Falls, S.D., 57108.
- Tabor, R.W., S.E. Ellen, M.M. Clark, P.A. Glancy, and T.L. Katzer, 1983, *Geology, geophysics, geologic hazards, and engineering and geologic character of earth materials in the Washoe Lake area, text to accompany the maps of the environmental series, Washoe City Quadrangle, Nevada*, Nevada Bureau of Mines and Geology Open File Report 83-7.
- Thomas, J.M., S.M. Carlton, and L.B. Hines, 1989, *Ground-Water hydrology and simulated effects of development in Smith Creek valley, a hydrologically closed basin in Lander County, Nevada*. U.S. Geological Survey Professional Paper 1409-E.
- Thompson, G.A., and C.H. Sandberg, 1958, *Structural significance of gravity surveys in the Virginia Range-Mount Rose Area, Nevada and California*, *Bull. Geol. Soc. America.*, 69, pp. 1269-1282.
- Urish, D.W., 1981, *Electrical resistivity-hydraulic conductivity relationships in glacial outwash aquifers*, *Water Resources Research*, 17(5), pp. 1401-1408.
- U.S. Geological Survey, 1992, *Water Data Report NV-91-1*, 481 p.
- Whitebread, D.H., 1976, *Alteration and geochemistry of volcanic rocks in parts of the Virginia City Quadrangle, Nevada*, U.S. Geological Survey Professional Paper 936.
- Winter, T.C., 1981, *Uncertainties in estimating the water balance of lakes*, *Water Resources Bulletin*, 17(1), pp. 82-115.

APPENDIX A: DRIFT CORRECTIONS

Gravity and magnetic data need to be corrected for secular drift. The causes of drift are different for the two methods, and there are different ways of making the drift corrections, depending upon the degree of accuracy desired. When only moderate accuracy is required, a linear drift correction employing one or more base stations is usually adequate.

Gravity

The primary causes of secular drift in gravity surveys are tidal effects caused by the sun and moon, and drift of the instrument due to temperature variations. Because the LaCoste and Romberg gravimeter is temperature-stabilized, instrumental drift is normally small unless an instrument problem or extreme conditions are encountered. The tidal effects of the sun and moon are entirely predictable and programs are available with which to make tidal corrections. However, unless extreme accuracy is required, such as for micro-gravity surveys, most of the tidal effect can be "captured" by frequent reoccupation of base stations. At Washoe Lake, gravity base stations were occupied, at a minimum, at the beginning of data collection, near mid-day, and at the end of data collection. Base stations were occupied more frequently whenever possible. The sensitivity of the LaCoste and Romberg Gravimeter is 0.01 milligals (mg). Diurnal variations in gravity are typically on the order of 0.05 to 0.10 mg., although the error encountered in measuring this variation is probably much less. These errors are small relative to the amplitude of the gravity anomaly of the area, which is about 10 mg.

Magnetics

Most magnetic drift is caused by electromagnetic phenomena in or above the earth's atmosphere. While it is diurnal in nature, it is somewhat less predictable than gravitational tidal effects. With modern recording magnetometers, the present field procedure is to leave one magnetometer at a base station recording the magnetic field at pre-selected time intervals. At the end of each field day, the data sets are merged into a computer and the field data drift corrected automatically. However, this requires the added expense of a second magnetometer, which was not available on an academic budget. The sensitivity of the magnetometers employed is 1 nanotesla (nT). The amplitude of the diurnal magnetic drift (excluding magnetic storms) is on the order of 20-40 nT. Because this drift is rather smoothly-varying, most of it can be captured, as with gravity, by occupying base stations at the beginning of data collection, near mid-day, and at the end of data collection, plus whenever else is convenient. This generally provides an accuracy of corrected data on the order of a few nT. Because the magnitude of the variations due to lithologic sources in the subsurface of Washoe Valley is on the order of 300 nT, errors of a few nT are acceptable.

Base Stations

The main base station for both the gravity and magnetic surveys was at the wooden park sign immediately east of the paved parking area on the east side of Highway 395 at exit 44 (the Bellevue exit). Other temporary base stations were established as necessary through the course of the gravity and magnetic surveys.

Drift Correction Algorithm

The following algorithm was used to correct both the gravity and magnetic data. It requires that a base station be occupied at the beginning and the end of the time

period during which the field stations were recorded. It applies a simple linear drift correction to the data, that is, it assumes that the drift in the field during the time interval between occupation of the base station(s) was simply linear. While the actual fields do not necessarily vary linearly, this is usually an adequate approximation for time periods up to a few hours.

The following algorithm is generalized in that it can handle drift corrections when multiple base stations are employed. That is, different base stations can be occupied at the beginning and end of the data recording period in question. This can offer great logistical convenience for surveys over large areas (it is tacitly assumed that the base stations have been previously leveled to a common datum). The true gravity value, $X(I)$, at a station I is given by:

$$X(I) = GB1 + [D(I) - DB1] * CONS - [T(I) - TB1] * DELTA(I)$$

Where:

$$DELTA(I) = \frac{(DB2 - DB1) * CONS - (GB1 - GB2)}{TB2 - TB1}$$

and where:

GB1 = Gravity at Base 1

GB2 = Gravity at Base 2

DB1 = Dial reading at Base 1

DB2 = Dial reading at Base 2

D(I) = Dial reading at station(I)

TB1 = Time at Base 1

TB2 = Time at Base 2

T(I) = Time at station(I)

CONS = the meter constant. For magnetics, the value of CONS is 1.0. For gravity, it is a number slightly greater than 1.0. The exact value is meter-specific, and is provided in the operators manual that comes with the instrument.

APPENDIX B: GRAVITY DATA

Free air, Bouguer, Latitude, and terrain corrections were made to the gravity stations collected for this thesis to obtain complete Bouguer gravity values, using the formula:

$$BG = OG - LC + FAC - BC + TC$$

where

BG = the complete Bouguer Gravity

OG = the observed gravity (after drift correction)

LC = the latitude correction = 7.958×10^{-4} mgal/m.

FAC = the free air correction = 0.3086 mgal/m \times E, where E = the elevation in meters.

BC = the Bouguer Correction = 0.112 mgal/m \times E, where E = the elevation in meters, and assuming a Bouguer reduction density of 2.67 g/cm³.

All of the data from this survey were reduced to a common datum. The data were then merged with the regional data to produce the contour map shown in Figure 6. Based on a comparison of 5 common station, a value of 177.22 milligals was subtracted from our data to level it with the regional data. The standard deviation for the 5 stations was about +/- 0.25 mgal.

Full terrain corrections would have been too time consuming. However, rough terrain corrections were estimated in the following manner: The total terrain corrections for all of the regional stations were gridded and contoured with SURFER. These contours were overlain on our data, and terrain corrections for each station were picked off the contours. This method was judged to be a reasonable compromise between making no correction at all, and going through the tedium of full terrain

corrections. There is an obvious near terrain correction from the nearby mountain ranges. However, it was assumed that the total terrain correction would not vary much over the survey area.

Most gravity stations were read at points where GPS elevations were available. These were accurate to a few centimeters, which was more than adequate for gravity reduction on this scale. For the few stations that did not have GPS data, elevations were estimated by interpolating between stations of known elevation. Given the relatively flat topography of the lake bed, this was judged to be acceptable.

The principal facts for the gravity stations of this survey are tabulated on the following pages.

WASHOE LAKE REDUCED GRAVITY

	10/18/91	11/08/91	11/23/91	12/05/91	12/05/91
CONS	1.02257	1.02257	1.02257	1.02257	1.02257
GB1	70.16	70.16	70.16	67.91	67.91
GB2	70.16	70.16	70.16	67.91	67.91
DB1	69.73	69.65	70.16	68.7	69.24
TB1	9.4	12.15	13.33	12.37	13.2167
DB2	69.82	69.7	70.22	68.78	69.17
TB2	14.433	16.5833	16.5	17.43	14.8

LATITUDE CORRECTION FACTOR

0.011533	0.019355	0.016167	-0.04521	0.0007958	400
----------	----------	----------	----------	-----------	-----

X-COORD	Y-COORD	RAWGRV	TIME	CORGRV	ELEV	BC	FAC	LC	BG
53.047	-2083.34	71.17	1624	70.37059	1535.069	170.29798	473.7158	-1.65798	-24.5536
41.227	-1845.76	70.85	1617	70.04526	1534.986	170.28877	473.6902	-1.46891	-25.0844
29.595	-1610.45	70.69	1612	69.88299	1534.93	170.28256	473.673	-1.28164	-25.445
29.501	-1379.14	70.22	1605	69.40427	1534.87	170.2759	473.6544	-1.09756	-26.1196
24.17	-1161.78	70.1	1601	69.28264	1534.83	170.27146	473.6421	-0.92458	-26.4222
13.13	-922.2	70.12	1557	69.30417	1534.767	170.26447	473.6227	-0.73391	-26.6037
6.133	-694.362	70.36	1552	69.55094	1534.756	170.26325	473.6193	-0.55259	-26.5405
0.403	-464.877	70.61	1548	69.80766	1534.721	170.25937	473.6085	-0.36996	-26.4733
-1.27	-233.21	71	1544	70.20754	1534.731	170.26048	473.6115	-0.1856	-26.2558
0	0	71.19	1539	70.40317	1534.836	170.27213	473.6439	0	-26.225
-1.285	227.158	71.38	1535	70.59854	1534.711	170.25826	473.6054	0.180779	-26.2351
-1.285	227.158	70.17	1552	70.64887	1534.711	170.25826	473.6054	0.180779	-26.1848
-2.0735	341.165	70.18	1545	70.66044	1534.751	170.2627	473.6177	0.271509	-26.256
-2.862	455.172	70.12	1539	70.60024	1534.791	170.26714	473.6301	0.362239	-26.3991
-3.43	578.18	69.97	1534	70.44782	1534.813	170.26958	473.6368	0.460132	-26.645
-4.006	701.19	69.86	1602	70.32995	1534.835	170.27202	473.6436	0.558027	-26.8565
-6.7515	824.4095	69.84	1607	70.30854	1534.9465	170.28439	473.678	0.656088	-26.9539
-9.497	947.629	69.88	1633	70.34445	1535.058	170.29676	473.7125	0.75415	-26.994
-11.8945	1070.334	69.86	1618	70.32688	1535.1225	170.30391	473.7324	0.851802	-27.0965
-14.292	1193.038	69.77	1622	70.23408	1535.187	170.31107	473.7523	0.949453	-27.2742
-17.123	1314.396	69.75	1627	70.21267	1535.179	170.31018	473.7498	1.046034	-27.3938
-14.586	1435.661	69.75	1633	70.21151	1536.264	170.43055	474.0846	1.14254	-27.277
-113.645	714.7685	69.32	1233	69.81794	1534.852	170.2739	473.6489	0.568833	-27.3759
-223.283	728.347	68.81	1237	69.29566	1534.869	170.27579	473.6541	0.579639	-27.9056
-337.559	738.763	68.41	1246	68.8849	1534.88	170.27701	473.6575	0.587929	-28.3225
-451.834	749.179	67.97	1251	68.43401	1534.891	170.27823	473.6609	0.596218	-28.7795
-568.355	753.5755	67.46	1257	67.91135	1534.9653	170.28647	473.6838	0.599717	-29.291
-684.876	757.972	67.03	1302	67.47068	1535.0395	170.2947	473.7067	0.603216	-29.7205
-801.397	762.3685	66.6	1315	67.02848	1535.1138	170.30294	473.7297	0.606714	-30.1515
-917.918	766.765	66.27	1320	66.69007	1535.188	170.31118	473.7526	0.610213	-30.4788
-1035.5	769.7725	65.85	1326	66.25943	1535.4955	170.34529	473.8475	0.612607	-30.851
-1153.08	772.78	65.35	1333	65.7468	1535.803	170.3794	473.9424	0.615	-31.3052
-1271.34	777.6968	64.95	1341	65.33624	1536.3254	170.43736	474.1036	0.618913	-31.6165

-1271.34	777.6968	64.95	1341	65.33624	1536.3254	170.43736	474.1036	0.618913	-31.6165
-1300.9	778.926	66.23	1439	65.34739	1536.456	170.45185	474.1439	0.619891	-31.5805
-1392.62	784.083	64.72	1346	65.10009	1536.5292	170.45997	474.1665	0.623995	-31.8174
-1453.77	787.521	65.86	1444	64.96769	1536.578	170.46538	474.1815	0.626732	-31.9429
-1621.45	797.755	65.61	1450	64.71043	1536.696	170.47847	474.2179	0.634876	-32.185
-1794.62	808.67	65.45	1503	64.54332	1536.893	170.50033	474.2787	0.643563	-32.3218
-1945.22	817.275	65.4	1509	64.49057	1537.202	170.53461	474.3741	0.650411	-32.3204
-2130.02	827.936	65.4	1515	64.48896	1537.426	170.55946	474.4432	0.658895	-32.2862
-1505.39	-1730.22	67.91		67.91	1538.305	170.65697	474.7145	-1.37696	-26.6556
348.197	-1165.5	71.85	1337	70.59699	1534.815	170.2698	473.6375	-0.92754	-25.1078
672.224	-1169.22	73.05	1343	71.82859	1534.8	170.26813	473.6328	-0.9305	-23.8762
1018.985	-1171.74	74.11	1349	72.91704	1534.825	170.27091	473.6405	-0.9325	-22.7808
1364.977	-1176.23	74.51	1356	73.33134	1534.943	170.284	473.677	-0.93608	-22.3396
1709.018	-1177.98	75.1	1402	73.93918	1535.411	170.33592	473.8214	-0.93747	-21.6379
-328.33	-1157.91	69.96	1410	68.6892	1534.899	170.27912	473.6634	-0.9215	-27.005
-661.636	-1155.83	69.71	1419	68.44034	1535.212	170.31384	473.76	-0.91984	-27.1937
-1007.59	-1154.83	69.31	1427	68.03734	1535.668	170.36443	473.9007	-0.91905	-27.5074
-1343.4	-1154.32	69.15	1433	67.87825	1536.744	170.4838	474.2327	-0.91864	-27.4542
-1687.26	-1152.56	68.79	1440	67.5154	1536.997	170.51187	474.3108	-0.91724	-27.7684
2007.912	-2677.55					0	0	-2.13087	-397.869
113.994	701.19	70.57	1420	71.07558	1534.93	170.28256	473.673	0.558027	-26.092
231.994	701.19	71.22	1425	71.73929	1535.03	170.29365	473.7038	0.558027	-25.4086
349.994	701.19	71.85	1431	72.38236	1535.13	170.30474	473.7347	0.558027	-24.7457
467.994	701.19	72.37	1437	72.91294	1535.23	170.31584	473.7655	0.558027	-24.1954
585.994	701.19	72.97	1444	73.52514	1535.33	170.32693	473.7964	0.558027	-23.5634
703.994	701.19	73.39	1452	73.95308	1535.43	170.33802	473.8272	0.558027	-23.1157
821.994	701.19	73.75	1456	74.32044	1535.53	170.34912	473.8581	0.558027	-22.7286
52.456	1436			70.16	1533.7536	170.15205	473.3099	1.14281	-27.8249
290.2	2258.96	73.06	1332	73.12152	1534.668	170.25349	473.5921	1.797744	-25.3376
-106.04	2258.96	71.3	1347	71.31696	1534.9728	170.2873	473.6862	1.797744	-27.0819
716.92	1667.648	74.58	1404	74.6655	1535.8872	170.38875	473.9683	1.327162	-23.0821
716.92	2039.504	74.89	1409	74.98089	1537.1064	170.524	474.3446	1.623095	-22.8216
716.92	2423.552	75.53	1414	75.63372	1537.1064	170.524	474.3446	1.928731	-22.4744
716.92	2838.08	76.58	1419	76.7058	1538.9352	170.72689	474.9089	2.258625	-21.3708
991.24	1222.64	76.17	1426	76.28429	1535.8872	170.38875	473.9683	0.973012	-21.1091
1923.928	1192.16	77.68	1431	77.82676	1541.3736	170.9974	475.6614	0.948755	-18.458
2216.536	-185.536	77.27	1445	77.40299	1534.3632	170.21968	473.498	-0.14765	-19.171
-2904.1	399.68	64.39	1600	64.20809	1537.4112	170.55782	474.4386	0.318077	-32.2292
-2209.16	369.2	64.8	1607	64.62509	1535.5824	170.35493	473.8743	0.29382	-32.1494
190	-3639	71.77	1101	72.21648	1537.1811	170.53229	474.3676	-2.89602	-21.0522
190	-3517	71.82	1112	72.26426	1537.0152	170.51388	474.3164	-2.79893	-21.1343
190	-3395	71.74	1125	72.17849	1536.8492	170.49547	474.2652	-2.70184	-21.3499
190	-3273	71.98	1140	72.41934	1536.6833	170.47707	474.214	-2.60475	-21.239
190	-3151	71.97	1150	72.40606	1536.5174	170.45866	474.1628	-2.50766	-21.3821
190	-3029	71.8	1200	72.22918	1536.3515	170.44025	474.1116	-2.41056	-21.6889
190	-2907	71.72	1206	72.14554	1536.1856	170.42185	474.0604	-2.31347	-21.9024
190	-2785	71.38	1218	71.79421	1536.0196	170.40344	474.0092	-2.21638	-22.3836
190	-2663	71.18	1228	71.58665	1535.8537	170.38503	473.958	-2.11929	-22.7211
190	-2551	70.94	1239	71.33788	1535.7014	170.36813	473.911	-2.03016	-23.0891
190	-2439	70.73	1247	71.1207	1535.5491	170.35124	473.864	-1.94103	-23.4255
190	-2327	70.58	1255	70.96488	1535.3968	170.33434	473.817	-1.85189	-23.7006
190	-2206	70.37	1305	70.74709	1535.2322	170.31608	473.7662	-1.7556	-24.0472
190	-2086	70.19	1313	70.56059	1535.069	170.29798	473.7158	-1.6601	-24.3614

APPENDIX C: MAGNETIC DATA

After drift correction, an ambient magnetic field of 51000 nT was removed from all magnetic stations to obtain the contoured maps of Figures 7 and 9. The data are tabulated on the following pages in x, y, and z co-ordinates. the x and y co-ordinates are in meters and the z value is the magnetic field at that point.

Washoe Valley Magnetic Data
 X and Y Co-ordinates in Meters
 Magnetic Field in nanoteslas -51000

X-COORD	Y-COORD	MAG		X-COORD	Y-COORD	MAG
=====	=====	=====		=====	=====	=====
-1505.38	-1730.22	628	Exit 44	-1008.23	-275.451	467
190	-3639	647.3932	Base	-1008.25	-242.881	469
190	-3608.5	675.4068		-1008.28	-210.312	477
190	-3578	679.4847		-1008.3	-177.743	472
190	-3547.5	671.6407		-1008.33	-145.174	487
190	-3517	684.7186		-1008.35	-112.604	473
190	-3486.5	667.3424		-1008.37	-80.0352	470
190	-3456	641.4983		-1008.4	-47.4659	486
190	-3425.5	604.5763		-1008.42	-14.8967	492
190	-3395	580.6542		-1008.45	17.67254	482
190	-3364.5	554.122		-1008.47	50.24178	475
190	-3334	597.278		-1008.49	82.81102	500
190	-3303.5	612.6678		-1008.52	115.3803	484
190	-3273	619.8237		-1008.54	147.9495	479
190	-3242.5	613.3695		-1008.57	180.5187	485
190	-3212	598.4475		-1008.59	213.088	472
190	-3181.5	607.5254		-1008.61	245.6572	452
190	-3151	613.6814		-1008.64	278.2264	474
190	-3120.5	619.0712		-1008.66	310.7957	462
190	-3090	628.2271		-1008.69	343.3649	476
190	-3059.5	632.3051		-1008.71	375.9342	494
190	-3029	635.3831		-1008.74	408.5034	495
190	-2998.5	636.6949		-1008.76	441.0726	459
190	-2968	629.8508		-1008.78	473.6419	451
190	-2937.5	633.9288		-1008.81	506.2111	473
190	-2907	634.0068		-1008.83	538.7803	470
190	-2876.5	632.2407		-1008.86	571.3496	469
190	-2846	640.3966		-1008.88	603.9188	497
190	-2815.5	634.5525		-1008.9	636.4881	468
190	-2785	635.7864		-1008.93	669.0573	462
190	-2754.5	638.0203		-1008.95	701.6265	479
190	-2724	632.1763		-1008.98	734.1958	469
190	-2693.5	627.3322		-1009	766.765	469
190	-2663	619.5661		-1009	799.265	465
190	-2635	621.722		-1009	831.765	473
190	-2607	620.878		-1009	864.265	491
190	-2579	620.0339		-1009	896.765	471
190	-2551	618.1898		-1009	929.265	461
190	-2523	620.4237		-1009	961.765	479
190	-2495	618.6576		-1009	994.265	460
190	-2467	617.8136		-1009	1026.765	465
190	-2439	618.0475		-1009	1059.265	479
190	-2411	612.2034		-1009	1091.765	476
190	-2383	615.3593		-1009	1124.265	484
190	-2355	614.5153		-1009	1156.765	472

X-COORD	Y-COORD	MAG	X-COORD	Y-COORD	MAG
190	-2327	611.6712	-1009	1189.265	483
190.25	-2296.88	608.8271	-1009	1221.765	492
190.5	-2266.75	608.061	-1009	1254.265	475
190.75	-2236.63	602.2169	-1009	1286.765	478
191	-2206.5	596.3729	-1009	1319.265	479
191.25	-2176.38	591.5288	-1009	1351.765	474
191.5	-2146.25	595.6847	-1009	1384.265	477
191.75	-2116.13	598.8407	-1009	1416.765	490
192	-2086	597.9186	-1009	1449.265	487
-3.43	578.18	549.404	-1009	1481.765	486
-3.574	608.9325	536.5758	-1009	1514.265	485
-3.718	639.685	530.7475	-1009	1546.765	496
-3.862	670.4375	521.9192	-684.876	757.972	487
-4.006	701.19	527.2626	-684.876	726.472	490
-4.69288	731.9979	514.6061	-684.876	694.972	500
-5.37975	762.8058	519.9495	-684.876	663.472	510
-6.06663	793.6136	522.1212	-684.876	631.972	492
-6.7535	824.4215	511.2929	-684.876	600.472	506
-7.44038	855.2294	508.4646	-684.876	568.972	500
-8.12725	886.0373	496.6364	-684.876	537.472	509
-8.81413	916.8451	497.8081	-684.876	505.972	522
-9.501	947.653	484.1515	-684.876	474.472	512
-10.0999	978.3261	485.3232	-684.876	442.972	522
-10.6988	1008.999	476.4949	-684.876	411.472	528
-11.2976	1039.672	487.6667	-684.876	379.972	537
-11.8965	1070.346	481.0101	-684.876	348.472	536
-12.4954	1101.019	479.1818	-684.876	316.972	524
-13.0943	1131.692	472.3535	-684.876	285.472	542
-13.6931	1162.365	478.5253	-684.876	253.972	547
-14.292	1193.038	477.697	-684.876	222.472	548
-14.9998	1223.378	477.8687	-684.876	190.972	546
-15.7075	1253.717	487.0404	-684.876	159.472	554
-16.4153	1284.057	476.2121	-684.876	127.972	556
-17.123	1314.396	487.5556	-684.876	96.472	552
-16.4888	1344.712	493.7273	-684.876	64.972	550
-15.8545	1375.029	485.899	-684.876	33.472	551
-15.2203	1405.345	494.2424	-684.876	1.972	547
-14.586	1435.661	520.4141	-684.876	-29.528	544
-840.292	1193.038	475.2038	-684.876	-61.028	544
-810.792	1193.038	484.121	-684.876	-92.528	546
-781.292	1193.038	482.0382	-684.876	-124.028	545
-751.792	1193.038	472.0382	-653.376	-124.028	556
-722.292	1193.038	474.9554	-621.876	-124.028	560
-692.792	1193.038	471.8726	-590.376	-124.028	572
-663.292	1193.038	477.707	-558.876	-124.028	561
-633.792	1193.038	475.5414	-527.376	-124.028	588
-604.292	1193.038	492.4586	-495.876	-124.028	597
-574.792	1193.038	491.293	-464.376	-124.028	594
-545.292	1193.038	475.2102	-432.876	-124.028	612
-515.792	1193.038	480.1274	-401.376	-124.028	610

X-COORD	Y-COORD	MAG	X-COORD	Y-COORD	MAG
-486.292	1193.038	478.0446	-369.876	-124.028	618
-456.792	1193.038	479.9618	-338.376	-124.028	614
-427.292	1193.038	477.879	-306.876	-124.028	618
-397.792	1193.038	479.7962	-275.376	-124.028	638
-368.292	1193.038	473.7962	-243.876	-124.028	619
-338.792	1193.038	482.7134	53.047	-2083.33	585.0366
-309.292	1193.038	480.6306	87.76512	-2083.88	595.0976
-279.792	1193.038	484.5478	122.4832	-2084.42	600.1585
-250.292	1193.038	483.465	157.2014	-2084.97	606.2805
-220.792	1193.038	481.3822	191.9195	-2085.52	610.3415
-191.292	1193.038	471.2994	226.6376	-2086.06	614.4024
-161.792	1193.038	477.2166	261.3557	-2086.61	617.5244
-132.292	1193.038	474.1338	296.0738	-2087.16	625.6463
-102.792	1193.038	474.051	330.792	-2087.7	629.7683
-73.292	1193.038	476.9682	365.5101	-2088.25	636.8293
-43.792	1193.038	468.8854	400.2282	-2088.8	639.8902
-14.292	1193.038	473.7197	434.9463	-2089.34	644.9512
15.208	1193.038	477.4076	469.6644	-2089.89	653.9512
44.708	1193.038	474.4904	504.3826	-2090.44	659.0122
74.208	1193.038	483.5732	539.1007	-2090.99	667.0732
103.708	1193.038	474.6561	573.8188	-2091.53	678.1341
133.208	1193.038	480.7389	608.5369	-2092.08	683.1951
162.708	1193.038	481.8217	643.255	-2092.63	688.2561
192.208	1193.038	478.9873	677.9732	-2093.17	698.3171
221.708	1193.038	489.1529	712.6913	-2093.72	699.378
251.208	1193.038	486.2357	747.4094	-2094.27	697.439
280.708	1193.038	506.3185	782.1275	-2094.81	699.5
310.208	1193.038	500.4013	816.8456	-2095.36	694.561
339.708	1193.038	496.4841	851.5638	-2095.91	691.6829
369.208	1193.038	500.5669	886.2819	-2096.45	688.8049
398.708	1193.038	496.6497	921	-2097	682.9268
428.208	1193.038	482.7325	957.5649	-2097.3	679.9878
457.708	1193.038	476.8981	994.1298	-2097.6	677.9878
487.208	1193.038	494.9809	1030.695	-2097.89	673.1098
516.708	1193.038	493.0637	1067.26	-2098.19	670.1707
546.208	1193.038	500.1465	1103.824	-2098.49	666.2317
575.708	1193.038	505.3121	1140.389	-2098.79	662.2317
605.208	1193.038	515.3949	1176.954	-2099.09	657.2927
634.708	1193.038	510.4777	1213.519	-2099.39	650.2927
664.208	1193.038	545.5605	1250.084	-2099.68	644.3537
693.708	1193.038	535.5605	1286.649	-2099.98	639.4146
-663.292	1193.038	468.7834	1323.214	-2100.28	629.4146
-663.292	1222.538	474.8662	1359.779	-2100.58	624.4756
-663.292	1252.038	443.949	1396.344	-2100.88	617.5366
-663.292	1281.538	483.0318	1432.909	-2101.18	615.5976
-663.292	1311.038	470.1975	1469.473	-2101.47	607.5976
-663.292	1340.538	481.2803	1506.038	-2101.77	604.6585
-663.292	1370.038	471.3631	1542.603	-2102.07	602.6585
-663.292	1399.538	476.4459	1579.168	-2102.37	598.7195
-663.292	1429.038	482.4459	1615.733	-2102.67	600.7805

X-COORD	Y-COORD	MAG	X-COORD	Y-COORD	MAG
-663.292	1458.538	475.5287	1652.298	-2102.96	599.7805
-663.292	1488.038	481.6115	1688.863	-2103.26	600.8415
-663.292	1517.538	480.6943	1725.428	-2103.56	604.9024
-663.292	1547.038	482.7771	1761.993	-2103.86	610.9634
-663.292	1576.538	493.8599	1798.557	-2104.16	616.0244
-663.292	1606.038	501.9427	1835.122	-2104.46	632.0854
-663.292	1635.538	501.0255	1871.687	-2104.75	632.1463
-663.292	1665.038	492.0255	1908.252	-2105.05	641.1463
-663.292	1694.538	494.1083	1944.817	-2105.35	651.2073
-663.292	1724.038	504.1911	190	-2327.23	618.2143
-663.292	1753.538	497.2739	160.5	-2327.23	613.3214
-663.292	1783.038	498.2739	131	-2327.23	613.5357
-663.292	1812.538	503.3567	101.5	-2327.23	613.75
-663.292	1842.038	508.4395	72	-2327.23	615.9643
-663.292	1871.538	496.5223	42.5	-2327.23	620.0714
-663.292	1901.038	503.6051	13	-2327.23	617.0714
-663.292	1930.538	506.6879	-16.5	-2327.23	612.1786
-663.292	1960.038	521.7707	-46	-2327.23	605.2857
-663.292	1989.538	504.9363	-75.5	-2327.23	589.2857
-663.292	2019.038	519.0191	-105	-2327.23	580.3929
-663.292	2048.538	514.1019	-134.5	-2327.23	572.5
-663.292	2078.038	504.1019	-164	-2327.23	564.6071
53.047	-2083.33	586.004	-193.5	-2327.23	561.6071
51.5695	-2053.63	590.16	-223	-2327.23	555.7143
50.092	-2023.94	593.316	-252.5	-2327.23	557.8214
48.6145	-1994.24	590.472	-282	-2327.23	558.9286
47.137	-1964.55	594.784	-311.5	-2327.23	554.9286
45.6595	-1934.85	602.94	-341	-2327.23	560.0357
44.182	-1905.15	603.096	-370.5	-2327.23	564.1429
42.7045	-1875.46	605.252	-400	-2327.23	571.25
41.227	-1845.76	609.408	-429.5	-2327.23	575.3571
39.773	-1816.35	616.564	-459	-2327.23	588.4643
38.319	-1786.93	617.72	-488.5	-2327.23	594.5714
36.865	-1757.52	622.876	-518	-2327.23	602.6786
35.411	-1728.11	624.032	-547.5	-2327.23	610.7857
33.957	-1698.69	625.188	-577	-2327.23	613.7857
32.503	-1669.28	628.344	-606.5	-2327.23	615.8929
31.049	-1639.86	627.5	-636	-2327.23	617
29.595	-1610.45	626.62	-665.5	-2327.23	618.1071
29.58325	-1581.54	625.776	-695	-2327.23	620.1071
29.5715	-1552.62	628.932	-724.5	-2327.23	621.2143
29.55975	-1523.71	623.088	-754	-2327.23	600.3214
29.548	-1494.8	620.244	-783.5	-2327.23	588.4286
29.53625	-1465.88	620.4	-813	-2327.23	577.5357
29.5245	-1436.97	616.556	-842.5	-2327.23	560.75
29.51275	-1408.05	615.712	-872	-2327.23	545.75
29.501	-1379.14	611.024	-901.5	-2327.23	511.75
28.83463	-1351.97	615.18	-931	-2327.23	501.8571
28.16825	-1324.8	613.336	-960.5	-2327.23	473.9643
27.50188	-1297.63	616.492	-990	-2327.23	464.0714

X-COORD	Y-COORD	MAG	X-COORD	Y-COORD	MAG
26.8355	-1270.46	614.648	-1019.5	-2327.23	465.1786
26.16913	-1243.29	617.804	-1049	-2327.23	463.2857
25.50275	-1216.12	620.96	-1078.5	-2327.23	496.3929
24.83638	-1188.95	621.116	-1108	-2327.23	470.5
24.17	-1161.78	622.428	-1137.5	-2327.23	475.6071
22.79	-1131.83	625.584	-1167	-2327.23	522.7143
21.41	-1101.89	623.74	-1196.5	-2327.23	545.8214
20.03	-1071.94	626.896	-1226	-2327.23	570.9286
18.65	-1041.99	627.052	-1255.5	-2327.23	562.0357
17.27	-1012.04	624.208	-1285	-2327.23	587.25
15.89	-982.095	625.364	-1314.5	-2327.23	572.3571
14.51	-952.148	628.52	-1344	-2327.23	572.3571
13.13	-922.2	629.52	-1373.5	-2327.23	548.4643
12.25538	-893.72	629.676	-1403	-2327.23	574.5714
11.38075	-865.241	633.832	-1432.5	-2327.23	582.6786
10.50613	-836.761	634.988	-1462	-2327.23	570.7857
9.6315	-808.281	633.144	-1491.5	-2327.23	585.8929
8.756875	-779.801	639.3	-1521	-2327.23	616.8929
7.88225	-751.322	642.456	-1196.5	-2327.23	538.0714
7.007625	-722.842	640.612	-1203.88	-2290.29	495.1786
6.133	-694.362	641.768	-1211.25	-2253.36	527.1786
5.41675	-665.676	644.924	-1218.63	-2216.42	526.2857
4.7005	-636.991	653.08	-1226	-2179.49	495.3929
3.98425	-608.305	648.236	-1233.38	-2142.55	518.5
3.268	-579.62	649.392	-1240.75	-2105.62	564.6071
2.55175	-550.934	653.548	-1248.13	-2068.68	544.9286
1.8355	-522.248	660.704	-1255.5	-2031.74	518.0357
1.11925	-493.563	662.86	-1262.88	-1994.81	504.1429
0.403	-464.877	663.016	-1270.25	-1957.87	511.25
0.820594	-461.019	666.172	-1277.63	-1920.94	554.3571
0.521938	-428.474	671.328	-1285	-1884	568.375
0.223281	-395.93	668.484	-1285.79	-1853.6	575.6875
-0.07537	-363.386	662.64	-1286.58	-1823.19	556.6875
-0.37403	-330.842	650.796	-1287.38	-1792.79	587
-0.67269	-298.298	645.952	-1288.17	-1762.39	592.3125
-0.97134	-265.754	647.108	-1288.96	-1731.98	595.3125
-1.27	-233.21	654.264	-1289.75	-1701.58	562.625
-1.11125	-204.059	657.42	-1290.54	-1671.18	531.625
-0.9525	-174.908	645.576	-1291.33	-1640.77	533.9375
-0.79375	-145.756	643.732	-1292.13	-1610.37	544.25
-0.635	-116.605	645.888	-1292.92	-1579.97	539.5625
-0.47625	-87.4538	627.044	-1293.71	-1549.56	561.875
-0.3175	-58.3025	645.2	-1294.5	-1519.16	527.1875
-0.15875	-29.1513	651.356	-1295.29	-1488.76	584.5
0	0	650.512	-1296.08	-1458.35	577.8125
-0.16063	28.39475	639.668	-1296.88	-1427.95	560.125
-0.32125	56.7895	637.824	-1297.67	-1397.55	544.4375
-0.48187	85.18425	627.136	-1298.46	-1367.14	493.75
-0.6425	113.579	616.292	-1299.25	-1336.74	558.0625
-0.80313	141.9738	607.448	-1300.04	-1306.34	562.375

X-COORD	Y-COORD	MAG	X-COORD	Y-COORD	MAG
-0.96375	170.3685	627.604	-1300.83	-1275.93	599.6875
-1.12438	198.7633	630.76	-1301.63	-1245.53	559.6875
-1.285	227.158	623.76	-1302.42	-1215.13	522
-0.76663	255.6598	617.916	-1303.21	-1184.72	470.3125
-0.24825	284.1615	642.228	-1304	-1154.32	532.3125
0.270125	312.6633	583.54	954.941	-214.562	582.5
0.7885	341.165	595.696	984.1195	-214.181	579.4444
1.306875	369.6668	582.852	1013.298	-213.801	568.3889
1.82525	398.1685	584.008	1042.476	-213.42	574.3889
2.343625	426.6703	563.32	1071.655	-213.04	574.3333
2.862	455.172	593.476	1100.833	-212.659	575.2778
1.289	485.924	565.632	1130.012	-212.278	579.2222
-0.284	516.676	562.632	1159.19	-211.898	575.1667
-1.857	547.428	540.788	1188.369	-211.517	565.1111
-31.4629	704.5846	518.8276	1217.547	-211.137	573.0556
-58.8658	707.9793	512.6724	1246.726	-210.756	578
-86.2686	711.3739	514.5172	1275.904	-210.376	585
-113.672	714.7685	518.3621	1305.083	-209.995	590.9444
-141.074	718.1631	513.2069	1334.261	-209.614	599.8889
-168.477	721.5578	510.0517	1363.44	-209.234	591.8889
-195.88	724.9524	513.8966	1392.618	-208.853	597.8333
-223.283	728.347	502.5862	1421.797	-208.473	595.7778
-251.852	730.951	495.431	1450.975	-208.092	621.7778
-280.422	733.555	508.2759	954.941	-214.562	581.1111
-308.991	736.159	501.1207	923.0673	-215.184	591.0556
-337.561	738.763	501.9655	891.1936	-215.805	601
-366.13	741.367	492.6552	859.3199	-216.427	614.9444
-394.699	743.971	494.5	827.4462	-217.048	633.8889
-423.269	746.575	503.1897	795.5725	-217.67	619.8889
-451.838	749.179	492.0345	763.6988	-218.292	621.8333
-480.968	750.2781	496.8793	731.8251	-218.913	631.7778
-510.098	751.3773	490.7241	699.9514	-219.535	631.7778
-539.228	752.4764	495.569	668.0777	-220.156	639.7222
-568.358	753.5755	487.4138	636.204	-220.778	636.6667
-597.488	754.6746	493.2586	604.3303	-221.4	642.6111
-626.618	755.7738	485.1034	572.4566	-222.021	644.6111
-655.748	756.8729	478.9483	540.5829	-222.643	641.5556
-684.878	757.972	466.7931	508.7092	-223.264	651.5
-714.008	759.0711	479.6379	476.8355	-223.886	653.4444
-743.138	760.1703	483.4828	444.9618	-224.508	664.3889
-772.268	761.2694	474.3276	413.0881	-225.129	672.3333
-801.398	762.3685	468.0172	381.2144	-225.751	662.2778
-830.528	763.4676	475.8621	349.3407	-226.372	661.2222
-859.658	764.5668	472.7069	317.467	-226.994	648.1667
-888.788	765.6659	468.5517	285.5933	-227.616	653.1111
-917.918	766.765	465.3966	253.7196	-228.237	658.0556
-947.312	767.5169	465.2414	221.8459	-228.859	664
-976.706	768.2688	469.0862	189.9722	-229.48	661
-1006.1	769.0206	459.931	158.0985	-230.102	658.9444
-1035.49	769.7725	469.6207	126.2248	-230.724	659.8889

X-COORD	Y-COORD	MAG	X-COORD	Y-COORD	MAG
-1064.89	770.5244	469.4655	94.3511	-231.345	658.8333
-1094.28	771.2763	461.3103	62.4774	-231.967	661.8333
-1123.68	772.0281	464.1552	30.6037	-232.588	663.7778
-1153.07	772.78	450	-1.27	-233.21	657.6667
-1182.64	774.0164	460.8448	-30.7956	-231.066	675.6111
-1212.2	775.2528	455.6897	-60.3211	-228.921	671.5556
-1241.77	776.4892	444.5345	-89.8467	-226.777	660.5
-1271.33	777.7256	458.3793	-119.372	-224.632	703.4444
-1300.9	778.962	502.5345	-148.898	-222.488	662.4444
-1331.47	780.6738	464.069	-178.423	-220.343	637.3889
-1362.05	782.3856	461.9138	-207.949	-218.199	635.3333
-1392.62	784.0974	465.9138	-237.474	-216.054	639.2778
-1423.2	785.8092	462.7586	-267	-213.91	631.2778
-1453.77	787.521	471.4483	-1304	-1154	493.7753
285	1456	487.5652	-1304.42	-1122.82	474.9663
285	1485.5	470.288	-1304.84	-1091.65	479.1573
285	1515	486.0109	-1305.26	-1060.47	516.1573
285	1544.5	486.4565	-1305.68	-1029.3	446.3483
285	1574	492.9022	-1306.1	-998.119	447.5393
285	1603.5	503.625	-1306.52	-966.943	445.5393
285	1633	515.3478	-1306.94	-935.766	483.7303
285	1662.5	508.7935	-1307.35	-904.59	460.9213
285	1692	490.2391	-1307.77	-873.414	471.1124
285	1721.5	512.962	-1308.19	-842.238	457.3034
285	1751	510.6848	-1308.61	-811.062	442.4944
224	1780.5	536.3587	-1309.03	-779.885	434.6854
224	1810	525.8043	-1309.45	-748.709	435.6854
224	1839.5	528.25	-1309.87	-717.533	415.8764
224	1869	524.9728	-1310.29	-686.357	428.0674
224	1898.5	525.6957	-1310.71	-655.18	435.2584
224	1928	527.4185	-1311.13	-624.004	430.4494
224	1957.5	527.1413	-1311.55	-592.828	430.4494
224	1987	530.8641	-1311.97	-561.652	448.6404
224	2016.5	522.587	-1312.39	-530.475	446.8315
224	2046	527.0326	-1312.81	-499.299	447.0225
224	2075.5	523.7554	-1313.23	-468.123	451.0225
224	2105	525.4783	-1313.65	-436.947	466.2135
224	2134.5	528.2011	-1314.06	-405.771	441.4045
224	2164	536.6957	-1314.48	-374.594	432.5955
224	2193.5	525.3696	-1314.9	-343.418	429.7865
15	1435.661	486.7931	-1315.32	-312.242	436.9775
15	1465.161	441.6379	-1315.74	-281.066	424.1685
15	1494.661	444.4828	-1316.16	-249.889	428.3596
15	1524.161	491.3276	-1316.58	-218.713	414.5506
15	1553.661	476.3276	-1317	-187.537	410.5506
15	1583.161	486.1724	-1317.42	-156.361	415.7416
15	1612.661	493.1724	-1317.84	-125.185	419.9326
15	1642.161	491.0172	-1318.26	-94.0083	426.9326
15	1671.661	503.8621	-1318.68	-62.8321	436.1236
15	1701.161	512.7069	-1319.1	-31.6559	446.3146

X-COORD	Y-COORD	MAG	X-COORD	Y-COORD	MAG
15	1730.661	498.5517	-1319.52	-0.47965	436.3146
15	1760.161	494.3966	-1319.94	30.69658	429.0787
15	1789.661	498.3966	-1320.35	61.87281	419.2697
15	1819.161	503.2414	-1320.77	93.04903	421.4607
15	1848.661	495.0862	-1321.19	124.2253	419.4607
15	1878.161	491.931	-1321.61	155.4015	438.6517
15	1907.661	494.931	-1322.03	186.5777	420.8427
10	-1161.76	636	-1322.45	217.7539	427.8427
-18.1942	-1161.44	636	-1322.87	248.9302	437.0337
-46.3883	-1161.12	635	-1323.29	280.1064	421.2247
-74.5825	-1160.8	629	-1323.71	311.2826	422.2247
-102.777	-1160.48	625	-1324.13	342.4588	427.4157
-130.971	-1160.16	622	-1324.55	373.6351	443.4157
-159.165	-1159.84	617	-1324.97	404.8113	421.6067
-187.359	-1159.51	614	-1325.39	435.9875	420.7978
-215.553	-1159.19	610	-1325.81	467.1637	427.7978
-243.748	-1158.87	609	-1326.23	498.34	418.9888
-271.942	-1158.55	609	-1326.65	529.5162	409.1798
-300.136	-1158.23	599	-1327.06	560.6924	419.3708
-328.33	-1157.91	599	-1327.48	591.8686	412.5618
-357.386	-1157.74	591	-1327.9	623.0449	414.7528
-386.442	-1157.56	592	-1328.32	654.2211	417.9438
-415.498	-1157.39	586	-1328.74	685.3973	436.1348
-444.553	-1157.21	586	-1329.16	716.5735	441.3258
-473.609	-1157.04	575	-1329.58	747.7498	423.5169
-502.665	-1156.87	569	-1330	778.926	427.7079
-531.721	-1156.69	560	-1300.9	778.926	479.8989
-560.777	-1156.52	561	-1331.76	780.785	447.0899
-589.833	-1156.34	560	-1362.61	782.644	447.2809
-618.888	-1156.17	571	-1393.47	784.503	449.4719
-647.944	-1155.99	567	-1424.33	786.362	453.6629
-677	-1155.82	564	-1455.18	788.221	460.8539
-706.667	-1155.74	569	-1486.04	790.08	463.236
-736.333	-1155.65	569	-1516.9	791.939	444.427
-766	-1155.57	569	-1547.76	793.798	450.618
-795.667	-1155.49	548	-1578.61	795.657	459.809
-825.333	-1155.4	565	-1609.47	797.516	460.809
-855	-1155.32	527	-1640.33	799.375	464
-884.667	-1155.24	516	-1671.18	801.234	466.191
-914.333	-1155.15	517	-1702.04	803.093	465.382
-944	-1155.07	519	-1732.9	804.952	472.382
-973.667	-1154.99	523	-1763.75	806.811	494.573
-1003.33	-1154.9	523	-1794.61	808.67	483.764
-1033	-1154.82	530	-1825.1	810.4182	479.764
-1062.55	-1154.77	529	-1855.59	812.1664	482.9551
-1092.09	-1154.73	519	-1886.08	813.9145	476.1461
-1121.64	-1154.68	549	-1916.57	815.6627	469.1461
-1151.18	-1154.64	558	-1947.06	817.4109	480.3371
-1180.73	-1154.59	546	-1977.55	819.1591	479.5281
-1210.27	-1154.55	551	-2008.04	820.9073	464.7191

X-COORD	Y-COORD	MAG	X-COORD	Y-COORD	MAG
-1239.82	-1154.5	538	-2038.53	822.6555	511.9101
-1269.36	-1154.46	544	-2069.02	824.4036	528.1011
-1298.91	-1154.41	554	-2099.51	826.1518	478.1011
-1328.45	-1154.37	546	-2130	827.9	467.2921
-1358	-1154.32	547	-1794.61	808.67	476.4382
-1387.93	-1154.16	563	-1792.93	778.0189	463.6292
-1417.86	-1154	572	-1791.25	747.3678	456.8202
-1447.8	-1153.84	590	-1789.57	716.7167	462.8202
-1477.73	-1153.68	591	-1787.88	686.0656	450.0112
-1507.66	-1153.52	554	-1786.2	655.4145	448.2022
-1537.59	-1153.36	543	-1784.52	624.7634	439.3933
-1567.52	-1153.2	561	-1782.84	594.1123	451.3933
-1597.45	-1153.04	553	-1781.16	563.4613	455.5843
-1627.39	-1152.88	556	-1779.48	532.8102	450.7753
-1657.32	-1152.72	535	-1777.8	502.1591	445.7753
-1687.25	-1152.56	494	-1776.11	471.508	454.9663
52.57136	-1162.12	623	-1774.43	440.8569	440.1573
80.97273	-1162.46	625	-1772.75	410.2058	447.1573
109.3741	-1162.79	628	-1771.07	379.5547	429.3483
137.7755	-1163.13	631	-1769.39	348.9036	440.5393
166.1768	-1163.47	640	-1767.71	318.2525	473.7303
194.5782	-1163.81	636	-1766.03	287.6014	433.9213
222.9795	-1164.14	641	-1764.34	256.9503	449.1124
251.3809	-1164.48	639	-1762.66	226.2992	431.1124
279.7823	-1164.82	652	-1760.98	195.6481	454.3034
308.1836	-1165.16	654	-1759.3	164.997	480.4944
336.585	-1165.5	661	-1757.62	134.3459	471.6854
364.9864	-1165.83	660	-1755.94	103.6948	454.8764
393.3877	-1166.17	663	-1754.26	73.04375	453.0674
421.7891	-1166.51	660	-1752.57	42.39266	478.0674
450.1905	-1166.85	661	-1750.89	11.74156	491.2584
478.5918	-1167.18	663	-1749.21	-18.9095	450.2584
506.9932	-1167.52	660	-1747.53	-49.5606	480.4494
535.3945	-1167.86	659	-1745.85	-80.2117	433.6404
563.7959	-1168.2	658	-1744.17	-110.863	406.6404
592.1973	-1168.53	657	-1742.49	-141.514	480.8315
620.5986	-1168.87	656	-1740.81	-172.165	485.0225
649	-1169.21	657	-1739.12	-202.816	496.2135
677.0769	-1169.4	652	-1737.44	-233.467	469.4045
705.1538	-1169.6	647	-1735.76	-264.118	462.4045
733.2308	-1169.79	641	-1734.08	-294.769	510.5955
761.3077	-1169.99	640	-1732.4	-325.42	494.7865
789.3846	-1170.18	640	-1730.72	-356.072	484.9775
817.4615	-1170.38	637	-1729.04	-386.723	499.1685
845.5385	-1170.57	636	-1727.35	-417.374	516.3596
873.6154	-1170.77	638	-1725.67	-448.025	479.3596
901.6923	-1170.96	634	-1723.99	-478.676	496.5506
929.7692	-1171.16	638	-1722.31	-509.327	490.7416
957.8462	-1171.35	637	-1720.63	-539.978	486.7416
985.9231	-1171.55	638	-1718.95	-570.629	479.9326

X-COORD	Y-COORD	MAG	X-COORD	Y-COORD	MAG
1014	-1171.74	636	-1717.27	-601.28	478.1236
1041.417	-1172.11	639	-1715.58	-631.931	518.3146
1068.833	-1172.49	629	-1713.9	-662.583	515.5056
1096.25	-1172.86	629	-1712.22	-693.234	498.6966
1123.667	-1173.24	619	-1710.54	-723.885	491.6966
1151.083	-1173.61	621	-1708.86	-754.536	488.8876
1178.5	-1173.99	623	-1707.18	-785.187	501.8876
1205.917	-1174.36	615	-1705.5	-815.838	511.0787
1233.333	-1174.73	611	-1703.81	-846.489	483.0787
1260.75	-1175.11	604	-1702.13	-877.14	517.2697
1288.167	-1175.48	601	-1700.45	-907.791	486.4607
1315.583	-1175.86	598	-1698.77	-938.442	480.6517
1343	-1176.23	604	-1697.09	-969.093	521.8427
1371.155	-1176.36	598	-1695.41	-999.745	512.8427
1399.31	-1176.5	591	-1693.73	-1030.4	491.0337
1427.466	-1176.63	589	-1692.04	-1061.05	480.2247
1455.621	-1176.77	584	-1690.36	-1091.7	531.4157
1483.776	-1176.9	581	-1688.68	-1122.35	445.6067
1511.931	-1177.04	583	-1687	-1153	487.7978
1540.087	-1177.17	584	1977.478	-2677.11	700.8
1568.242	-1177.31	584	1947.044	-2676.67	700.8
1596.397	-1177.44	588	1916.609	-2676.23	698
1624.552	-1177.58	600	1886.175	-2675.79	684.2
1652.708	-1177.71	602	1855.741	-2675.35	683.4
1680.863	-1177.85	601	1825.307	-2674.91	687.6
1709.018	-1177.98	591	1794.872	-2674.46	673.6
25.494	701.19	543.204	1764.438	-2674.02	669.8
54.994	701.19	543.204	1734.004	-2673.58	680
84.494	701.19	544.048	1703.57	-2673.14	681
113.994	701.19	576.892	1673.136	-2672.7	673.2
143.494	701.19	569.736	1642.701	-2672.26	661.4
172.994	701.19	567.58	1612.267	-2671.82	648.6
202.494	701.19	578.424	1581.833	-2671.38	641.6
231.994	701.19	588.268	1551.399	-2670.94	643.8
261.494	701.19	603.112	1520.964	-2670.5	643
290.994	701.19	598.956	1490.53	-2670.06	642.2
320.494	701.19	604.8	1460.096	-2669.62	638.4
349.994	701.19	605.488	1429.662	-2669.17	632.6
379.494	701.19	611.332	1399.228	-2668.73	625.8
408.994	701.19	629.176	1368.793	-2668.29	630
438.494	701.19	632.02	1338.359	-2667.85	629.2
467.994	701.19	634.864	1307.925	-2667.41	621.2
497.494	701.19	635.708	1277.491	-2666.97	617.4
526.994	701.19	637.552	1247.056	-2666.53	606.6
556.494	701.19	642.396	1216.622	-2666.09	602.8
585.994	701.19	645.084	1186.188	-2665.65	596
615.494	701.19	657.928	1155.754	-2665.21	588
644.994	701.19	638.772	1125.32	-2664.77	587.2
674.494	701.19	647.616	1094.885	-2664.33	592.4
703.994	701.19	660.46	1064.451	-2663.88	603.6

X-COORD	Y-COORD	MAG	X-COORD	Y-COORD	MAG
733.494	701.19	656.304	1034.017	-2663.44	622.8
762.994	701.19	656.148	1003.583	-2663	639
792.494	701.19	642.992	973.1484	-2662.56	657
821.994	701.19	650.68	942.7142	-2662.12	667.2
851.494	701.19	642.524	912.28	-2661.68	672.4
880.994	701.19	649.368	854.4976	-2661.79	683.6
910.494	701.19	650.056	825.6064	-2661.84	697
939.994	701.19	685.744	796.7152	-2661.89	698
-328.33	-1393.91	584	767.824	-2661.94	700.2
-328.33	-1364.41	588	738.9328	-2662	692.4
-328.33	-1334.91	588	710.0416	-2662.05	696.6
-328.33	-1305.41	590	681.1504	-2662.1	685.8
-328.33	-1275.91	595	652.2592	-2662.16	693.8
-328.33	-1246.41	597	623.368	-2662.21	706
-328.33	-1216.91	601	594.4768	-2662.26	717.2
-328.33	-1187.41	604	565.5856	-2662.31	732.4
-328.33	-1157.91	603	536.6944	-2662.37	746.6
-328.33	-1128.41	609	507.8032	-2662.42	755.6
-328.33	-1098.91	613	478.912	-2662.47	756.8
-328.33	-1069.41	613	450.0208	-2662.52	752
-328.33	-1039.91	611	421.1296	-2662.58	736
-328.33	-1010.41	620	392.2384	-2662.63	718.2
-328.33	-980.91	619	363.3472	-2662.68	700.2
-328.33	-951.41	622	334.456	-2662.74	679.4
-328.33	-921.91	623	305.5648	-2662.79	668.6
-328.33	-892.41	624	276.6736	-2662.84	649.6
-328.33	-862.91	629	247.7824	-2662.89	636.8
-328.33	-833.41	633	218.8912	-2662.95	625
-328.33	-803.91	636	190	-2663	612
-328.33	-774.41	643	955.981	-185.062	589.3422
-328.33	-744.91	641	957.021	-155.562	597.27
-328.33	-715.41	643	958.061	-126.062	599.1977
-328.33	-685.91	649	959.101	-96.562	603.1255
-328.33	-656.41	650	960.141	-67.062	606.0532
-328.33	-626.91	650	961.181	-37.562	618.981
-328.33	-597.41	653	962.221	-8.062	619.9087
-328.33	-567.91	663	963.261	21.438	617.9087
-328.33	-538.41	659	964.301	50.938	614.8365
-328.33	-508.91	656	965.341	80.438	635.8365
-328.33	-479.41	660	966.381	109.938	632.7643
-328.33	-449.91	658	967.421	139.438	637.692
-328.33	-420.41	656	968.461	168.938	648.6198
-328.33	-390.91	653	969.501	198.438	649.5475
-328.33	-361.41	650	970.541	227.938	657.5475
-328.33	-331.91	648	971.581	257.438	652.4753
-328.33	-302.41	639	972.621	286.938	657.2586
358	-2083.33	624.6274	973.661	316.438	676.1863
356.8667	-2052.61	619.5551	974.701	345.938	693.1863
355.7333	-2021.89	618.5551	975.741	375.438	690.1141
354.6	-1991.18	626.4829	976.781	404.938	681.0418

X-COORD	Y-COORD	MAG	X-COORD	Y-COORD	MAG
353.4667	-1960.46	631.4106	977.821	434.438	675.0418
352.3333	-1929.74	634.3384	978.861	463.938	693.9696
351.2	-1899.02	644.2662	979.901	493.438	676.8973
350.0667	-1868.3	651.1217	980.941	522.938	700.8251
348.9333	-1837.58	658.0494	981.981	552.438	684.6806
347.8	-1806.87	660.9772	955.981	-185.062	589.3422
346.6667	-1776.15	673.9049	957.021	-155.562	597.27
345.5333	-1745.43	682.8327	958.061	-126.062	599.1977
344.4	-1714.71	686.6882	959.101	-96.562	603.1255
343.2667	-1683.99	695.616	960.141	-67.062	606.0532
342.1333	-1653.27	701.5437	961.181	-37.562	618.981
341	-1622.56	705.5437	962.221	-8.062	619.9087
339.8667	-1591.84	710.3992	963.261	21.438	617.9087
338.7333	-1561.12	711.327	964.301	50.938	614.8365
337.6	-1530.4	711.2548	965.341	80.438	635.8365
336.4667	-1499.68	709.038	966.381	109.938	632.7643
335.3333	-1468.96	709.9658	967.421	139.438	637.692
334.2	-1438.25	708.8213	968.461	168.938	648.6198
333.0667	-1407.53	710.749	969.501	198.438	649.5475
331.9333	-1376.81	701.6768	970.541	227.938	657.5475
330.8	-1346.09	697.6046	971.581	257.438	652.4753
329.6667	-1315.37	688.5323	972.621	286.938	657.2586
328.5333	-1284.65	683.4601	973.661	316.438	676.1863
327.4	-1253.94	677.3878	974.701	345.938	693.1863
326.2667	-1223.22	677.3878	975.741	375.438	690.1141
325.1333	-1192.5	671.3156	976.781	404.938	681.0418
324	-1161.78	676.1711	977.821	434.438	675.0418
323.3939	-1133.64	668.3042	978.861	463.938	693.9696
322.7879	-1105.5	669.2319	979.901	493.438	676.8973
322.1818	-1077.36	668.1597	980.941	522.938	700.8251
321.5758	-1049.23	667.0875	981.981	552.438	684.6806
320.9697	-1021.09	668.0875	472	1360	506.1568
320.3636	-992.949	667.0152	498	1340	527.2647
319.7576	-964.811	667.943	524	1320	534.3725
319.1515	-936.672	674.7985	550	1300	548.5882
318.5455	-908.534	675.7985	575.7575	1280.303	552.696
317.9394	-880.395	673.654	601.5151	1260.606	581.8039
317.3333	-852.257	672.5817	627.2727	1240.909	599.9117
316.7273	-824.118	676.5095	653.0303	1221.212	613.0196
316.1212	-795.98	674.4373	678.7878	1201.515	632.1274
315.5152	-767.841	682.365	704.5454	1181.818	627.2352
314.9091	-739.703	681.2205	730.303	1162.121	632.3431
314.303	-711.564	675.1483	756.0606	1142.424	633.5588
313.697	-683.426	677.076	781.8181	1122.727	612.6666
313.0909	-655.287	679.0038	807.5757	1103.03	636.7745
312.4848	-627.149	673.9316	833.3333	1083.333	639.8823
311.8788	-599.01	677.8593	859.0909	1063.636	627.9901
311.2727	-570.872	675.7871	884.8484	1043.939	601.098
310.6667	-542.733	673.7871	910.606	1024.242	595.2058
310.0606	-514.595	675.7148	936.3636	1004.545	606.3137

X-COORD	Y-COORD	MAG	X-COORD	Y-COORD	MAG
920.711	-2158.09	671.2624	1881.25	-138.333	631.5686
921.2861	-2126.77	672.2624	1895.833	-162.222	626.6764
921.8613	-2095.45	676.3346	1910.416	-186.111	623.7843
922.4364	-2064.13	680.4068	1925	-210	623.8921
923.0115	-2032.81	712.4791	1957.5	-204	632.3235
923.5866	-2001.49	694.5513	1990	-198	625.4313
924.1618	-1970.17	695.6236	2022.5	-192	629.5392
924.7369	-1938.85	694.6236	2055	-186	627.647
925.312	-1907.53	689.6958	2087.5	-180	633.7549
925.9036	-1876.42	679.7681	2120	-174	636.8627
926.4953	-1845.31	673.8403	2152.5	-168	627.9705
927.0869	-1814.19	675.8403	2185	-162	621.0784
927.6785	-1783.08	677.9125	2217.5	-156	619.1862
928.2701	-1751.97	682.9848	2250	-150	620.2941
928.8618	-1720.86	687.057	2251.562	-120.625	616.4019
929.4534	-1689.74	698.1293	2253.125	-91.25	617.6176
930.045	-1658.63	700.2015	2254.687	-61.875	615.7254
930.7274	-1628.16	702.2738	2256.25	-32.5	612.8333
931.4098	-1597.7	701.2738	2257.812	-3.125	615.049
932.0921	-1567.23	695.346	2259.375	26.25	613.1568
932.7745	-1536.76	692.4183	2260.937	55.625	616.3725
933.4569	-1506.29	688.4905	2262.5	85	615.4803
934.1393	-1475.83	686.5627	2264.062	114.375	618.5882
934.8216	-1445.36	688.635	2265.625	143.75	619.696
935.504	-1414.89	692.7072	2267.187	173.125	614.8039
935.5101	-1384.34	689.7795	2268.75	202.5	622.9117
935.5163	-1353.79	692.8517	2270.312	231.875	618.0196
935.5224	-1323.24	691.8517	2271.875	261.25	615.1274
935.5285	-1292.69	684.924	2273.437	290.625	607.2352
935.5346	-1262.14	685.9962	2275	320	615.3431
935.5408	-1231.59	678.0684	2276.562	349.375	601.5588
935.5469	-1201.04	670.2129	2278.125	378.75	607.6666
935.553	-1170.49	638.3574	2279.687	408.125	594.6666
936.0147	-1140.69	664.4297	2281.25	437.5	600.7745
936.4763	-1110.88	658.5019	2282.812	466.875	589.8823
936.938	-1081.08	654.5019	2284.375	496.25	589.9901
937.3997	-1051.28	651.5741	2285.937	525.625	584.098
937.8613	-1021.48	646.6464	2287.5	555	619.098
938.323	-991.672	643.7186	2289.062	584.375	583.2058
938.7847	-961.869	644.7909	2290.625	613.75	592.3137
939.2463	-932.066	638.8631	2292.187	643.125	596.4215
939.708	-902.263	637.9354	2293.75	672.5	599.4215
940.1697	-872.46	625.9354	2295.312	701.875	609.5294
940.6313	-842.657	619.0076	2296.875	731.25	615.6372
941.093	-812.854	616.0798	2298.437	760.625	611.8529
941.5547	-783.051	614.2243	2300	790	613.3921
942.0163	-753.248	610.2966	2141	764	602.7156
942.478	-723.445	614.2966	1982	738	588.9313
942.9397	-693.642	607.3688	1823	712	574.147
943.4013	-663.839	609.4411	1664	686	607.3627

X-COORD	Y-COORD	MAG	X-COORD	Y-COORD	MAG
309.4545	-486.456	666.6426	962.1212	984.8484	621.4215
308.8485	-458.318	665.4981	987.8787	965.1515	619.5294
308.2424	-430.179	663.4981	1013.636	945.4545	631.6372
307.6364	-402.041	661.3536	1039.393	925.7575	630.745
307.0303	-373.902	663.2814	1065.151	906.0606	618.9607
306.4242	-345.764	660.2814	1090.909	886.3636	635.0686
305.8182	-317.625	657.2091	1116.666	866.6666	636.1764
305.2121	-289.487	658.1369	1142.424	846.9696	639.2843
304.6061	-261.348	650.0646	1168.181	827.2727	644.3921
304	-233.21	653.9924	1193.939	807.5757	658.5
897.352	-3421.26	580.0837	1219.696	787.8787	663.7156
897.9758	-3389.67	661.1559	1245.454	768.1818	658.8235
898.5995	-3358.08	602.2281	1271.212	748.4848	667.9313
899.2233	-3326.49	601.3004	1296.969	728.7878	663.0392
899.847	-3294.9	589.3726	1322.727	709.0909	679.147
900.4708	-3263.31	622.4449	1348.484	689.3939	668.2549
901.0945	-3231.72	649.5171	1374.242	669.6969	672.3627
901.7183	-3200.13	671.5894	1400	650	625.4705
902.342	-3168.55	690.6616	1414.583	626.1111	656.7941
902.9658	-3136.96	686.7338	1429.166	602.2222	661.0098
903.5895	-3105.37	675.8061	1443.75	578.3333	657.1176
904.2133	-3073.78	669.8783	1458.333	554.4444	657.1176
904.837	-3042.19	655.9506	1472.916	530.5555	644.2254
905.4608	-3010.6	654.0228	1487.5	506.6666	633.3333
906.0845	-2979.01	660.0228	1502.083	482.7777	620.4411
906.7083	-2947.42	668.0951	1516.666	458.8888	622.549
907.332	-2915.83	671.1673	1531.25	435	618.6568
907.9505	-2884.06	681.2395	1545.833	411.1111	612.7647
908.569	-2852.29	689.3118	1560.416	387.2222	607.8725
909.1875	-2820.52	696.384	1575	363.3333	608.9803
909.806	-2788.76	706.4563	1589.583	339.4444	609.0882
910.4245	-2756.99	710.5285	1604.166	315.5555	602.196
911.043	-2725.22	705.6008	1618.75	291.6666	603.3039
911.6615	-2693.45	698.673	1633.333	267.7777	606.4117
912.28	-2661.68	703.7452	1647.916	243.8888	600.5196
912.898	-2629.89	704.7452	1662.5	220	599.6274
913.516	-2598.11	712.8175	1677.083	196.1111	602.8431
914.134	-2566.32	719.8897	1691.666	172.2222	605.1666
914.752	-2534.54	721.962	1706.25	148.3333	611.2745
915.37	-2502.75	718.962	1720.833	124.4444	621.3823
915.988	-2470.96	716.0342	1735.416	100.5555	625.4901
916.606	-2439.18	707.0342	1750	76.66666	629.598
917.224	-2407.39	696.6122	1764.583	52.77777	629.7058
917.6599	-2376.23	689.6844	1779.166	28.88888	624.8137
918.0958	-2345.07	684.7567	1793.75	5	625.9215
918.5316	-2313.9	678.8289	1808.333	-18.8888	632.0294
918.9675	-2282.74	674.9011	1822.916	-42.7777	633.1372
919.4034	-2251.58	672.9734	1837.5	-66.6666	633.245
919.8393	-2220.42	670.0456	1852.083	-90.5555	627.3529
920.2751	-2189.25	669.1901	1866.666	-114.444	624.4607

X-COORD	Y-COORD	MAG	X-COORD	Y-COORD	MAG
943.863	-634.036	611.5133	2300	790	616.8431
944.3247	-604.233	611.5856	2278.947	811.5789	623.9509
944.7863	-574.43	616.5856	2257.894	833.1578	616.0588
945.248	-544.627	617.6578	2236.842	854.7368	601.1666
945.7097	-514.824	616.73	2215.789	876.3157	611.2745
946.1713	-485.021	612.8023	2194.736	897.8947	597.3823
946.633	-455.218	604.8745	2173.684	919.4736	599.4901
947.6715	-425.136	601.9468	2152.631	941.0526	598.7058
948.71	-395.054	597.019	2131.578	962.6315	599.8137
949.7485	-364.972	597.0913	2110.526	984.2105	583.9215
950.787	-334.89	590.1635	2089.473	1005.789	596.0294
951.8255	-304.808	594.2357	2068.421	1027.368	590.1372
952.864	-274.726	591.308	2047.368	1048.947	626.245
953.9025	-244.644	585.3802	2026.315	1070.526	599.3529
954.941	-214.562	583.6692	2005.263	1092.105	579.4607
-1007.58	-1154.82	498	1984.21	1113.684	591.5686
-1007.6	-1122.25	483	1963.157	1135.263	587.6764
-1007.63	-1089.68	491	1942.105	1156.842	606.7843
-1007.65	-1057.11	502	1921.052	1178.421	621.8921
-1007.68	-1024.54	520	1900	1200	619
-1007.7	-991.974	511	700	1650	493
-1007.72	-959.405	485	1000	1650	531
-1007.75	-926.835	497	1275	1650	584
-1007.77	-894.266	493	1550	1650	576
-1007.8	-861.697	502	2000	1650	655
-1007.82	-829.128	500	1900	2040	570
-1007.84	-796.558	500	1550	2050	481
-1007.87	-763.989	502	1275	2050	514
-1007.89	-731.42	485	1000	2050	483
-1007.92	-698.851	491	700	2050	507
-1007.94	-666.281	475	1000	2450	546
-1007.97	-633.712	491	1275	2450	536
-1007.99	-601.143	490	1550	2450	607
-1008.01	-568.574	487	1900	2400	605
-1008.04	-536.004	486	2000	1425	658
-1008.06	-503.435	487	2250	1675	669
-1008.09	-470.866	471	2850	2000	627
-1008.11	-438.297	478	700	1250	564
-1008.13	-405.728	487	1000	1250	588
-1008.16	-373.158	489	1275	1250	623
-1008.18	-340.589	467	1550	1250	679
-1008.21	-308.02	483			

APPENDIX D: TERRAIN CONDUCTIVITY DATA

The terrain conductivity were collected with a Geonics EM-34. Data were collected at 20 and 40 meter spacings. Both vertical and horizontal coil readings were taken for the 40 meter separation. Because the data were somewhat noisy, the 40 meter vertical coil data were first smoothed with a three point running average. These smoothed data are plotted on Figure 14. The survey proceeded from the northwest end of Profile 1, traversing south. The line then turned southwestward, following a creek, through a gap in the sand dunes, and then turned northwestward and followed the shore of Washoe Lake. Profile 2 was read from southeast to northwest.

The data are presented on the following page.

Washoe Lake EM34 data, February 1, 1993

STA	40vc	3 ptavg	40hc	20vc	20hc	Bearing
0	25		28	18	20	Bearing
1	22	23	26	18	20	SE
2	22	22.666667	26	16	20	
3	24	23.333333	28	18	19	
4	24	23.666667	26	18	18	
5	23	23.666667	26	16	19	
6	24	24.333333	30	16	18	
7	26	26.666667	30	18	20	
8	30	29.333333	35	25	25	
9	32	31	26	30	20	
10	31	31	34	24	25	
11	30	30	32	24	17	
12	29	29	34	24	26	
13	28	27.666667	28	22	18	
14	26	26.333333	31	21	22	
15	25	25.666667	32	20	21	
16	26	25.666667	30	21	21	
17	26	25.333333	31	20	21	
18	24	25	28	19	20	
19	25	24.333333	28	19	22	
20	24	24	26	19	21	
21	23	23.666667	28	18	20	
22	24	23	28	18	20	
23	22	22.666667	28	18	22	
24	22	22.666667	26	18	20	
25	24	23.666667	27	19	21	
26	25	24.666667	25	21	20	
27	25	24	26	18	21	Bearing
28	22	22.666667	28	17	22	SW
29	21	21.666667	28	18	22	
30	22	22.333333	30	18	24	
31	24	23.333333	28	19	22	
32	24	23.666667	29	20	22	
33	23	23.333333	28	18	22	
34	23	23.333333	27	19	22	
35	24	24	28	20	24	
36	25	25	28	22	24	
37	26	25.666667	29	22	23	
38	26	26	30	20	23	Bearing
39	26	26.666667	30	21	25	NW
40	28	27.666667	34	22	24	
41	29	28.666667	34	22	26	
42	29	29	33	22	25	
43	29	29.333333	34	22	26	
44	30	29.666667	33	25	24	
45	30	29.666667	30	24	24	
46	29	29	32	22	24	
47	28	27.666667	31	20	24	
48	26	27.333333	32	23	22	
49	28	27	32	22	22	
50	27	27	32	19	20	
51	26	26.333333	30	20	22	
52	26		31	20	20	

APPENDIX E: GLOBAL POSITIONING (GPS) DATA

The Global Positioning data were collected with a Trimble 4000SDT GPS receiver with a geodetic antenna mounted on a Suburban. Most of the pre-staked stations on the dry lake bed were accessed relatively rapidly in this manner. In order to keep baselines short, a base station was occupied near the middle of the lake and all other co-ordinates referenced to it. Readings were also taken at several locatable points around the periphery of the lake to obtain better ties. The GPS co-ordinates of the sign at the Exit 44 (Bellevue Road) wooden park sign is:

Latitude = 39 degrees 14 minutes 50.51384 seconds

Longitude = -119 degrees 48 minutes 38.74052 seconds

Elevation = 1538.3054 meters.

APPENDIX F: WELL DATA

Initial estimates of transmissivities were made from specific capacity tests from a number of water wells available from Rush's report, USGS data bases, and the state engineer, using the following relationship(Freeze and Cherry, 1979):

$$T = CQ/\Delta h$$

where:

Q = pumping rate

Δh = drawdown

C = a constant depending on the system of units being used.

While a majority of wells which have had specific capacity tests run on them are clustered to the southwest, there are enough wells in other locations to make initial estimates of the areal distribution of hydraulic properties.

Data quality was highly variable. Many of the wells were multiply screened, and thus it was often not possible to attribute the discharge to a particular interval or hydrostratigraphic unit, or to tell whether the unit was confined or unconfined. The data seem to be more consistent to the southwest.

WASHOE VALLEY WATER LEVELS ca. 1965

T16N, R19E WEST SIDE OF VALLEY

SEQUENC NUMBER	SEC	1/4 1/4	ALTUTUD	WATER LEVEL	WELL DEPTH	HOLE DEPTH	ALT - WTR LVL	C/U ?
2	3	NENW	5080	11			5069	
3	3	SWNW	5160	29	239		5131	
	3	SWNW	5160		996			
4	3	SESW	5050		475			
5	10	NENE	5035	FLOWING	138			
6	10	SENE	5040	FLOWING				
	10	NENW	5055	9			5046	
7	10	NENW	5055	4			5051	
	10	SWNW	5100					
8	10	SENWNW	5065	6	94		5059	
	11	SWSW	5035	FLOWING				
10	11	NESESW	5035	FLOWING	135			
11	14	SWNW	5045	FLOWING	162			
12	14	SESW	5050	7	90		5043	
13	15	SWNW	5160	4	131		5156	
14	15	SENW	5060		500			
	15	NESW	5085	10	450		5075	
15	16	NESE	5200	4	60		5196	
16	16	SESE	5190	1	235		5189	
	21	SENE	5200	FLOWING				
17	22	NESE	5150		590			
18	22	SWSE	5200	72	122		5128	
	22	SENW	5200	1	622		5199	
19	23	SWSW	5180	27	130		5153	
20	23	NWSE	5040	15	70		5025	
	23	NWSE	5040	11	70		5029	
21	25	NENW	5060	1	100		5059	
22	26	NWNE	5170	20	130		5150	
23	26	SENWSE	5120	15	138	156	5105	
24	26	SESE	5060	FLOWING	84			
	26	SWSE	5160	15	156		5145	
25	35	SESUNE	5240		76	76		
26	35	SESUNE	5240	2	6		5238	
27	35	SWSENE	5250		116	220		
28	35	NWSE	5250	33	155		5217	
	35	NWNE	5180	0			5180	
29	36	NWNW	5070	50			5020	
30	36	SWNW	5170	3	170		5167	

DATE	REMARKS
=====	=====
10/65	
01/63	
	RUSH
10/65	
10/65	
10/65	RUSH
10/65	
	RUSH
03/68	FRANKTOWN, W/TIM
10/65	RASMUSSEN FLOWI
10/65	
10/65	
07/50	
10/65	
04/49	
10/65	
10/65	
01/64	
10/65	
10/65	
06/62	
10/65	RUSH,DUP
10/65	
10/65	
07/60	TIME SERIES DATA
10/65	
10/65	
	TIME SERIES DATA
05/76	TIME SERIES DATA
	TIME SERIES DATA
11/63	
10/65	
01/65	
07/59	

T16N, R20E EAST SIDE OF VALLEY

SEQUENC NUMBER	SEC	1/4 1/4	ALTUTUD	WATER LEVEL	WELL DEPTH	HOLE DEPTH	ALT - WTR LVL
31	5	SWNE	5150	50	80		5100
32	5	SWSW	5075	1	242		5074
33	6	NENE	5085	39	83		5046
34	6	NWNE	5080	46	83		5034
35	6	NENW	5055	11	87		5044
36	6	NESW	5045	FLOWING			
37	6	SESE	5070	22	66		5048
38	17	SWNE	5060	13	225	225?	5047
39	17	NESE	5120	56			5084

T17N, R19E WEST SIDE OF VALLEY

SEQUENC NUMBER	SEC	1/4 1/4	ALTUTUD	WATER LEVEL	WELL DEPTH	HOLE DEPTH	ALT - WTR LVL
40	23	SENE	5075	13	70		5062
41	23	SE	5070	5			5065
42	23	SWSE	5080	19	76		5061
43	24	NESWNW	5050	13	417		5037
			5040?				5027?
44	25	SENE	5075	40	92		5035
45	26	NENE	5050	FLOWING	120		
46	27	NESWSE	5160				
47	34	NENE	5075	16			5059
48	34	NESE	5085	17	63		5068

T17N, R20E EAST SIDE OF VALLEY

SEQUENC NUMBER	SEC	1/4 1/4	ALTUTUD	WATER LEVEL	WELL DEPTH	HOLE DEPTH	ALT - WTR LVL
49	30	SWSW	5065	27			5038
50	31	SWNE	5080	34			5046
51	31	NENW	5070	13			5057
52	31	NESW	5130	86			5044
RUSH	31	SWNE	5100		317		

C/U ? DATE REMARKS

10/65
05/54
10/65
04/64
01/66
01/66
01/66
10/65
01/66

C/U ? DATE REMARKS

10/65
10/65
10/65
10/65

10/65
10/65

10/65
10/65

DAVIS CR. PARK WEL

C/U ? DATE REMARKS

10/65
01/66
01/66
01/66

SPECIFIC CAPACITY DATA

SEQUENC NUMBER	SEC	1/4 1/4	ALTUTUD	PROD LEVEL	WATER LEVEL	DRAW- DOWN	DIS- CHARGE	T gal/dy/ft	T m**2/s	T m**2/day
3	3	SWNW	5160	92	29	63	88	368.762	5.3E-05	4.57265
4	3	SESW	5050			56	4100	19328.6	0.00278	239.674
11	14	SWNW	5045			75	300	1056	0.00015	13.0944
14	15	SESW	5060			140	1200	2262.86	0.00033	28.0594
15	16	NESE	5200	60	4	56	3	14.1429	2E-06	0.17537
16	16	SESE	5190	26	1	25	18	190.08	2.7E-05	2.35699
	22	NWSE	5200	622	1	145	800	1456.55	0.00021	18.0612
18	22	SWSE	5200		72		25		0	0
20	23	NWSE	5040	40	10	30	20	176	2.5E-05	2.1824
27	35	SWSENE	5250	47	1	46	50	286.957	4.1E-05	3.55826
RUSH	35	NWSE	5250			72	9	33	4.8E-06	0.4092
30	36	SWNW	5170	80	3	77	20	68.5714	9.9E-06	0.85029

T17N, R19E WEST SIDE OF VALLEY

32	5	SWSW	5080	1	20	0	0
34				44	32	0	0
36					0.5 FLOWING	0	0

T16N, R20E EAST SIDE OF VALLEY

38	17	SWNE	5060	68	13	55	2000	9600	0.001382	119.04
----	----	------	------	----	----	----	------	------	----------	--------

T17N, R19E WEST SIDE OF VALLEY

42	23	SWSE	5080	69	19	50	15	79.2	1.14E-05	0.98208
44	25	SENE	5075	92	40	52	5	25.38462	3.66E-06	0.314769
45	26	NENE	5050	120		58	20	91.03448	1.31E-05	1.128828

T17N, R20E EAST SIDE OF VALLEY

31	SWNE	5100	317	9	13	381.3333	5.49E-05	4.728533
----	------	------	-----	---	----	----------	----------	----------

DATA FROM DRILLER'S LOGS, T16N, R19E

SEQUENC NUMBER	SEC	1/4 1/4	ALTUTUD	PROD LEVEL	CASING	TD	WATER LEVEL	DRAW-DOWN	DIS-CHARGE	T gal/dy/ft	T m**2/s	T m**2/day
22		NENE		6-60	0-42	354	6	26	50	507.6923	7.31E-05	6.295385
22		SWNE		430-622	430-622	622	25	170	800	1242.353	0.000179	15.40518
				100-270	100-270							
22		NESE		315-4??	50-585	587	3	239	350	386.6109	5.57E-05	4.793975
22		SESE		183-218	183-218	218	25	135	30	58.66667	8.45E-06	0.727467
22		SESE		18-249	90-220	249	10		124			
22		SWSW		90-243	60-250	250			170			
22		SWSE		80-242	60-242	242			175			
23		NENW			60-300	468	11	55	310	1488	0.000214	18.4512
23		SESW			many	350		25	80	844.8	0.000122	10.47552
23		NWSE			100-245	248						
25		SENE			TEST	380	TEST	175	100	150.8571	2.17E-05	1.870629
26		SESE			69-201?	320	3					
26		SENE			186-206	210						
35		SWNE		FLOWING	50-116	220	FLOWING	47	55	308.9362	4.45E-05	3.830809
								20	60	792	0.000114	9.8208